



Norwegian University of
Science and Technology

Cuttings Transport in Inclined Sections

Birgitte Ruud Kosberg

Master of Science in Petroleum Geoscience and Engineering

Submission date: June 2017

Supervisor: Pål Skalle, IGP

Co-supervisor: Jan David Ytrehus, SINTEF

Norwegian University of Science and Technology
Department of Geoscience and Petroleum

PREFACE

This study was conducted as the product of the course *TPG4910 – Petroleum Engineering – Drilling Engineering, Master thesis*. The course gives 30 credits at the *Norwegian University of Science and Technology (NTNU)*, with its objective to manage self-standing work within drilling by the use of scientific methods.

The thesis is written in cooperation with *NTNU* and *SINTEF Petroleum*. A series of experiments were performed with the aim to control the rheology during drilling operations and analyse the deviations. The learning outcome also included the physics of cuttings transport in deviated wells, with the effect from velocity and rotational drill pipe. Rheology measurements were conducted in the laboratory of the *Petroleum Technical Centre (PTS)*, while cuttings transport experiments were performed by *SINTEF* in the experimental-hall at *SINTEF Petroleum*.

I first and foremost would like to thank my supervisor *Pål Skalle* from *NTNU*, who provided me with understanding within the field of fluid mechanics and rheology. I would like to thank my supervisor, *Jan David Ytrehus*, at *SINTEF Petroleum* for including me in the project and giving me close follow-up. *Ali Taghipour* has been in great help during the flow-loop set-up offering his expertise, being solution oriented and patient. *Bjørnar Lund* from *SINTEF* has been a solid support in questions regarding hydraulics and mathematical modelling. Thanks to *Roger Overå* for his guidance and always being available in the case of need in the laboratory. A big thanks to *Knut Richard Gyland* from *M.I Swaco – A Schlumberger Company*, for taking the time to help with the experimental rheology-procedures. The same goes for *Benjamin Werner*, which has been a great help for this thesis by providing data from his article published previously this year (2017) and with his guidance during performing the experiments. A special thanks to *SINTEF* for offering a pleasant work environment with good equipment and facilities.

Trondheim June 2017

Birgitte Ruud Kosberg

ABSTRACT

Mud rheology is a key parameter in hole cleaning efficiency. Field data suggests that oil-based drilling fluids perform better compared to water based drilling fluids in the field, even with identical rheological properties. This reason for this is not fully understood. Studies and experimental work is conducted to see the rheological properties in context with cuttings transport in inclined and horizontal wellbores. Cuttings particles settling in the wellbore can result in mechanical pipe sticking and other unfortunate cost- and safety-hazards. Operational parameters as annular velocity and drill pipe rotation can influence the hole cleaning efficiency significantly. Models are developed to estimate cuttings bed height based on operational data and rheology. The literature study suggests that the field is in need of a universal model to be utilized for all cases.

The objective of this thesis was to engage in a hole cleaning experiment conducted by *SINTEF Petroleum*. Set-up of a semi full-scale flow-loop and monitoring rheological properties over time during experiments was performed. Continuous fluid control ensured that the mud kept the original quality without unfortunate effect to the experiments. The experimental procedure was already published, based on testing samples of water-based Laptonite-fluids. For this thesis, an oil-based WARP fluid was tested in Anton Paar and Fann 35. Fluids were tested with 0h and 24h resting time, with and without pre-stirring at 1022 s^{-1} , prior to obtaining a flow curve after API specifications. The objective was to investigate the effect pre-stirring had on reproducibility of rheology measurements.

Cuttings transport was modelled for inclined and horizontal boreholes. The model estimates the cuttings bed height as a function of velocity and rotation of the drill pipe in annuli. The critical, local velocity where the sum of forces acting upon a cuttings particle was zero was utilized to find the cuttings bed height without rotation. The mass balance between shear force acting on the bed, induced by the rotating drill pipe, and gravitational forces was used to estimate the height at which the cuttings were lifted from the bed. Further, we analysed if this lift height was sufficient to transport the particle out of the section by axial drag forces along annuli, combined with particle slip velocity.

Pre-stirring of the mud-sample prior to measuring the flow curve in accordance to API specifications, show clear advantage for reproducing results for both OBM WARP and Laptonite-fluids. Laptonite-fluids showed increased reproducibility by pre-stirring when relatively low salt concentrations was added to the fluid. Laptonite fluids seemed to be affected by gelling without pre-stirring, while OBM WARP had the opposite effect; less shear stress was developed compared to samples with pre-stirring. In general, Fann 35 deviated from Anton Paar, especially with lower shear stress in the high-shear area.

The cuttings bed model showed less effect of increasing velocity on cuttings bed height, compared to experimental data. Estimated values were affected by excluded physics that would influence cuttings bed height, and simplifying assumptions. The fluid mechanics of cuttings transport requires more comprehensive modelling. Research in developing well-fitted fluid models for drilling fluids, as well as a statistical method in analysing a flow pattern with both different flow regimes in the axial and cross-sectional directions, should be in focus in the future.

SAMMENDRAG

Borevæske-reologi er en nøkkelparameter i hullrensings-effektivitet. Ifølge felt-data vil oljebaserte borevæsker prestere bedre i felt sammenlignet med vannbaserte borevæsker, selv om de har like reologiske egenskaper. Man har enda ikke helt kartlagt hva som forårsaker dette. Studier og eksperimentelt arbeid er utført for å se reologiske egenskaper i sammenheng med transport av borekaks i høyavviks- og horisontalbrønner. Avsetning av borekaks-partikler i brønnen kan forårsake at borestrengen blir sittende fast i brønnen samt andre kostbare og tidskrevende utfordringer. Operasjonelle data, som hastighet i annulus og rotasjon av borestrengen, kan ha signifikant påvirkning på hullrensings-effektiviteten. Flere modeller er utviklet for å estimere høyden på borekaks-avsetningen i brønnen som resultat av operasjonelle data og borevæskens reologi. Litteratur studier anslår at man trenger en mer universell modell som er anvendbar for felt-data.

Målet med denne masteroppgaven var å delta i et hullrensningseksperiment utført av SINTEF Petroleum. Under oppgaven ble det satt opp en strømningsløyfe for å kjøre hullrensings-eksperiment, samt utført testing av reologien av borevæsken over tid før og under eksperimentene. Kontinuerlig fluid-kontroll sikret at borevæsken holdt stabil kvalitet under forsøkene uten at endringer påvirket eksperimentene. Eksperimentell prosedyre i laben var allerede publisert, basert på reologiske målinger av vannbaserte Laptonitt-fluider. I denne masteroppgaven ble en olje-basert WARP-væske testet i Anton Paar og Fann 35. Borevæsken ble testet med både 0 og 24 timer hviletid etter at den bli pre-skjært i en blender, med og uten for-røring ved 1022 s^{-1} i reometeret og viskometeret, før den ble testet etter API-spesifikasjoner. Målet var å anslå hvorvidt for-røring påvirket reproduserbarheten av reologi-målingene.

Borekaks-transport ble modellert for høyavvik- og horisontalbrønner. Modellen estimerer høyden av akkumulert borekaks som funksjon av aksiell hastighet av borevæsken og rotasjon av borestrengen. Kritisk, lokal hastighet som ble funnet hvor kreftene som virker på en borekaks-partikkel var null, ble brukt til å finne høyden av kakset for hullrensning uten rotasjon av borestrengen. Kraftbalanse mellom skjærkrefter fra den roterende borestrengen og gravitasjonseffekt på partikkelen ble brukt til å estimere høyden partikkelen ble transportert opp fra det akkumulerte

borekakset. Videre brukte vi denne høyden til å estimere hvor langt partikkelen ble transportert som funksjon av aksial hastighet av borevæsken og fall-hastigheten til partikkelen.

Væsker som ble rørt i ti minutter i forkant av målinger etter API-spesifikasjoner i Anton Paar og Fann 35, viste bedre evne til å gi reproduserbare resultater, for både OBM WARP og WBM Laptonitt. Reproduserbarheten økte betydelig ved tilsetning av lave salt konsentrasjoner i Laptonitt-væskene ved for-røring. Laptonitt-væskene så ut til å vise effekt av økt gelestruktur ved målinger uten for-røring ved høyt skjær, mens OBM WARP hadde motsatt effekt; mindre skjærstress-målinger i målinger uten for-røring, sammenlignet med målinger med for-røring. Fann 35 avvirket generelt sett fra Anton Paar, spesielt i høyskjær-området.

Modellen som predikerte høyden av borekaks-avsetningen i brønnen viste lavere variasjon i kaks-høyde av økt hastighet, sammenlignet med eksperimentelle data. Estimerte verdier var påvirket av usikkerhet av enkle antakelser. Fluid mekanikken relatert til borekaks-transport trenger en mer omfattende modell. I fremtiden bør man fokusere på å bedre reologiske modeller til å passe borevæskens reologi, samt å modellere borekaks-transport med statistiske metoder ved å analysere strømningsregimer både for aksielle- og radielle retninger.

TABLE OF CONTENTS

PREFACE	III
ABSTRACT	V
SAMMENDRAG	VII
LIST OF FIGURES	XI
LIST OF TABLES	XIII
1 INTRODUCTION	1
2 PREVIOUS KNOWLEDGE	3
3 THEORY	9
3.1 BASIC PRINCIPLES	9
3.2 RHEOLOGY MODELS	11
3.3 FLOW REGIMES	14
3.4 FACTORS AFFECTING HOLE CLEANING	16
4 EXPERIMENTAL FLUID CHARACTERIZATION	23
4.1 FLOW-LOOP SET-UP.....	24
4.2 TESTED FLUIDS	28
4.3 RHEOLOGICAL CHARACTERIZATION	30
4.4 MEASUREMENT CHALLENGES	46
5 ANALYSIS AND EVALUATION OF LABORATORY OBSERVATIONS	55
5.1 OBSERVATIONS	55
5.2 PHYSICS INVOLVED.....	58
5.3 COMPARISON WITH LABORATORY DATA	75
6 SELF-ASSESSMENT	81
6.1 UNCERTAINTY AND LIMITATIONS	81
6.2 FUTURE WORK AND IMPROVEMENT AREAS	85
7 CONCLUSION	87
NOMENCLATURE	89
REFERENCES	93
APPENDICES	97
APPENDIX A: FLOW CURVES FOR PROCEDURE EVALUATION	99
APPENDIX B: FLOW CURVES FOR RHEOLOGY CONTROL (<i>SINTEF</i>).....	101

APPENDIX C: LABORATORY PROCEDURES	103
<i>C.1 PROCEDURE FOR FANN 35-VISCOMETER AND ES MEASUREMENTS</i>	103
<i>C.2 PROCEDURE FOR ANTON PAAR-RHEOMETER</i>	103
<i>C.3 PROCEDURE FOR DENSITY MEASUREMENTS WITH PYCNOMETER</i>	104
APPENDIX D: RISK ASSESSMENT	105

LIST OF FIGURES

FIGURE 1 SHEAR STRESS AND SHEAR RATE ACTING ON A FLUID (THIS AUTHOR)	10
FIGURE 2 DIFFERENT FLOW CURVES; (1) NEWTONIAN FLUID, (2) BINGHAM PLASTIC FLUID, (3) SHEAR-THICKENING FLUID AND (4) SHEAR-THINNING FLUID (CAENN ET AL., 2011)	11
FIGURE 3 COMMON RHEOLOGY MODELS APPLIED ON DIFFERENT DRILLING FLUIDS (THIS AUTHOR)	12
FIGURE 4 LAMINAR VS. TURBULENT FLOW REGIMES (THIS AUTHOR)	14
FIGURE 5 TRANSITIONAL FLOW REGIME (THIS AUTHOR)	15
FIGURE 6 SLIP VELOCITY IN VERTICAL, INCLINED AND HORIZONTAL WELLBORES (THIS AUTHOR)	17
FIGURE 7 THE AFFECT OF ECCENTRICITY ON THE VELOCITY PROFILE IN ANNULI (TOMREN, 1979)	20
FIGURE 8 FULL-SCALE FLOW-LOOP (THIS AUTHOR)	24
FIGURE 9 SAND INJECTION UNIT	25
FIGURE 10 TEST SECTION WITH ROTATING DRILL STRING-MOTOR	26
FIGURE 11 SAND FILTRATION UNIT WITH MUD TANK AND MIXER	26
FIGURE 12 FRICTION COEFFICIENTS FOR STEEL ON CONCRETE (LEFT) VS STEEL ON STEEL (RIGHT) (THIS AUTHOR)	27
FIGURE 13 FANN 35-VISCOMETER (FANN, 2016)	30
FIGURE 14 ANTON PAAR MODULAR COMPACT RHEOMETER (MCR) (ANTON ANTON-PAAR, 2011)	31
FIGURE 15 ANTON PAAR BOB FULLY IMMERSSED IN MUD (KOSBERG, 2016)	32
FIGURE 16 OFITE EMULSION STABILITY TESTER (OFI TESTING EQUIPMENT, 2014)	33
FIGURE 17 RHEOLOGY PROFILE IN IBC-TANK 1 AND 2 (FANN 35) AND THE FIRST MEASUREMENT FROM FLOW-LOOP EXPERIMENTS (FANN 35 & AP)	34
FIGURE 18 FLOW CURVES FROM INDIVIDUAL MEASUREMENTS IN FANN 35 AND ANTON PAAR OF OBM WARP AT 50°C FROM WEEK 1 IN THE FLOW-LOOP	36
FIGURE 19 PRESSURE GRADIENTS FOR THREE EXPERIMENTS WITHOUT SAND INJECTION AND ROTATION, VS. SUPERFICIAL VELOCITY (SINTEF, 2017)	37
FIGURE 20 THE FOUR DIFFERENT COMBINATIONS OF PROCEDURE FOR PRE-STIRRING IN FANN 35 AND ANTON PAAR	40
FIGURE 21 RHEOLOGY PROFILE OF FLUID 1A AT 24 C (WERNER ET AL., 2017)	41
FIGURE 22 RHEOLOGY PROFILE OF FLUID 1B AT 24 C (WERNER ET AL., 2017)	41
FIGURE 23 RHEOLOGY PROFILE OF FLUID 2A (WERNER ET AL., 2017)	42
FIGURE 24 RHEOLOGY PROFILE OF FLUID 2B (WERNER ET AL., 2017)	42
FIGURE 25 RHEOLOGY PROFILE OF FLUID 2C (WERNER ET AL., 2017)	43
FIGURE 26 ANTON PAAR MEASUREMENTS WITH AND WITHOUT PRE-STIRRING OF 1B AT 24°C (WERNER ET AL., 2017) ..	43
FIGURE 27 EFFECT OF PRE-STIRRING OF OBM WARP IN ANTON PAAR AT 25°C	44
FIGURE 28 EFFECT OF PRE-STIRRING OF OBM WARP IN FANN 35 AT 25°C	45
FIGURE 29 FLOW CURVE OF OBM WARP WITH LINEAR CURVE FITTING (BINGHAM PLASTIC)	47
FIGURE 30 TANK WEIGHT MEASUREMENT VS. TIME WITH NOISE FROM VIBRATING PUMP, WITH THE VELOCITY RAMPED UP 0.3-0.5-0.7-0.9-1.1 TO 1.3 (SINTEF, 2017)	50
FIGURE 31 AVERAGE AND MEDIAN WEIGHT DIFFERENCES VERSUS AVERAGE PRESSURE DROP OF THREE EXPERIMENTS, WITHOUT ROTATION AND SAND-INJECTION (SINTEF, 2017)	51

FIGURE 32 DENSITY OF OBM WARP MEASURED AT THE TOP AND AT THE BOTTOM OF AN IBC-TANK BEFORE AND AFTER AGITATION.....	52
FIGURE 33 OBM WARP IN THE IBC-TANK FROM <i>M.I. SWACO – A SCHLUMBERGER COMPANY</i>	53
FIGURE 34 DENSITY MEASUREMENTS OF OBM WARP IN FLOW-LOOP OVER TIME FROM 10.05.17 TO 04.06.17	53
FIGURE 35 ILLUSTRATION OF THE MAIN COMPONENTS IN THE FULL-SCALE FLOW LOOP (YTREHUS J, 2015).....	55
FIGURE 36 FLOW CURVE OF OBM C OBTAINED BY FANN 35 (WERNER ET AL., 2016B).....	57
FIGURE 37 EFFECT OF ROTATION ON HOLE CLEANING IN INCLINED AND HORIZONTAL EXPERIMENTS (SINTEF, 2017).....	58
FIGURE 38 FORCES ACTING UPON A CUTTINGS PARTICLE (RAMADAN ET AL., 2003).....	62
FIGURE 39 VELOCITY PROFILE WITH THE CRITICAL VELOCITY (U_c), AVERAGE VELOCITY ($U_{MEAN, BED}$), MAX VELOCITY (U_{MAX}) AND DISTANCE (Y) TO THE CRITICAL VELOCITY FROM THE BED (THIS AUTHOR).....	64
FIGURE 40 FLOW CHART FOR FINDING CUTTINGS BED FLOW AREA WITHOUT ROTATION	65
FIGURE 41 CUTTINGS TRANSPORT OF ROP- AND RPM-FEED (THIS AUTHOR).....	66
FIGURE 42 RADIUS OF PARTICLE LIFTING (THIS AUTHOR)	67
FIGURE 43 FLOW BETWEEN AN INNER CONCENTRIC, ROTATING CYLINDER AND AN OUTER FIXED CYLINDER	70
FIGURE 44 MAX HEIGHT FOR N PARTICLES, TRANSPORTED BY THE ROTATING DRILL PIPE (THIS AUTHOR)	71
FIGURE 45 TRANSPORT DISTANCE FOR CUTTINGS TRANSPORT DEPENDING ON RADIUS LENGTH FROM THE ROTATING DRILL PIPE SEEN FROM ABOVE (THIS AUTHOR).....	71
FIGURE 46 FLOW CHART FOR CALCULATING CUTTINGS BED REDUCTION	74
FIGURE 47 COMPARISON OF MODEL AND EXPERIMENTAL DATA FROM SINTEF FOR CUTTINGS TRANSPORT WITHOUT ROTATION.....	75
FIGURE 48 COMPARISON OF MODEL AND EXPERIMENTAL DATA FROM SINTEF FOR CUTTINGS TRANSPORT WITH 50 RPM	77
FIGURE 49 FORCES ACTING UPON A CUTTINGS PARTICLE SUSPENDED IN MUD, IN HORIZONTAL AND INCLINED ANNULI	78
FIGURE 50 COMPARISON OF MODEL AND EXPERIMENTAL DATA FROM SINTEF FOR CUTTINGS TRANSPORT WITH 150 RPM	78
FIGURE 51 MODELLED CUTTINGS BED HEIGHT IN INCLINED AND HORIZONTAL SECTIONS FOR 0, 50, 80 AND 150 RPM.....	80
FIGURE 52 CUTTINGS BED HEIGHT VS. CUTTINGS HOLD-UP (SINTEF, 2017)	80

LIST OF TABLES

TABLE 1 FLUID COMPOSITION OF THE LAPTONITE FLUIDS UTILIZED IN THE PUBLISHED WORK OF WERNER ET AL. (2017).	29
TABLE 2 TEST SCHEDULE FOR FLOW-LOOP EXPERIMENTS.....	34
TABLE 3 AVERAGE DENSITY MEASUREMENTS OF TOP AND BOTTOM OF OBM WARP IN IBC TANKS, AND AN INDIVIDUAL MEASUREMENT FROM THE FIRST FLOW-LOOP EXPERIMENT.....	35
TABLE 4 TANK TEMPERATURES AT THE START AND END OF HYDRAULIC EXPERIMENT 1-3 IN THE FLOW LOOP WITHOUT ROTATION AND SAND INJECTION	46
TABLE 5 AVERAGE TANK WEIGHT DIFFERENCE IN AVERAGE AND MEDIAN FOR EACH VELOCITY-STEP, IN THREE EXPERIMENTS WITHOUT ROTATION AND SAND INJECTION (SINTEF, 2017)	50
TABLE 6 DIMENSIONS OF FACTORS CONTRIBUTING TO CUTTINGS TRANSPORT	56
TABLE 7 HERSCHEL BULKLEY PARAMETERS FOR OBM C (SAYINDLA ET AL., 2016)	57
TABLE 8 UNCERTAINTIES RELATED TO RHEOLOGICAL CHARACTERIZATION AND FLOW-LOOP EXPERIMENTS	83

1 INTRODUCTION

The drilling process includes the work of a rock cutting drill bit, leading to a rate of penetration, which is a result of the rocks properties, weight on bit (WOB) and the imposed rotary movement of the drill pipes (RPM). The pieces of rock cut by the drill bit is transported away from the drill bit and back up to surface, achieved by pumping drilling fluids down through the drill pipe and up the annular space. At the surface, pieces of cuttings larger than a certain minimum size are removed from the drilling fluid by a shale shaker or hydro cyclones before recycling the fluid back to the wellbore. Optimizing the drilling fluids rheology and the drilling parameters is important to improve hole cleaning of a well. Successful hole cleaning is an increasingly demanding process characterized by increasingly longer and more inclined wells. At inclinations around 30-50 degrees, Barite together with cuttings may slide backwards (sagging), potentially resulting in demanding hazards related to poor hole cleaning (Ozbayoglu et al., 2008).

The consequence of inadequate hole cleaning can result in a series of hazardous incidents during drilling. Mechanical pipe sticking is the case if the cuttings remain in the hole and surrounds the drill pipe when pulling out. It is likely to experience premature bit wear as a result of not being able to transport the cuttings away from the bit while drilling. Inadequate hole cleaning can be costly as it will slow down the drilling process and create difficulties in logging- in cementing-operations. In serious cases, low degree of cuttings transport can lead to high wellbore pressures resulting in fracture of the formation and result in lost well control.

Drilling fluids rheology is expected to have an intermediate effect on hole cleaning. Drilling fluids are often separated into two main categories based on their base fluid content; water-based mud with water as the base fluid, and oil-based mud with water emulsified in the base fluid, oil. Studies have been performed to study and map their rheological differences. Field data has shown that even with the same rheological properties, oil-based mud performs better in respect to hole cleaning efficiency. Changes

in mud properties over time during a drilling operation, may affect the hole cleaning capability. Such evaluation will increase knowledge of the documented rheological differences for water-based and oil-based drilling fluids.

A more dominating effect on hole cleaning efficiency is drill pipe rotation. Different models are utilized to predict the cuttings accumulation in inclined sections. The objective of this study is two-folded:

- Investigate the rheological stability of drilling fluids during the drilling process
- Investigate the relative effect of drill string rotation on cuttings transport relative to hydraulic transport

A mechanistic model will be utilized and further developed in this thesis to include rotating effects on cuttings bed height. Transportation and deposition of cuttings is a result of the many forces acting upon a particle in a fluid system. The model will be used to analyse data from the laboratory and provide explanation for unexpected behaviour between cuttings bed height and velocity in annuli.

2 PREVIOUS KNOWLEDGE

The rheological effects on mud properties for transport of cuttings in inclined or horizontal wells have previously been studied both experimentally and theoretically (Okrajni and Azar, 1986). In order to optimize hole-cleaning efficiency, the rheological properties must be designed for that purpose. During daily drilling operations it is therefore important to monitor the drilling fluids properties to ensure it maintains the designed quality. In the drilling industry today, Fann 35 is the most common viscometer used to monitor drilling fluid rheology. Experimental studies are previously performed to understand the differences in hole-cleaning efficiency with different water-based and oil-based drilling fluids, even with identical rheological profile.

Ytrehus et al. (2014) tested two different water-based drilling fluids with equivalent rheological properties, whereas one was based on KCl and the other on Bentonite, in a semi full-scale flow-loop. The flow-loop consisted of a 12 m long section with a freely rotating drill string and sand particles were injected into the drilling fluid, while circulating in horizontal position. The aim was to better understand their hole cleaning abilities through realistic experiments. They found that the KCl provided better hole cleaning at lower shear rates and the Bentonite-fluid provided better efficiency at higher shear rates. Their results showed that more accurate rheological characterization should be made to better understand their functionality of cuttings transport.

As a result of the industry's need for more accurate procedures, Werner et al. (2017) studied the effect of preconditioning and aging on rheological properties of thixotropic drilling fluids. The fluid samples were mixed at low shear for two minutes in a Waring blender, before one sample was put to rest and the other pre-stirred in the Fann 35 or Anton Paar MCR for 10 minutes at 1022 s^{-1} before starting measuring the flow curve. The fluid samples were API-tested both immediately after mixing and after 24 hours at rest. It was concluded that most reproducible results were obtained by pre-stirring the fluid, which was supported by previous work (Assembayev and Skalle, 2015), as well as they indicated that the pre-stirring had larger effect for a longer period of resting time for the fluid (24h compared to 0h).

Numerous studies have been pursued to investigate hole-cleaning efficiency in deviated or horizontal wells. These studies can be divided into two main groups; experimental and theoretical.

Firstly, experimental studies give a clear insight in what degree different parameters affects hole cleaning. In a four year experimental study on contributing factors to hole cleaning, mud weight, annular mud velocity, hole angle and drill pipe rotation was listed as the major effects to influence hole cleaning, while rheology was listed as a moderate effect (Sifferman and Becker, 1992). Drill pipe rotation had largest effect on reducing cuttings build-up under conditions where the well is horizontal, cuttings size is small and ROP (rate of penetration) is low. Rotational pipe was later confirmed as an important contributor by Ravi and Hemphill (2006) who also pointed out that the effect is particularly while the drill pipe is eccentric placed within annuli and that efficient hole cleaning is not possible with axial flow alone.

Kim et al. (2008) studied laminar and turbulent flow through both concentric and eccentric annuli with solid particles, both numerically and experimentally. Rotation of drill pipe gave better particle-transport, with high effect with lower velocities and lower effect in higher flow rates. Radial distribution of the solid fraction was significantly improved from 0 to 400 rpm at 30° inclined annuli with a velocity of 0.6 m/s.

Another aspect of rotation of the drill pipe is that analytical, experimental and numerical results show that for laminar flow, the eccentricity and rotational movement increases axial friction drop (Ooms and Kampman-Reinhartz, 2000). Saasen (1998) demonstrated that frictional pressure loss was the main contributor to hole cleaning and that a significantly high-pressure loss was needed to achieve a relatively good hole cleaning.

Secondly, theoretical and mathematical studies have been conducted to predict the hole cleaning efficiency in deviated and horizontal wells with a basis in the experimental results. The most acknowledged models can be divided into three groups:

- 1) Two-layer model
- 2) Three-layer model

3) Mechanistic model

A two-layered model was developed by Gavignet and Sobey (1989) and compared to experimental data from Iyoho (1980), to investigate the major effects observed under bed formation. The model, which includes the solid phase and wet phase, suggested a criterion where thick bed-formation in highly deviated wells should not be based on saltation, but a simple momentum balance between the flowing mud and the cuttings bed. The criterion was strongly dependent on the cuttings size, cross-sectional area and pipe eccentricity. They discovered that a critical flow rate would hinder cuttings accumulation and therefore a bed would not form. The study also highlights the importance of friction factor between the borehole wall and cuttings particles in bed formation in high inclinations.

Wang et al. (2010) developed a three-layer model with a stationary, suspended cuttings bed, a dynamic cuttings layer and a solid phase layer suspended in the drilling fluid. Their finding was that ECD could help monitor and control the cutting bed height. For efficient hole cleaning, it was recommended to use low viscosity drilling fluids, high flow rate and drill pipe rotation. As the equipment and its capacity usually limit the flow rate, pipe rotation was found as the most efficient method to increase the hole cleaning efficiency. In the very high inclinations, when the bed height reached 10% of the annular space, flushing needs to be utilized.

A mechanistic model for cuttings transport was developed by Clark and Bickham (1994). The mechanistic model shows how the different forces acting upon a cuttings particle contributes to transport. The three different transport mechanisms in the model are settling, lifting and rolling. Analysing these mechanisms can tell us what effect is dominant at what angle. Compared to experimental data for cuttings transport in the study, the model showed good agreement to the data below critical values, but critical flow rates were underestimated. In this mechanistic model it is possible to vary operational inputs, mud rheology input, cuttings properties and the geometry of the well.

Ramadan et al. (2003) developed a similar mechanistic model taking into account the rolling and lifting mechanisms working on a cuttings particle. In their study a local velocity was found for both of the mechanisms where the summation of lifting and rolling-forces were zero. The lowest critical value of mean velocity gave the dominating mechanism and sat the transport criterion for flow rates in annuli. Hence both the mechanisms where working simultaneously. Both the model and experimental data in the study gave a direct relationship between acceleration of the cuttings particle and the particle removal rate from the bed. The work in this study will lay the foundation of the modelling in Chapter 5.

The concept of a critical velocity's ability to prevent cuttings bed build-up was also investigated by Ozbayoglu et al. (2007). They proposed an equation to estimate the cuttings bed area over total area, based on the critical value for velocity. The velocity could be predicted within an accuracy of $\pm 15\%$ in comparison with most experiments, using water as drilling fluid at different ROP's and inclinations. One of their most important observations was that shear stress was one of the most influencing parameters influencing the cuttings bed height.

Even though numerous models are developed for cuttings transport in high inclined and horizontal wellbores, it is stated by Azar and Sanchez (1997) that extremely complex problems are related to the topic. Faults and key issues in research methodology needs to be solved before finding a universal model for cuttings transport. The main issues in cuttings transport can be listed as following:

1. The models are comprehensive and required a lot of input data as well as variations from condition to condition. A Mechanistic model fits this criterion well, but an empirical-statistic method may be preferred. In addition, these two approaches may still not be enough to handle both the bed erosion from the axial flow as well as including the rotation of drill pipe in annuli. Appropriate theoretical analyses, experimental studies, statistic modelling and well developed research facilities are needed to get an accurate model of such a case.

2. The models developed get an “approved” or “not-approved” stamp by the industry. It needs a certain level of accuracy to be approved, and if it gets a “not-approved” the industry has a tendency to throw them away instead further research to find their real potential. A possible solution to the problem is for the industry to work more closely with academia.
3. The last main problem is the lack of understanding of cuttings transport and the need to make many assumptions or neglect an observation. An example is the lack of a method for calculating Herschel Bulkley-parametres (viscosity, flow regime etc.).

Addressing these issued would lead to a fuller understanding of the hole cleaning issues and development of better cutting transport models (Azar and Sanchez, 1997). A mechanistic cuttings model will in greater detail describe the erosion- and rotation effect on hole cleaning efficiencies in Chapter 5.

3 THEORY

This chapter presents the basic principles of rheology and characterisation of typical properties of different drilling fluids. We will also give a brief introduction to the terminology needed to understand the work done in this thesis.

3.1 BASIC PRINCIPLES

Rheology is defined as the science of a fluids deformation and their ability to flow (Skjeggstad, 1989). Rheology is of great importance for different industries on the basis of painting, cosmetics and food. Relevant for this thesis, the science of rheology is of importance when examining drilling fluids. In drilling technology, rheology also is important for produced fluids, cement fluids, completion- and workover-fluids (Schlumberger, 2016). In this subchapter we present further explanation to how colloidal particles can act together and create viscosity to a fluid.

For analysing a fluids ability to flow, two basic terms are central in rheology; *shear stress* and *shear rate*. For a fluid to flow, a force field parallel to the direction of the flow is needed, whether this is a differential pressure over the pipe or gravitational force. Shear stress is defined as the force in the flow direction (F) over the area between the liquid layers (A_l).

$$\tau = \frac{F}{A_l} \quad (2.1)$$

The laminar flow lines in Figure 1 can be thought of as layers with varying velocity profiles. In laminar flow regimes, velocity profiles in circular pipes have their maximum in the centre of the pipe and minimum against the pipe wall. The difference between two of these layer's velocities divided on the distance between them is referred to as the fluids shear rate (Caenn et al., 2011) as illustrated in Figure 1:

$$\dot{\gamma} = \frac{dv}{dr} \quad (2.2)$$

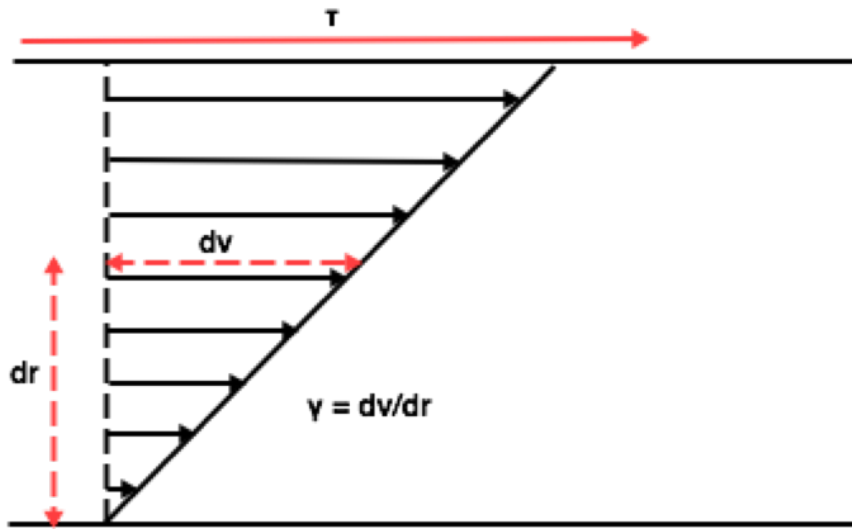


Figure 1 Shear stress and shear rate acting on a fluid (this author)

When analysing a drilling fluid it is common to plot these two properties, hence shear rate and shear stress, against each other in a flow curve. Their relationship can give a clear indication of the viscous properties of the fluid. Figure 2 indicates how flow-curves can illustrate what viscosity behaviour the fluid will have with increasing shear rates.

Curve (1) illustrates a Newtonian fluid with a linear relationship between shear stress and rate, which means that the viscosity is constant at every shear rate. Curve (2) illustrates the Bingham plastic curve. Curve (3) has an increasing slope for increased shear rates and therefore a higher viscosity at higher shear rates compared to low shear rates (shear-thinning). Slope (4) shows a shear-thickening fluid, where viscosity is increasing with higher shear rates (Caenn et al., 2011).

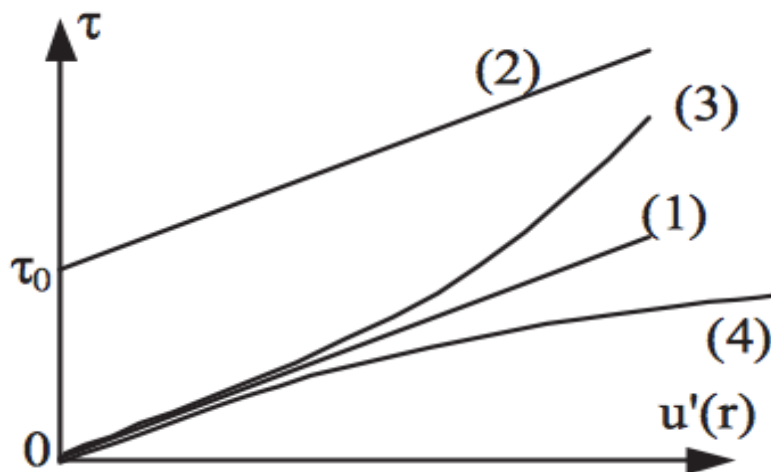


Figure 2 Different flow curves; (1) Newtonian fluid, (2) Bingham plastic fluid, (3) Shear-thickening fluid and (4) Shear-thinning fluid (Caenn et al., 2011)

3.2 RHEOLOGY MODELS

As explained in the previous subchapter, the properties of a drilling fluid is commonly analysed through a flow curve. Mathematically we are interested in finding a curve fitting that in a best possible way can overlap our experimental data from the laboratory. For different types of fluids we use different types of rheological modelling.

Newtonian fluid models are the simplest to analyse mathematically, as Newtonian fluids do not change their viscosity at constant pressure- and temperature conditions, with varying shear rates. Graphically this refers to the green, straight line in Figure 3 with a constant slope between shear rate and shear stress. In practical terms, Newtonian fluids are fluids that do not contain particles larger than molecules, such as water, oil and glycerine (Skjeggstad, 1989). In Newtonian fluid models, the slope of the curve is the fluid's viscosity given in the following form:

$$\mu_{eff} = \frac{\tau}{\dot{\gamma}} \quad (2.3)$$

A Bingham plastic fluid is similar to the Newtonian as its inclination is constant. A Bingham model's slope represents the fluid's plastic viscosity. At $\dot{\gamma}=0$, the Bingham-model in Figure 3 introduces a new term in rheology called the yield stress (τ_0). Yield stress is what separates the Bingham Plastic rheology model from the Newtonian model, where Newtonian fluids flows immediately, Bingham plastic needs a yield stress to set the fluid in motion. Fluids similar to drilling fluids will have a closer approximation through Bingham plastic compared to Newtonian, as yield point is a typical feature for fluids containing particles of a larger scale than molecules (Skjeggstad, 1989). Bingham plastic is expressed by equation (2.4):

$$\tau = \tau_0 + K \cdot \dot{\gamma} \quad (2.4)$$

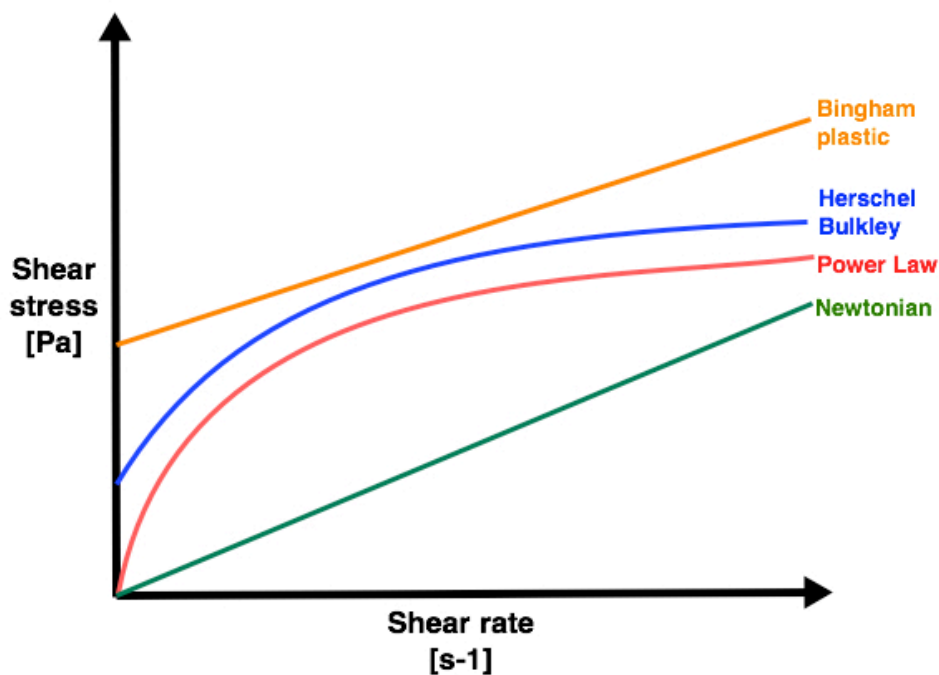


Figure 3 Common rheology models applied on different drilling fluids (this author)

The Power Law model deviates from the two previous as it has a non-linear trend shown in red in Figure 3, and describes shear thinning or shear thickening drilling fluids (Omosebi and Adenuga, 2012). The shear rate is exalted in an exponential constant (n),

which predicts the increase of the shear stress with the corresponding rate. The relationship between shear rate and shear stress is therefore exhibited as a straight line when plotted in a log-log graph. Power Law fluids remain with the same viscosity when left to rest, and therefore do not include a yield point or develop gel strength over time. Power Law is usually a good fit when measuring polymeric suspensions at low shear rates (Schlumberger, 2016). The Power Law equation is given on the form:

$$\tau = K \cdot \dot{\gamma}^n \quad (2.5)$$

The flow behaviour index's value (n) classifies the Power Law fluid if they are Newtonian, dilatant or pseudo-plastic. For Newtonian fluids, n=1, for dilatant fluids (shear thickening), n>1, and for pseudo-plastic fluids (shear thinning), n<1 (Omozebi and Adenuga, 2012).

Herschel Bulkley is often chosen as the best fit for drilling fluids (Werner et al., 2016b) and is a combination of Bingham plastic and Power Law; as its model has included Bingham plastic's yield point and the exponential relationship of the Power Law model. The relationship is given by equation (2.6):

$$\tau = \tau_0 + K \cdot \dot{\gamma}^n \quad (2.6)$$

Similar to the Power Law fluid model, Herschel Bulkley will also show a straight line when plotted in a log-log plot. From the log-log plot an yield point can be estimated for experimental data that has a best fit with Herschel Bulkley, where $\dot{\gamma} = 1$ by reading off the graph. From that point, subtracting the yield point and rearranging the equation (2.7) let you find the consistency factor (K) and flow behaviour index (n) by exponential curve fitting (Kosberg, 2016).

3.3 FLOW REGIMES

Flow can be divided into four regimes; plug-, laminar-, turbulent- and transitional flows. When studying drilling fluids, the three last mentioned are the most featured and relevant flow regimes. Reynolds number is applied to separate the flow regimes apart, and often sets a limit around $N_{Re} = 2300$, for a sharp transition between laminar and turbulent flow. Reynolds number in an annular space is calculated by equation (2.7):

$$N_{Re} = \frac{\rho \cdot v_{avg} \cdot (d_o - d_i)}{\mu_{eff}} \quad (2.7)$$

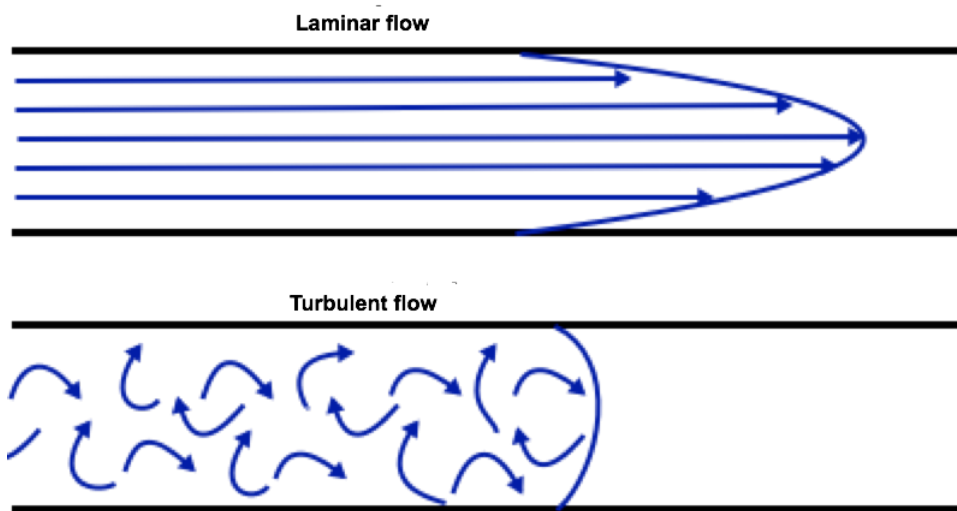


Figure 4 Laminar vs. turbulent flow regimes (this author)

Laminar- and turbulent flow regimes are illustrated in Figure 4. Laminar flow regimes often occur at $N_{Re} < 2300$, and is therefore associated with low velocities. A deck of cards can illustrate laminar flow where a force is applied on the top card in the direction parallel to the table. Because of friction the bottom card will lay still, while the cards in the middle will follow the top cards motion in different degrees. For a flow in a pipe, the fluid lines in the centre of the pipe will experience the highest velocity field, while it will be close to zero against the pipe wall (Caenn et al., 2011).

Turbulent flow regimes normally occur at $N_{Re} > 2300$, and is therefore associated with higher velocities. Random and local fluctuations characterize turbulent flow, where the maximum average velocity is in the middle axis and the lowest at the pipe's wall (Caenn et al., 2011).

In transitional flow regimes, small outbreaks of periodical turbulent fluctuations will occur as the Reynolds number increased towards the boundary of turbulent flow. This creates a breakdown of the laminar flow lines (White, 2016), illustrated by Figure 5.

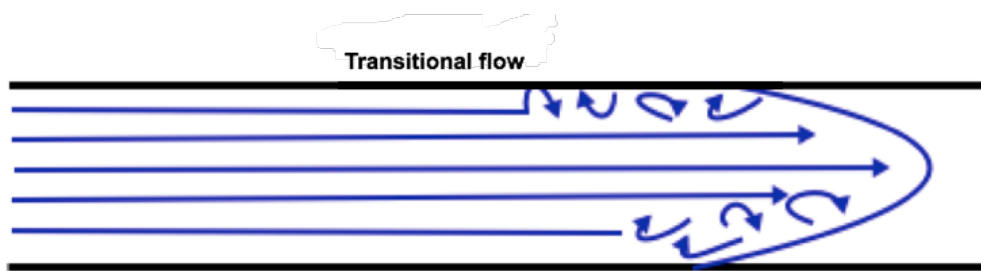


Figure 5 Transitional flow regime (this author)

In addition to accounting for the flow regime in the axial direction, flow regime radially around the drill pipe should be considered when studying fluid mechanisms in the annular space. During most of the drilling-related operations, the drill pipe will rotate inside in annuli, creating a velocity field perpendicular on the axial flow.

The flow regime around a rotating drill pipe can be defined by Taylor's number (Ta) from equation (2.8) (White, 2016):

$$Ta = \frac{r_i \cdot (r_o - r_i)^3 \cdot \Omega_i^2}{v_{avg}^2} \quad (2.8)$$

Taylor's number is derived for Newtonian fluids and does not take into account the shear thickening or shear thinning trend of a drilling fluid with a the occurrence of a yield point. In addition, Taylor's number does not take into account flow and flow regime in the axial direction of the annuli.

3.4 FACTORS AFFECTING HOLE CLEANING

This subsection will summarize the factors that have a significant influence on hole cleaning efficiency in the wellbore. It will provide the reader with basic knowledge of influencing operational parameters related to Chapter 5, where we will outline a mechanistic cuttings transport model.

Slip velocity

Slip velocity works as a result of the gravity force acting upon cuttings suspended in the drilling fluid. The velocity field is working in both axial and radial directions along the wellbore with the velocity-vectors defined by equation (2.9) and (2.10) (Okrajni and Azar, 1986):

$$v_{sa} = v_{slip} \cdot \cos \alpha \quad (2.9)$$

$$v_{sr} = v_{slip} \cdot \sin \alpha \quad (2.10)$$

where α is the inclination measured from a vertical point of view. As $\alpha = 0^\circ$ in vertical wellbores, axial slip velocity is the velocity in the gravitational direction ($v_{slip} = v_{sa}$). For horizontal wellbores where $\alpha = 90^\circ$, the slip velocity is only working in the radial direction ($v_{slip} = v_{sr}$). The travelling distance for the cuttings to form a sand bed against the wellbore wall is shorter for increasing inclination, which can be seen in Figure 6. In example, for the same particle size in the same fluid system, a sand bed will form more quickly in inclined sections when circulation stops.

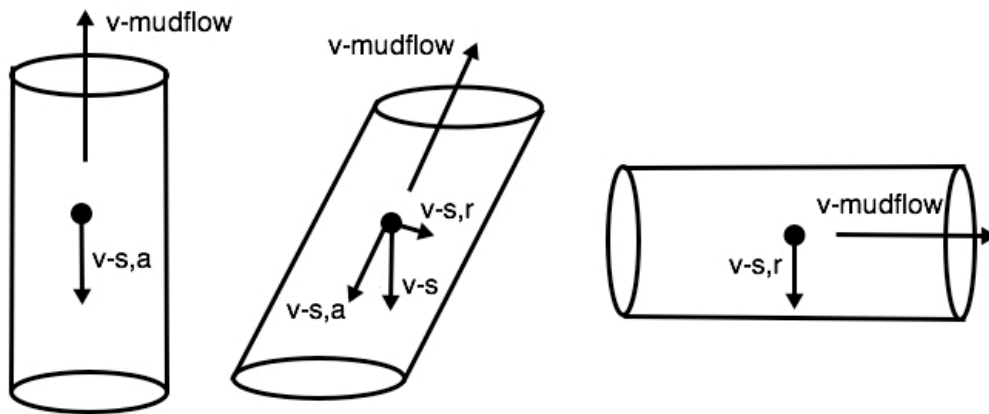


Figure 6 Slip velocity in vertical, inclined and horizontal wellbores (this author)

Annular Mud Velocity

To avoid cuttings settling in the bottom of the vertical section in a well, mudflow in the opposite direction with a higher velocity than the slip velocity will prevent occurrence of cuttings bed build-up. As can be seen in Figure 6, a higher inclination will decrease the axial component of slip velocity from maxima at vertical sections to zero at horizontal sections (see equation (2.9)). Even though the radial slip velocity is working perpendicular on the mud velocity, flow rate in annuli is of greater importance in high inclination- and horizontal wellbores. This is a result of the shorter travelling distance for a cuttings particle to the wall at higher inclinations compared to vertical wellbores (Okrajni and Azar, 1986).

Despite the fact that highest possible mud velocity is beneficial for hole cleaning, the mud flow rate is usually limited by several factors. The ECD (Equivalent Circulating Density) needs to stay within the pore pressure-, collapse- and fracture pressure gradients. ECD is mainly dependent on the borehole's depth and the drilling fluids velocity (friction pressure loss) and density. The mud velocity may also be limited by the influence of erosion against the open hole and formation.

Flow Regime

Flow regime in annuli has a great influence on hole cleaning efficiency. Independent of the cuttings size and shape, turbulent flow by the mud flowing in annulus will induce

turbulent flow of the particle's slip regime. In turbulent flow regimes, the momentum force of the mud is the only factor to decide the particle's slip velocity (Okrajni and Azar, 1986).

In laminar flow regimes, the particle's slip regime can either be turbulent or laminar, dependent on the particle's shape and size. It is however, expected that laminar flow will provide better transportation of cuttings compared to turbulent flow, and at the same time has a lower slip velocity. However, with increasing inclinations the axial slip velocity of a cuttings particle ceased and it can be expected that the advantages of having a laminar flow regime is not applicable (Okrajni and Azar, 1986).

Drill Pipe Rotation

Drill pipe rotation adds a lot of complexity into the matter of hole cleaning efficiency. A cuttings bed is often consolidated in contact with mud gelling properties. In seldom occasions pipe rotation can remove parts of the consolidated bed from the pipe wall before the mudflow will disperse the cuttings particles. In this way pipe rotation can increase hole-cleaning efficiency (Saasen and Løklingholm, 1998).

Another aspect of rotation of the drill pipe is that analytical, experimental and numerical results show that for laminar flow, the eccentricity and rotational movement increases axial friction drop (Ooms and Kampman-Reinhartz, 2000). As previously mentioned, a high frictional pressure loss was listed by Saasen (1998) as the main contributor to hole cleaning and is therefore a beneficial effect of rotation.

Mud Properties

A drilling fluid is designed for the specific area of drilling will reduce the risk of serious incidents related to poor hole cleaning. In Sifferman and Becker (1992) it is stated that drilling fluid density has a major effect on hole cleaning efficiency, whereas drilling fluid rheology is listed as a moderate contributing factor.

For improved rheological properties of drilling fluids in context with hole cleaning problems, the drilling fluid should be designed to meet a definite pressure loss rate in annulus as well as avoiding only basing its efficiency on the viscosity parameters

(Saasen, 1998). As the drilling fluid's gel formation in the cuttings bed is the primary source of problems regarding hole cleaning, hole cleaning would be optimized by the usage of low gel strength-muds and drilling fluids with low shear strength in the expected shear rates.

To prevent barite sag, high molecular weight polymer could be used, even though only short polymers should be used to create viscosity and avoid strong gel structure in the bed. Only a low degree of shear thinning trend would contribute to better hole cleaning efficiency (Saasen and Løklingholm, 2002).

A drilling fluid's rheological properties also have an effect on the mudflows velocity profile. The n -flow behaviour index defines the sharpness of the velocity front, where a lower value for n gives a flatter profile. In practical terms this reduces the cross sectional area where it is possible for faster settling of particles (Okrajni and Azar, 1986).

Choosing oil-based drilling fluids over water-based fluids have an advantage in hole cleaning efficiency from field experience (Werner et al., 2016a) without this being fully understood. Oil-based drilling fluids have better effect of sliding for the cuttings along the wellbore as a contributing factor to hole cleaning (Sifferman and Becker, 1992).

Geometry of the Drill Pipe in Annuli

A factor affecting the velocity profile during hole cleaning in annuli is eccentricity. As can be seen in Figure 7, mud flow through the tight areas around the pipes have a significant lower velocity profile compared to the spacious, as the flow always will choose the simplest way.

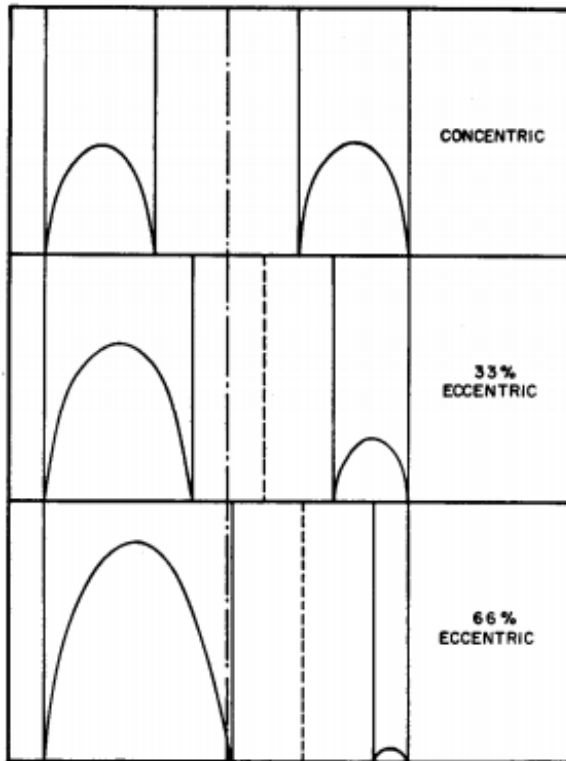


Figure 7 The affect of eccentricity on the velocity profile in annuli (Tomren, 1979)

Eccentricity of drill pipe in annuli affects the bed height of accumulated cuttings largely. With increasing height of cuttings bed, the interfacial area decreases as the height reaches the drill pipe's surface. To maintain a higher interfacial friction between the cuttings and mud, an increase in mud velocity is needed. As eccentricity normally increases with increasing inclination, higher mud velocities are needed for horizontal wells. The effect of eccentricity is only of importance when the drill pipe touches the cuttings bed (Gavignet and Sobey, 1989).

As we have illustrated previously in Figure 6, inclination has a dominant effect on hole cleaning. As the inclination increases, the force field parallel to the borehole wall will decrease. The friction force from the fluid against the bed must overcome the force from the sliding of bed along the wall in inclined sections. A bed formation is not probable when drilling a vertical well, as the travel distance from a cuttings particle is longer than for inclined wells, and if the cuttings particle would fall to the bottom, it will only return to the crushing bit on the bottom. In horizontal wells, there is no existence of a force causing backwards sliding for the bed, and the bed will continue growing until a critical

velocity is reached to erode the same volume that continues to build the bed (Gavignet and Sobey, 1989).

The size of drill pipe in annuli affects the flow rate needed to reach the critical velocity for transporting cuttings away from the cuttings bed. As the area for flow is increased by choosing a smaller drill pipe diameter, a higher flow rate is needed for efficient cuttings transport (Gavignet and Sobey, 1989).

Rate of Penetration (ROP)

It is important in drilling operations to remain a concentration of cuttings flow rate to mud flow rate lower than 5%. The ROP in itself is not important in hole cleaning efficiency as long as the mudflow rate can follow the pace (Gavignet and Sobey, 1989). Drilling with a high ROP can have beneficial advantages as lower casing wear and higher cost efficiency.

As it is estimated that the interfacial stress to be overcome between the particles in the bed is strongly dependent on the particle size, particle size is important in hole cleaning. Less drag force is needed to transport larger particles, as the drag on larger particles is greater. Therefore a higher mud velocity is needed to put the bed in motion for smaller particles (Gavignet and Sobey, 1989).

4 EXPERIMENTAL FLUID CHARACTERIZATION

Throughout a joint industry project by *SINTEF* with their clients, a full-scale flow-loop was utilized to study hole-cleaning efficiency. Field data show that oil-based drilling fluids perform better than water-based drilling fluids in terms of hole-cleaning efficiency. The industry project is a part of a larger study of hole cleaning in inclined annuli with different types of drilling fluids. In this specific project, oil-based WARP designed by *M.I. Swaco – A Schlumberger Company* was used to transport sand particles in annuli. Rheological data from experimental measurements in the lab will be seen in context with operational data from *SINTEF* to see the fuller picture of its function compared to other fluid types.

An Emulsion Stability-meter was used to monitor emulsion stability in the fluid during the full-scale experiments. For rheological purposes, a Fann 35-viscometer was used as the standardized tool for viscosity control over the flow-loop. Even though the Fann 35-viscometer has been used for decades, it has limited accuracy in the low-shear regions. To optimize the measurements, the Anton Paar-rheometer is used for adding more measuring points with higher accuracy, to be compared to the Fann 35-readings.

The first sub-chapter will provide information about the flow-loop designed and built by *SINTEF* as a part of the joint industry project. As the original start-up date for circulation experiments in the flow-loop was postponed, most of the work done in this thesis was prior to the experiments in context with building and testing the flow-loop. The second subchapter will provide information about the tested WARP-fluid circulated through the loop. Further, the same sub-chapter will demonstrate the published work done on evaluating the procedures in rheology measurements on a Laptonite WBM, as well as new work evaluating the procedure for OBM WARP. Problems and challenges met in context with the measurements will be presented in *Measurement Challenges*.

4.1 FLOW-LOOP SET-UP

As mentioned in the introduction of this chapter, the majority of laboratory time spent on this thesis was in contribution to building *SINTEF's* full-scale flow-loop illustrated by Figure 8. The flow loop will simulate cuttings transport in a horizontal and inclined borehole with different rotational speeds of an inner freely rotating drill pipe and variations of axial velocities of mudflow.

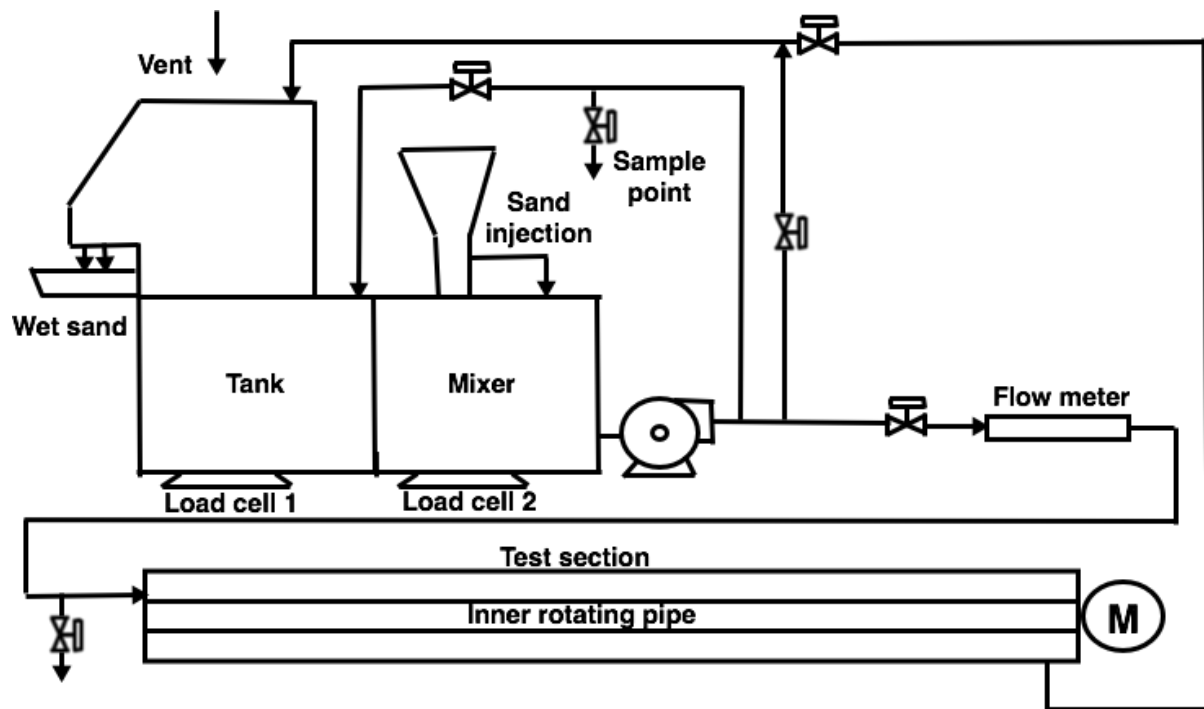


Figure 8 Full-scale flow-loop (this author)

The flow-loop was put together of several important components that give the ability to measure the weight of the cuttings bed developed in the test section. Experimental data in Chapter 5 is conducted from a similar flow-loop, with some small changes. The flow goes through the flow-loop in the following order:

1. The mudflow from the tank is mixed in the mixer with sand from the sand injection unit. Sand flows from the sand container down in the mixer through a screw pump. The sand injection unit can be seen in Figure 9.

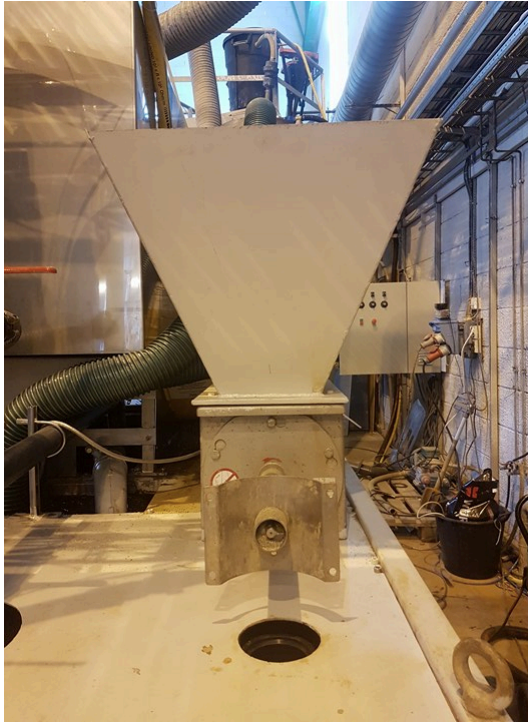


Figure 9 Sand injection unit

2. The total weight of the tank unit with the drilling fluid and sand is measured on *Load cells*. This is to have control of the sand content left in the test section as cuttings bed, after circulating through the loop.
3. The drilling fluid is pumped with a centrifugal pump through a flow meter for control of the velocity through the test section, with an option to send the fluid back as an anti-surge. From this pipe branching it is possible to take fluid samples from a drain. It is also possible to by-pass the flow-loop and send the fluid directly to the meshed filter for filtrating out wet sand.
4. From the flow meter, the fluid is sent through a hose and past a drain, designed for emptying the test section. The fluid fills the annulus and surrounds the inner rotating pipe, driven by a motor on the section's end, shown in Figure 10.



Figure 10 Test section with rotating drill string-motor

5. The drilling fluid flows back to the sand filtration unit shown in Figure 11, consisting of a meshed cloth, which carries the wet sand towards the deposition tray while the drilling fluid falls back into the tank. The sand is not re-injected.



Figure 11 Sand filtration unit with mud tank and mixer

- The loading cells will give an estimate of the amount of sand lost to the test section, by measuring the weight before sands are injected into the fluid and subtract this from the weight after bed forms inside the test section at a constant velocity. The weight of sand missing, is the weight of the cuttings bed with some other influencing effects discussed in *4.4 Measurement Challenges*.

In previous years, experiments have been conducted in the same flow loop with some small changes. The most important difference this year is that the annulus is now put together by an outer, static pipe of steel in some of the experiments, with an inner rotating steel-pipe. In previous years the outer annuli has been made up of concrete with a steel drill pipe.

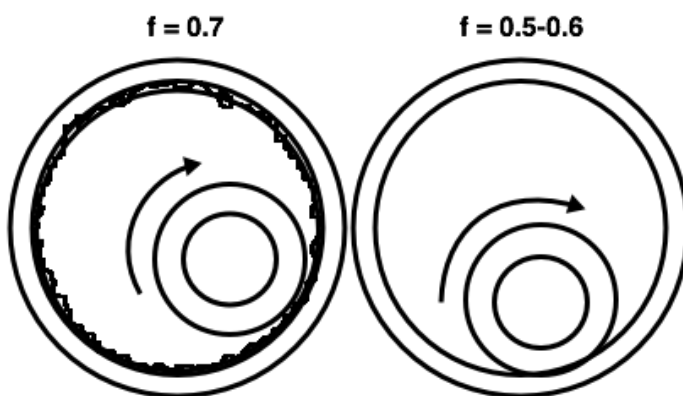


Figure 12 Friction coefficients for steel on concrete (left) vs steel on steel (right) (this author)

As can be seen in Figure 12, the friction for steel on concrete is higher than for steel on steel because of the coarser surface of concrete, approximately 0.7 vs 0.5-0.6 (Fischer and Kloiber, 2006). Because of this, a hypothesis is that the pipe will climb higher from the cuttings bed in the concrete wall compared to the steel wall. Steel against steel will have a lower resistance for sliding back down to the bottom. When the drill pipe is lifted from the cuttings bed, the pipe will experience less friction and rotate more freely.

4.2 TESTED FLUIDS

Conventional weighted drilling fluids can increase non-productive time (NPT) and create environmental and cost-effective challenges when drilling through a narrow mud-weight window down hole. The main challenge is maintaining low enough rheological properties to respect the ECD allowed for the section, and high enough for sufficient hole cleaning and at the same time avoiding barite sag.

Two fluids were tested in Fann 35 and Anton Paar during the period of this master thesis. Firstly, this master thesis was written in cooperation with *SINTEF* with the aim to obtain fluid control of oil-based WARP utilized in the flow-loop described in the previous sub-chapter. Secondly, the author of this thesis joined another project where the aim was to investigate several Laptonite-drilling fluids to test the procedure regarding aging and preconditioning of the fluids in Werner et al. (2017).

OBM WARP

The tested fluid in the flow loop was an oil-based mud (OBM) from *M-I Swaco's WARP Advanced fluids technology*. The fluid is relatively thin, as the field that it is designed for will need high flow rates and rotation to clean its long reservoir sections.

Firstly, OBM WARP is designed for avoiding Barite sag, both in static and dynamic situations. Secondly, it is supposed to lower the Equivalent Circulating Pressure (ECD), swag- and surge-pressure. When the mud returns to surface, the fine material will pass through three shale shakers more easily compared to conventional weighting agents (M.I-Swaco, 2011).

The WARP fluid technology is based on grinding weight material to extremely fine particles (0.1 to 10 microns). A high concentration of fine particles in the fluid will usually increase the rheology, but the OBM WARP is treated to avoid this effect. The weighting particles are one tenth of the size of conventional Barite. In addition, the fluid has a low yield point, low-shear viscosity and reduces friction in cased and open-hole. The exact composition of the fluid cannot be mentioned due to confidentiality the within company (M.I-Swaco, 2011).

WBM Laptonite

Prior to this hole cleaning project, procedure performance was evaluated for preconditioning and aging effect on a fluid's rheology by Werner et al. (2017). Five different Laptonite fluids were tested with different degrees of salinity. Laptonite is a synthetic clay built up of disc-like flakes, with the chemical composition $Na_{0.7}^{+}[(Si_8Mg_{5.5}Li_{0.3})O_{20}(OH)_4]_{0.7}^{-}$. Laptonite clays have a negative surface charge as a result of substitution of magnesium (Mg) by lithium (Li) (Werner et al., 2017).

The fluids were mixed by hydrating the Laptonite clay particles in water suspension prior to adding xanthan gum for viscosity and gel, Sodium Chloride (NaCl) for different concentrations of salt, Sodium hydroxide (NaOH) for base, and biocide, an additive that kills bacteria used in water-based drilling fluids containing starch or gum that is vulnerable to bacteria attack (Schlumberger, 2017).

In Table 1 we have listed the different fluid compositions of the Laptonite fluids (Werner et al., 2017). The fluids contained a) 0 g, b) 0.6 g and c) 12 g salt (NaCl) to see the effect of salt in the procedure evaluation.

Table 1 Fluid composition of the Laptonite fluids utilized in the published work of Werner et al. (2017)

Component	1		2		
	a	b	a	b	c
Water	Deionized water				
Laptonite RD [wt%]	1,50	1,50	1,50	1,50	1,50
Xanthan gum [wt%]	0,00	0,00	0,10	0,10	0,10
NaCl [g/l]	0,00	0,60	0,00	0,60	12,00
NaOH [mmol/l]	0,10	0,10	0,10	0,10	0,10
Biocide	0,00	0,00	0,10	0,10	0,10
pH value	10,07	10,31	10,51	10,21	9,31
Conductivity [mS]	0,58	1,53	0,55	1,38	17,70

4.3 RHEOLOGICAL CHARACTERIZATION

Rheological profiles and gel strength measurements were obtained by testing the fluid in the Fann 35-viscometer and the Anton Paar-rheometer. This sub-chapter will firstly present the characterization tools in greater detail, and secondly, present the results provided by these.

Fann 35-viscometer

Fann 35-viscometer is a direct-indicating viscometer illustrated in Figure 13. It is widely used in the oil- and gas industry and for research in the laboratory. The instrument is used to measure viscosity and gel strength of a fluid, and can perform rheological characterization on both Newtonian and non-Newtonian drilling fluids.

The Fann 35-viscometer consists of a gearbox and motor, rotating cylinder and bob with a torsion spring to give shear stress measurements from the bob. The apparatus also includes a thermo-cup to hold 350 ml of mud sample, which is the measuring volume defined by API specifications, as well as a thermometer to heat up the sample to a chosen temperature (Fann, 2016).

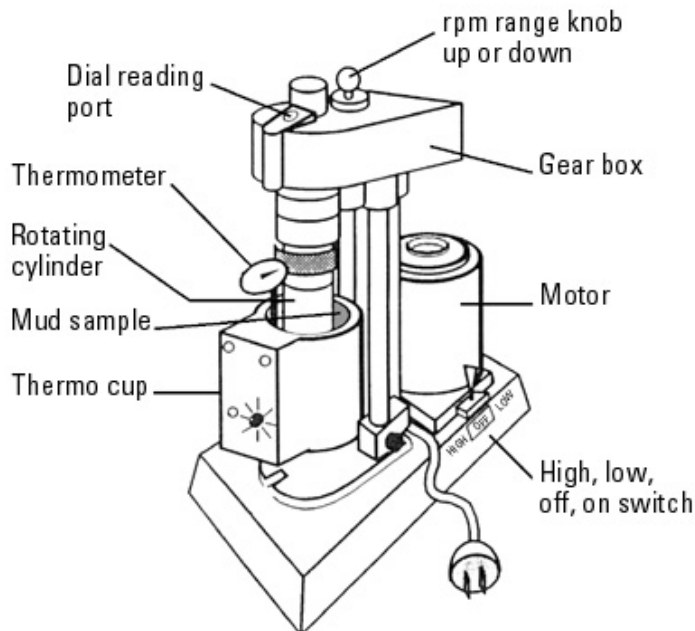


Figure 13 Fann 35-viscometer (Fann, 2016)

The *rpm range knob* chooses between high rpm (600 and 300 rpm), medium rpm (200 and 100 rpm) and low rpm (6 and 3 rpm). The *high/low/on/off-knob* chooses thereafter if the measurement should be the higher or lower value of rpm chosen by the *rpm range knob* (Fann, 2016). From API procedure the shear stress measurements for obtaining a flow curve starts at 600 rpm and is ramping down in the following order: 600-300-200-100-6-3 rpm. For obtaining a more reproducible result, the sample will be pre-stirred at 600 rpm (or 1022 s^{-1}) for 10 minutes (Werner et al., 2017).

Gel strength measurements are obtained by pre-stirring the sample at 600-rpm before the fluid rested for 10 seconds/10 minutes after flow curve measurements, and run the viscometer at 3 rpm after the wait. The dial reading read off from the display represents the gel strength of the fluid.

Anton Paar-rheometer

The Modular Compact Rheometer (MCR) in Figure 14 is a rheometer widely used in research within several industries. The measurements from Anton Paar are more comprehensive compared to Fann 35 and is therefore not as commonly used in the field. The apparatus is driven by an EC motor and is equipped with a temperature control and accessories fitted to the different measurement that the MCR can be used for (Anton-Paar, 2011).



Figure 14 Anton Paar Modular Compact Rheometer (MCR) (Anton Anton-Paar, 2011)

The Anton Paar MCR has an air intake for air bearing and water supply for cooling. Anton Paar also consists of a rotating bob to measure shear stress and a cup to contain mud, with a mark to show the level needed for the test. Small deviations in fluid level (5-6 mm) were tested by Assembayev and Skalle (2015) and did not seem to have an effect on the measurements. In this study we try to keep the fluid levels as similar as possible and fill the cup to the marked line, so that the bob will be completely immersed in the fluid, as shown in Figure 15.

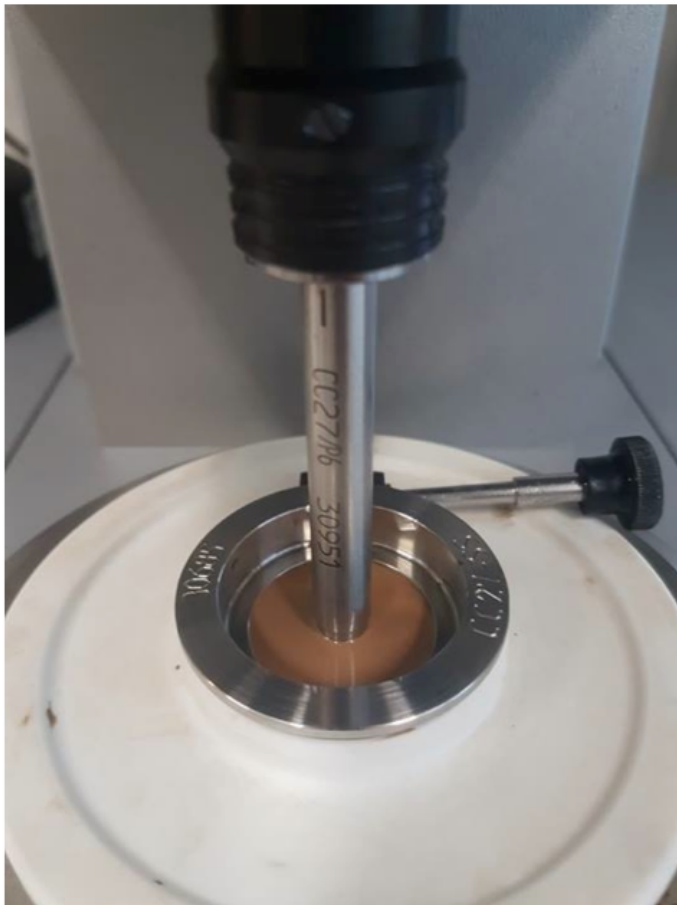


Figure 15 Anton Paar bob fully immersed in mud (Kosberg, 2016)

Anton Paar is a digital rheometer, which can be partly run from the menu-display seen in Figure 14, but is mainly run from a computer. In the *Rheoplus*-software it is possible to pre-set the shear rate testing plan, time duration for each measuring point and number of points. In all experiments obtained from Anton Paar in this thesis, the shear rates will ramp down from 1022 s^{-1} to 1 s^{-1} in 240 seconds, whereas a measured shear stress will be logged every 2 seconds with 120 measuring points. In similarity to Fann

35, 10 minutes pre-stirring will be applied to the fluid before running the test, as recommended by Werner et al. (2017).

Density and emulsion stability testing

The density of the fluid was normally 1.46 SG and was measured with a pycnometer for high accuracy. Measurements were taken two times a week. For measuring the electrical stability and thereby also the emulsion stability, we used an OFITE Emulsion Stability Tester (shown in Figure 16). Electric stability in volts was tested every day during Fann 35-measurements, excluding weekends.



Figure 16 OFITE Emulsion Stability Tester (OFI Testing Equipment, 2014)

Rheology control in tanks and flow-loop

The main objective for cooperating with *SINTEF* on their flow-loop project was to ensure fluid control of OBM WARP before and during the hole cleaning experiments. A test matrix was set-up for each week with experiments as listed in Table 2.

As can be seen in Table 2, full fluid-check was conducted twice a week, while the other weekdays simple Fann and Emulsion Stability-testing was conducted at both

temperatures (25°C and 50°C). After testing, the fluids were sent to *M.I. Swaco's* office in Stavanger for more advanced testing.

Table 2 Test schedule for flow-loop experiments

Test:	Mondays	Tuesdays	Wednesdays	Thursdays	Fridays
Fann 35	X	X	X	X	X
Anton Paar	X	-	-	X	-
Emulsion Stability	X	X	X	X	X
Pycnometer	X	-	-	X	-

Figure 17 shows rheology profiles in IBC-tank 1 and 2, measured in Fann prior to entering the flow-loop tank, compared to the tests in Anton Paar and Fann for the first flow-loop experiment. One sample was measured from both top and bottom of the tank to ensure similarity and exclude gravity-segregation effects after stirring. The values in Figure 17 are the average of the bottom and top in IBC-tanks in Fann, while the measurements from the first flow-loop experiment are two individual tests in Fann and Anton Paar. The two tanks show approximately the same fluid properties after mixing the tanks with a pressurized airflow, prior to sending the fluid to the flow-loop tank.

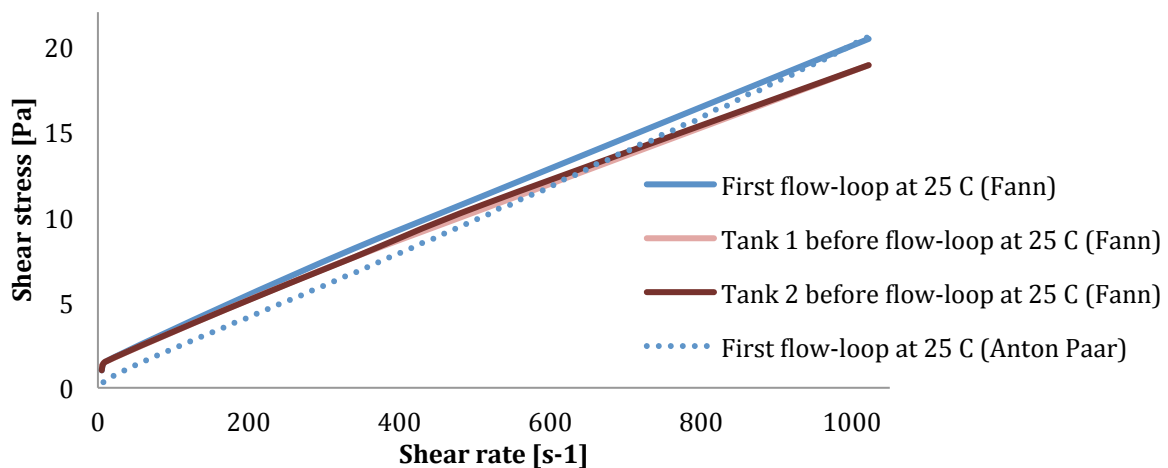


Figure 17 Rheology profile in IBC-tank 1 and 2 (Fann 35) and the first measurement from flow-loop experiments (Fann 35 & AP)

In the first flow-loop measurement at 25°C, the rheology was measured to be slightly higher than the tank measurements, especially at the higher shear rates. Anton Paar also

gave higher shear stress for the higher shear rates, but was significantly lower compared to all of the tests from Fann 35. This can be a result of more accurate testing points at lower shear rates compared to Fann 35, or simply because Fann 35 seems to overestimate the low shear-values. The increased deviation from Anton Paar can also be an effect of gelling with time towards lower shear rates under the measurements sequence in Fann 35. Anton Paar measurements also start in the high shear-area, but do not show this effect. It might as well be a geometric difference causing this deviation between Fann and Anton Paar.

As can be seen in Table 3, the first flow-loop experiment also had a lower density compared to the two tanks, but the low difference in density might be a result of measurement uncertainties and have to be seen in comparison to the total of flow-loop data.

Table 3 Average density measurements of top and bottom of OBM WARP in IBC tanks, and an individual measurement from the first flow-loop experiment

Average density measurements of OBM WARP (g/cm^3)		
Tank 1	Tank 2	First flow-loop experiment
1,468	1,467	1,462

Figure 18 shows flow curves obtained over the first week of measurements of OBM WARP at 50°C in Anton Paar and Fann 35. It is clear that Fann 35 deviates from Anton Paar in higher shear rates, where Fann 35 shows lower shear stress. In Figure 17 Fann 35 gives higher shear stress in the low shear area (3 & 6 rpm especially). Some inaccuracies may be from calibration and dial reading in Fann, as we switched to a new apparatus in between the measurements in Figure 17 and Figure 18.

A literature study shows that in general, Fann 35 is inaccurate at high shear measurements. The operator should always account for 6.78% error and multiply the shear stress from high shear rate-measurements with 1.0678. An error of 6.78% is not accounted for as a part of the API-standards, when giving the output in the unit $lb/100ft^2$ (M.I.Swaco, 2017).

Anton Paar gave unsteady measurement in a waveform around 600 s^{-1} at 50°C (Figure 18) and 500 s^{-1} for 25°C (see Appendix A) in rheology control-measurements from the flow-loop. This may be an effect of turbulence in the couette flow in the high-shear area.

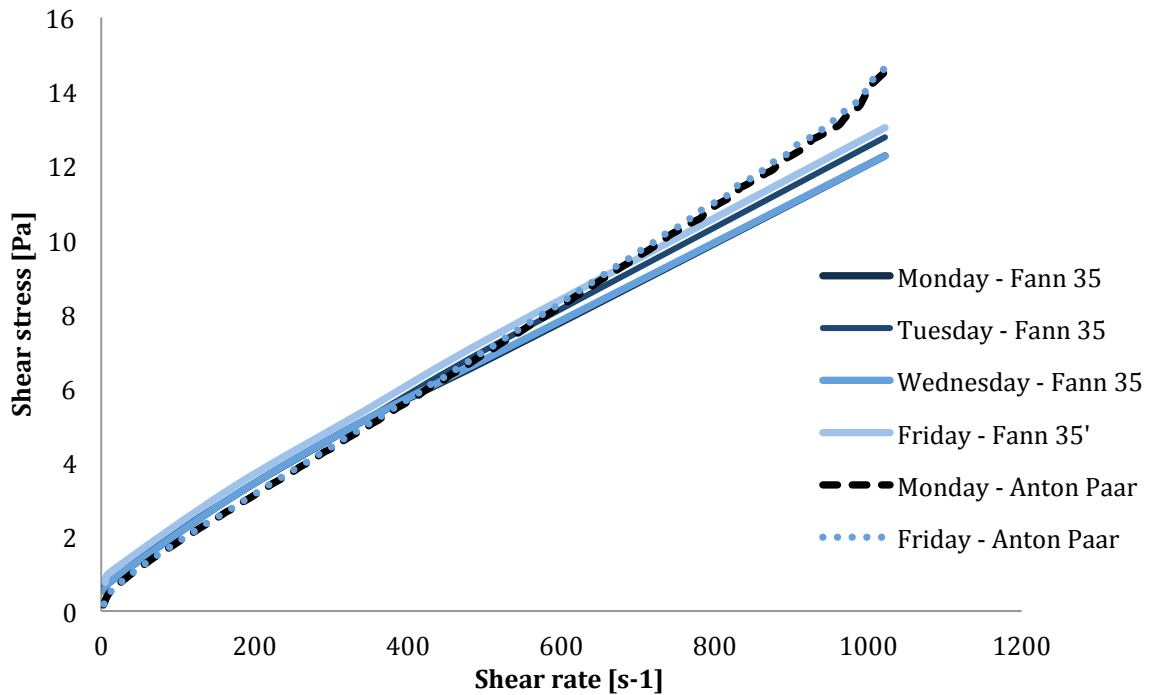


Figure 18 Flow curves from individual measurements in Fann 35 and Anton Paar of OBM WARP at 50°C from week 1 in the flow-loop

Reynolds number calculated for the flow-loop, show that we can expect turbulence at higher flow rates in the flow-loop. This is supported by pressure gradients versus velocity plotted in Figure 19 for three experiments in the flow-loop without rotation and sand injection. Included in the plot is also the modelled pressure gradients from a Herschel Bulkley-model by SINTEF (2017), based on the rheological parameters measured in Figure 18 by the author of this thesis. As can be seen by a rapid increase in pressure gradient in Figure 19, turbulence kicks off around 0.9 m/s in the model, and around 07 m/s for the experiments. In reality we will experience a transitional flow regime in between laminar and turbulent flow, and the experiments will therefore show a more gradual increase in pressure gradient. The velocities where turbulent occurs corresponds to a shear rate around $110\text{-}150 \text{ s}^{-1}$ for a Newtonian fluid, and turbulence in the high shear area in Anton Paar is therefore not unlikely.

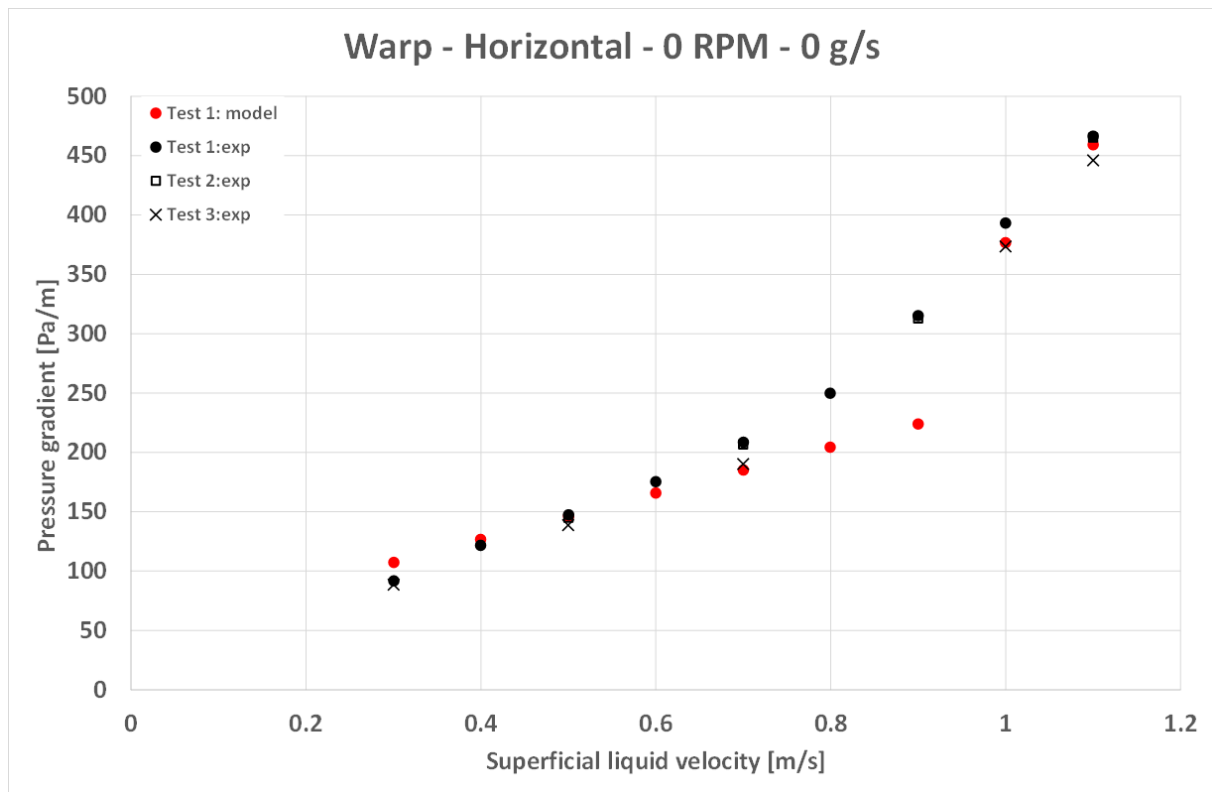


Figure 19 Pressure gradients for three experiments without sand injection and rotation, vs. superficial velocity (SINTEF, 2017)

The Taylor number according to equation (2.8) was well above the critical Taylor number for where Taylor-vortices occur ($Ta_c \approx 1708$). Comparatively one can also see that the OBM WARP has a more shear thinning trend when tested in Fann compared to Anton Paar, both in Figure 17 and Figure 18.

Procedure evaluation of measuring OBM WARP

The procedure utilized for Fann 35 for measuring the OBM WARP is listed in Appendix C. Pre-shearing the sample in a *Hamilton Beach* drink mixer for 15 minutes at 6000 rpm was done before obtaining the rheological profile of the fluid. A fluid sample was examined with two different approaches of pre-shearing to see the effect of cooling between mixing periods, which may be needed if the mixer heats up the fluid sample:

1. The fluid was pre-sheared for 15 minutes straight

2. The fluid was pre-sheared for 5 minutes in three intervals following a 5 minute rest period, with the last rest-period right before flow curve measurements

It was expected to show an effect of gelling, but the results were similar for the two samples (see Appendix A) and no difference between the two procedures could therefore be found.

When testing each sample, after being mixed for 15 minutes in *Hamilton Beach*, the sample was stirred for 10 minutes at 600 rpm in Fann 35 before taking measurements. 10 minutes pre-stirring was set for the sample to stabilize and reach the testing temperature (50°C), as API-standards do not describe pre-treatment of the drilling fluids prior to measurement. Especially oil-based drilling fluids have a tendency to not initially give stable values (Werner, 2017). Two time intervals for pre-stirring was measured:

1. 10 minutes pre-stirring at 1022 s^{-1} (600 rpm) in Fann 35
2. 8.5 minutes pre-stirring at 1022 s^{-1} (600 rpm) in Fann 35, which was the time for the sample to heat up to 50°C

No difference between the two tests was found with the small change in pre-stirring time (see Appendix A). It follows that this exact fluid sample does not need 10 minutes of pre-stirring to be stable. Even though the duration may be unnecessary long, it was decided to run all the tests with 10 minutes pre-stirring at 600 rpm, for less uncertainty in measuring technique.

The change in procedure was only tested on OBM WARP prior to starting the flow-loop, meaning that other fluids, and especially those thicker than the respective fluid, may act differently. A thicker fluid will typically need longer duration to stabilize in comparison.

Procedure evaluation on aging and preconditioning of WBM Laptonite and OBM WARP fluids

The scope of the work with the water-based Laptonite-fluids was to recommend guidelines in how to pre-treat a fluid prior to standard ISO-measuring the rheological properties. For measuring a fluid's viscosity and rheological properties, the ISO 10416 and ISO10414-1/2 standards are the common practise of procedure. However, the ISO-practises do not specify the common start point for which pre-treatment the fluids should be exposed to. This is quite important as some fluids are thixotropic and build gel over time while at rest, while others are the opposite and develop gel or increased viscosity with stirring-time (Werner et al., 2017). The data utilized for analysing rheological data is measured by the author and provided by Werner et al. (2017)

The different compositions of Laptonite fluids listed in Table 1 were tested in Fann 35 and Anton Paar to compare their rheological flow curves. The fluid samples were pre-sheared in a Waring blender at low speed for two minutes to obtain the same starting values for the fluid samples. The four procedures in Figure 20 were tested in Anton Paar and Fann 35 (Werner et al., 2017):

1. Pre-shearing in Waring-blender, then fluid rests for 0h prior to measuring flow curve with pre-stirring in viscometer/rheometer for 10 minutes at $1022s^{-1}$ (0h w/ pre-shear)
2. Pre-shearing in Waring-blender, then fluid rests for 0h prior to measuring flow curve without pre-stirring in viscometer/rheometer (0h wo/ pre-shear)
3. Pre-shearing in Waring-blender, then fluid rests for 24h prior to measuring flow curve with pre-stirring in viscometer/rheometer for 10 minutes at $1022s^{-1}$ (24h w/ pre-shear)
4. Pre-shearing in Waring-blender, then fluid rests for 24h prior to measuring flow curve without pre-stirring in viscometer/rheometer (24h wo/pre-shear)

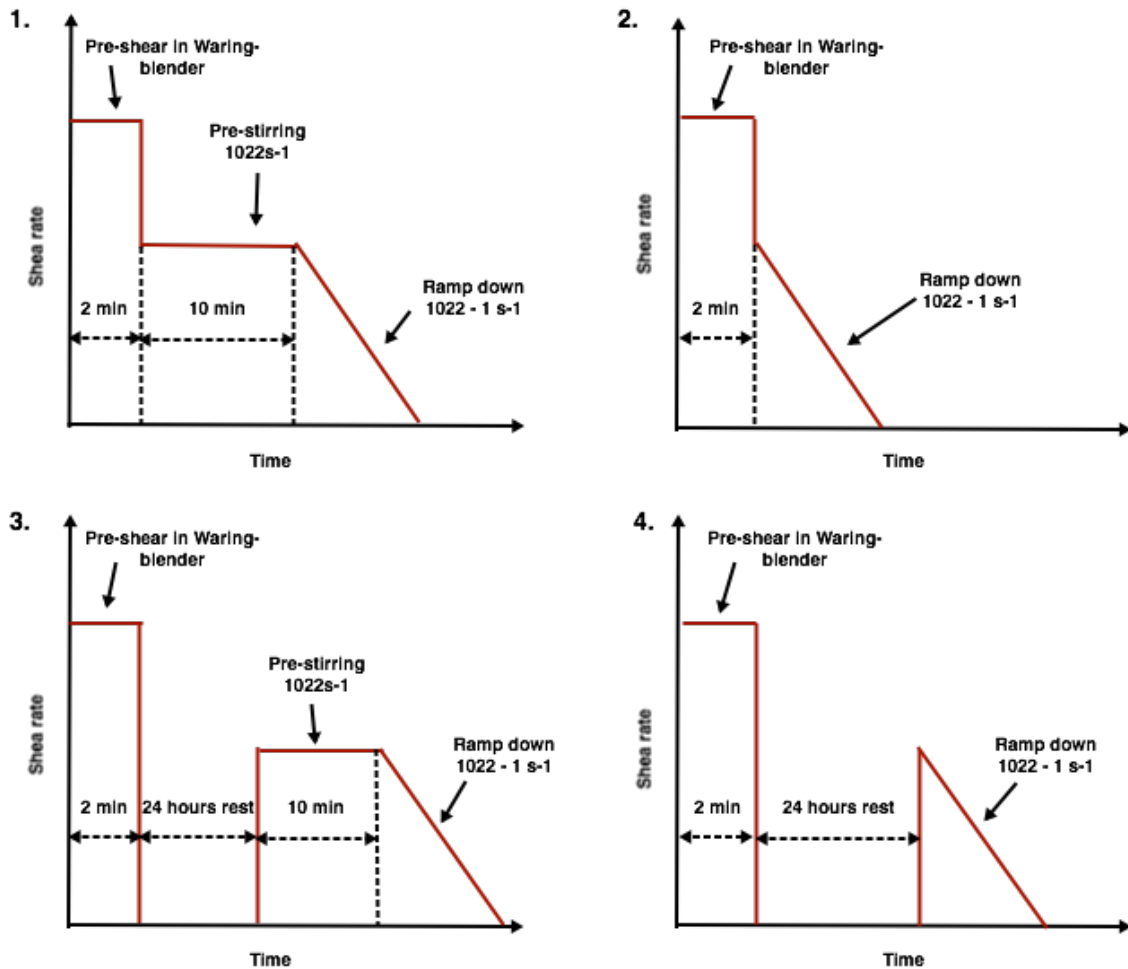


Figure 20 The four different combinations of procedure for pre-stirring in Fann 35 and Anton Paar

The tests without pre-stirring went directly to ramping down from a shear rate of 1022s^{-1} to the lowest possible for both the apparatus (5.11 s^{-1} in Fann 35 and 1 s^{-1} in Anton Paar) after the desired waiting time. Fluid 1 A & B were tested at both 24 and 50°C , while the other fluids (2 A, B & C) were tested at 24°C .

The measurements in Fann 35 showed that all samples that were pre-stirred had more reproducible results. As can be seen in Figure 21 and Figure 22, fluid 1 A and B both have the not-stirred sample with rest-time 24h as the one that deviates the most from the samples without resting time, especially at high shear rates. The two samples measured at 0h are quite similar for both procedures, and out of the two samples measured after 24h rest; the pre-stirred sample is most similar to those with 0h rest.

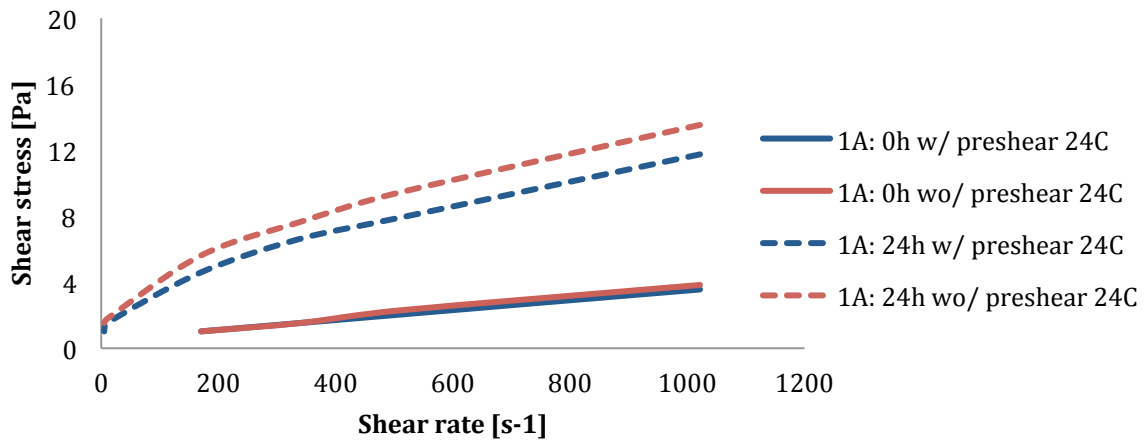


Figure 21 Rheology profile of fluid 1A at 24 C (Werner et al., 2017)

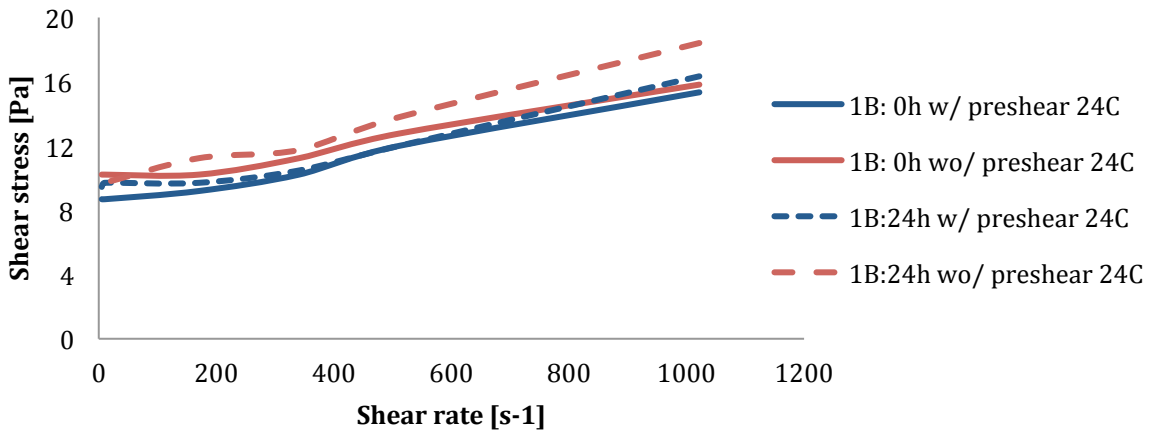


Figure 22 Rheology profile of fluid 1B at 24 C (Werner et al., 2017)

Figure 23, Figure 24 and Figure 25 show the rheology profile of three different salt-concentrations of the fluid 2, hence 0 g (2A), 0.6 g (2B) and 12 g (2C). From the three plots it can be seen that salt concentration has an impact on reproducibility in fluid 2, with high effect of adding relatively low concentrations of salt (0.6 g in 2B).

Comparing the two pre-stirred samples in Figure 23, Figure 24 and Figure 25, the samples with salt are significantly more alike. All of the Figures 21-25 show that 10 minutes pre-stirring cannot erase the fluid history with resting time, but has a significant effect on Laptonite fluids with relatively low salt concentrations. The effect is rather less for fluids with no salt (Werner et al., 2017).

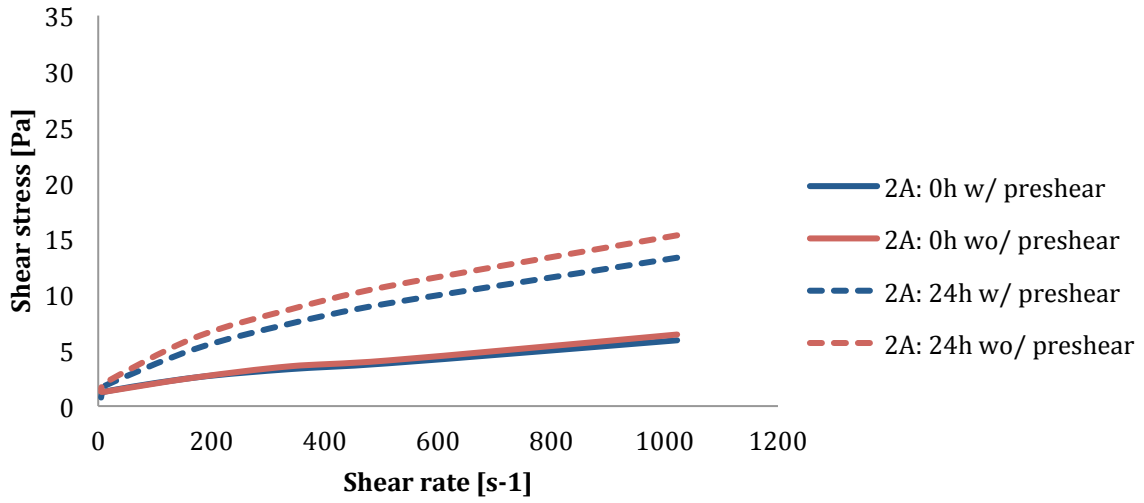


Figure 23 Rheology profile of fluid 2A (Werner et al., 2017)

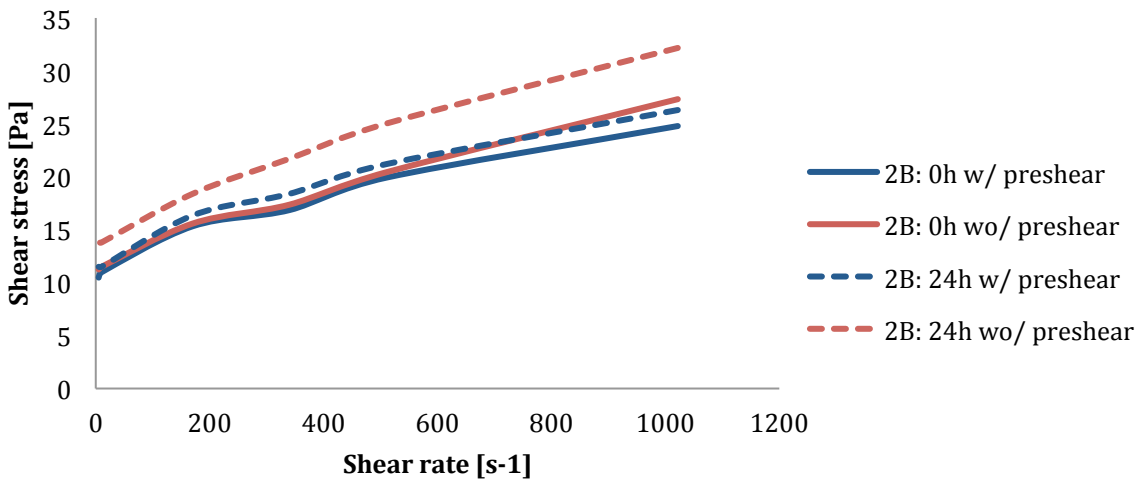


Figure 24 Rheology profile of fluid 2B (Werner et al., 2017)

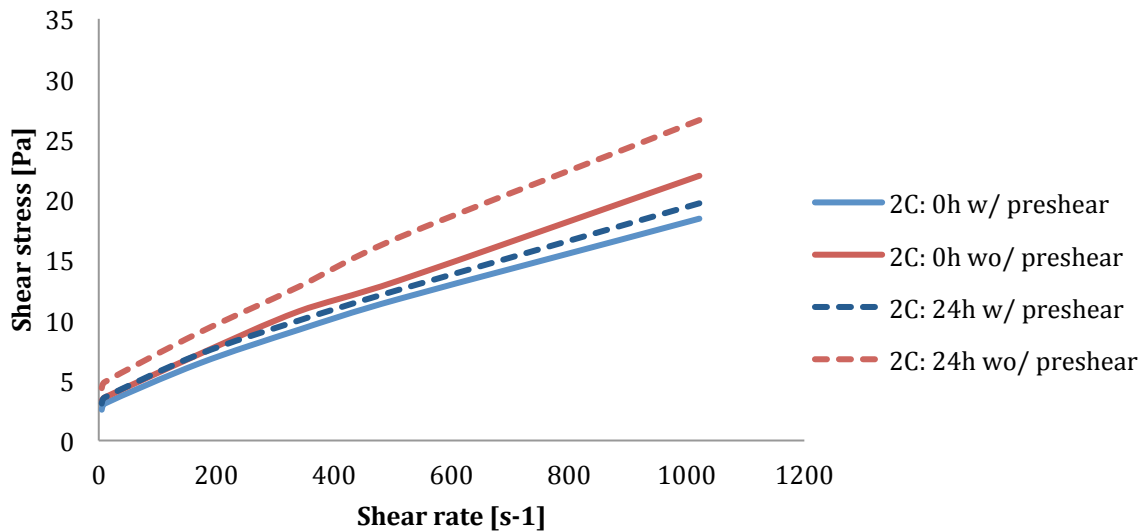


Figure 25 Rheology profile of fluid 2C (Werner et al., 2017)

In Anton Paar the significance of pre-stirring the fluid had an even clearer impact on 1B with 0.6 g salt, especially for the higher shear rates at 24°C in Figure 26. The pre-stirred samples are considered similar after 0h and 24h, while the two samples that are not pre-stirred has significant high slope at the start of measurement (high shear). This can be the breakdown of gel-structure in the fluid, which stabilizes more with time. For medium shear, the slope becomes more similar to the pre-stirred samples, while they hold a higher shear stress in general for all shear rates.

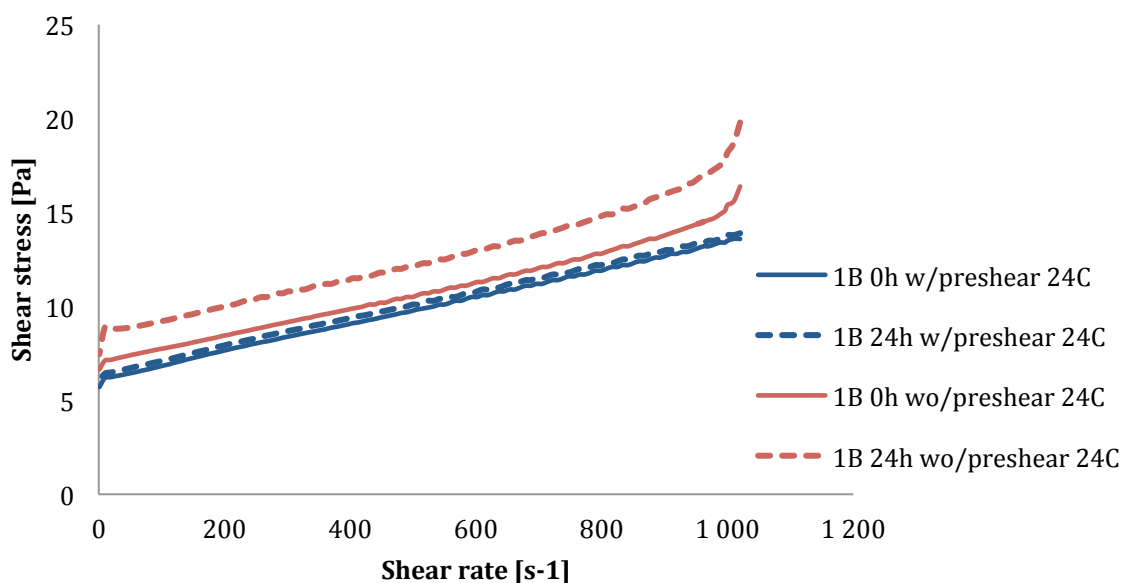


Figure 26 Anton Paar measurements with and without pre-stirring of 1B at 24°C (Werner et al., 2017)

To compare how different fluids will respond to a new procedure including pre-stirring for 10 minutes in Fann 35 and Anton Paar, the same experiment was conducted on OBM WARP from *M.I. Swaco – A Schlumberger Company*.

Figure 27 shows the flow curves obtained in Anton Paar with and without pre-stirring for 10 minutes, with 0h and 24h resting-time after pre-shearing the fluid in a Waring-blender. The pre-stirred samples and the sample without pre-stirring in Anton Paar and 0h rest-time, all have approximately the same rheology-profiles. The sample with 24h rest-time without pre-stirring in Anton Paar deviates from the other samples with lower shear stress per shear rate, especially at higher shear rates.

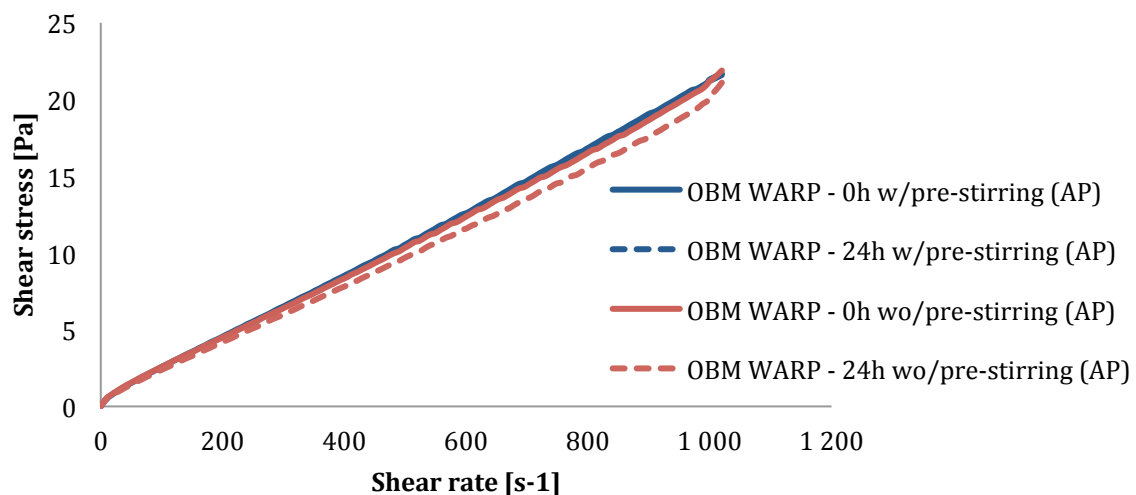


Figure 27 Effect of pre-stirring of OBM WARP in Anton Paar at 25°C

In Figure 28 the same measurements are shown for the Fann 35-viscometer. Pre-stirred samples with 24h rest had in general higher shear stress compared to the sample without rest (0h). For samples without pre-stirring, 24h rest-time had the opposite effect and had in general lower shear stress than measurements with 0h rest-time.

Compared to the measurements obtained in Anton Paar, Fann 35 validates that the sample without pre-stirring and a rest-time of 24h has the lowest measurements of shear stress versus shear rate. This is the opposite of the Laptonite fluids, which seemed to be influenced by gel structure at high shear rates.

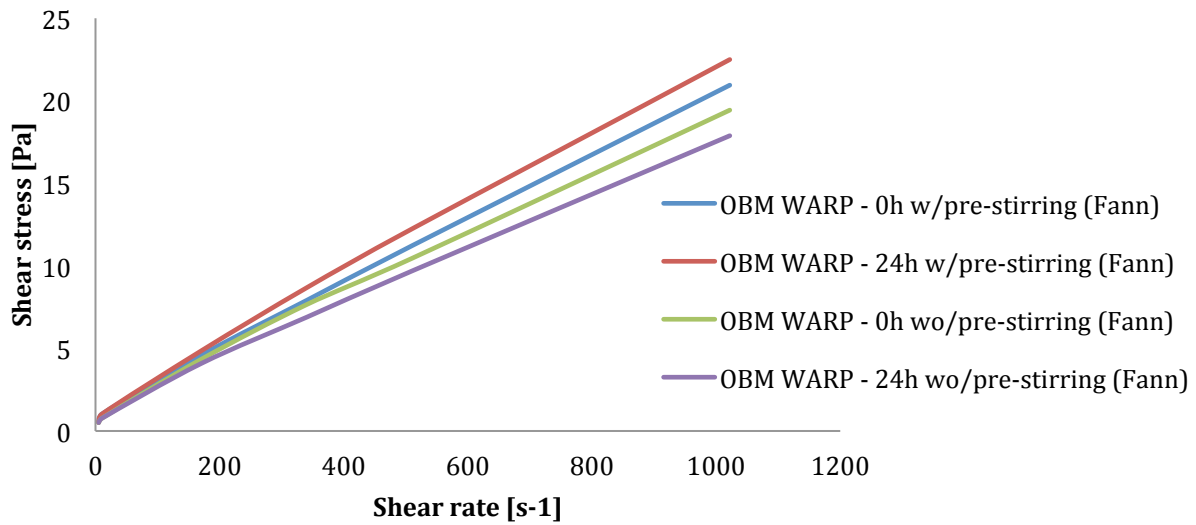


Figure 28 Effect of pre-stirring of OBM WARP in Fann 35 at 25°C

In general the measurements in Fann 35 deviated from the Anton Paar measurements, except OBM WARP – 0h w/pre-stirring. Several experiments should be conducted when testing a fluid in the Fann 35-viscometer to find an average value with less uncertainty, as the measure-points are based on individual experiments.

To check if the rheology deviations after 24h resting time influenced the hole cleaning data in the flow loop, pressure loss gradients in the test section was compared from several experiments.

The pressure loss gradients that are plotted in Figure 19 on page 37 show three similar experiments, ramping up the velocity with no sand injection and no rotation. The first test is where the fluid is exposed to the least pre-stirring, as it is the first circulation, while two and three has experienced more pre-stirring as a result of the previous experiments. The first experiment shows slightly higher pressure gradients compared to the second and third experiment. If the rheology-trends in Figure 27 and Figure 28 can imply that oil-based WARP will be thinner as a function of resting-time, we would expect the first experiment to have the lowest pressure gradient. In reality we see the opposite, where experiment 1 has either higher or similar pressure loss compared to experiment 2 and 3.

During the experiments it was observed that the temperature changed slightly, increasing from the beginning of experiment 1 until the end of experiment 3. Temperatures at the start and end of experiments are listed in Table 4:

Table 4 Tank temperatures at the start and end of hydraulic experiment 1-3 in the flow loop without rotation and sand injection

Experiment no:	Temperature start [°C]:	Temperature end [°C]:
#1	22.76	23.30
#2	23.83	24.30
#3	24.46	25.02

As rheological properties are highly dependent on temperature, an increasing temperature may cause lower viscosity of the fluid in the flow loop. This may again lower the pressure loss gradient and cause deviations between the experiments 1-3. The deviations in temperature make it difficult to conclude the cause for the results in Figure 27 and Figure 28.

The effect of pre-stirring seems to be significant both for Laptonite-fluids and OBM WARP. Immediately after pre-shearing the fluid in the HB-blender, it does not seem to play a difference with OBM WARP, while for Laptonite fluids, pre-stirring the fluid in Anton Paar and Fann should always be done to create more reproducible results. It is important to mention that pre-stirring the sample does not apply for studying their gel structure.

4.4 MEASUREMENT CHALLENGES

In this subchapter we will discuss the challenges met when characterizing the WARP OBM before and during flow-loop circulation, and how the challenges were dealt with.

Weighting error in flow loop

The tank unit in the flow-loop consists of a mixer, mud-tank, sand injection-unit, sand returns filter and a tray to collect the wet sand transported back with the mud. All these objects are weighted by the load cells, and with the all the sand in the sand injector unit, this weight is used as a reference point. Under experiments, sand is circulated with the

mud, and the new tank weight will be subtracted from the reference point. The weight difference will represent the mass of the sand cuttings bed.

As the cuttings bed height estimate is a function of the weight difference in the tank- and mixing unit, the weight of the tank unit should not be changed under the experiments by anything other than cuttings in and out of the tanks. As an example, one cannot touch or lean onto the tanks during experiments without influencing the results.

In previous years, *SINTEF* performed experiments without rotation and no sand injection, where the mud-velocity was ramped up from 0.5-0.7-0.9 to 1.1 m/s in the test section. At each step in velocity-increase, it was observed a decrease in tank-weight, measured by the load cells. As nothing was removed from the tank and the flow-rate was constant, this decrease in weight is believed caused by expansion of the hoses as a result of increasing pressure with increasing flow rates. It was requested by *SINTEF* to create a model that could estimate the decrease in weight caused by hose expansion with the following steps:

1. Characterize the oil-based WARP as a Bingham plastic fluid, illustrated by Figure 29, and find parameters n , K and μ_{pl} :

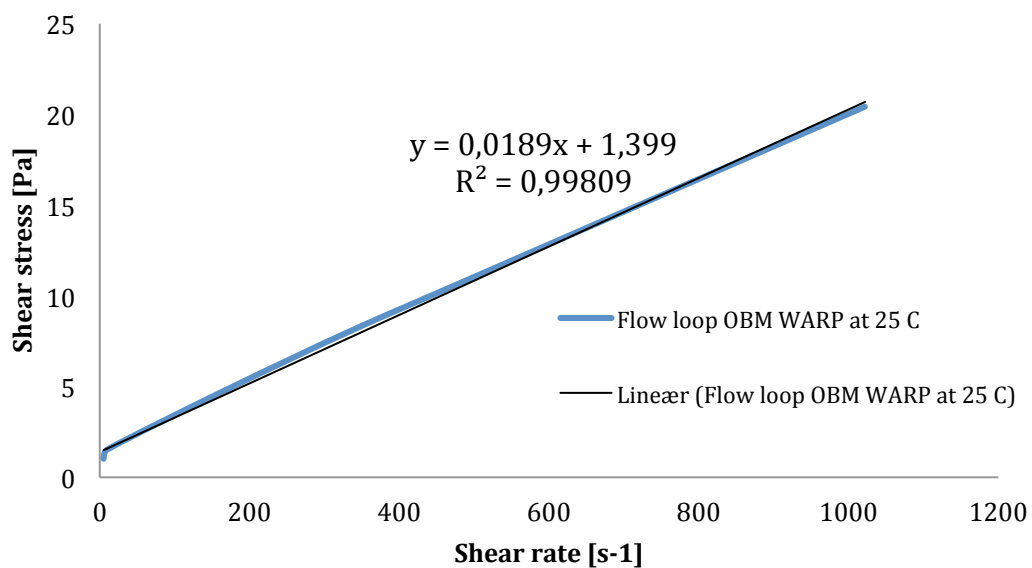


Figure 29 Flow curve of OBM WARP with linear curve fitting (Bingham plastic)

2. Calculate the Reynolds number (N_{Re}) and Bingham coefficient (K_p) by equation (4.1) and (4.2):

$$N_{Re} = \frac{d^n \cdot v_{avg}^{2-n} \cdot \rho}{K_p \cdot 8^{n-1}} \quad (4.1)$$

$$K_p = K \cdot \left(\frac{3n + 1}{4n} \right)^n \quad (4.2)$$

3. Measure the length of hoses from the pump to the test section with the rotating drill pipe, and the length from the test section back to the tank unit
4. Calculate the pressure drop for a Bingham plastic-fluid for different velocities by utilizing equation (4.3) for laminar flow and (4.4) for turbulent flow:

$$\Delta P_{hoses} = \frac{48\mu_{pl} \cdot L \cdot v_{avg}}{d_h^2} + \frac{6 \cdot L \cdot \tau_0}{d_o - d_i} \quad (4.3)$$

$$\Delta P_{hoses} = \frac{0.073 \cdot \rho_m^{0.8} \cdot v_{avg}^{1.8} \cdot \mu_{pl}^{0.2} \cdot L}{d_h^{1.2}} \quad (4.4)$$

5. Calculate the pressure drop over the test section by taking the average of the two DP-cells and multiply with the test sections length (L). Add the number to the pressure loss over the hoses to find the total pressure loss over the tank:

$$\Delta P = \frac{DP_1 + DP_2}{2} + \Delta P_{hoses} \quad (4.5)$$

This step has to be repeated for every velocity when the measurements have stabilized. Use the average value of ΔP for all stable values measurements at the same velocity.

6. Find ΔV from equation (4.6):

$$\Delta V = \Delta W / \rho_m \quad (4.6)$$

Where ΔV is the difference of volume in the tank at two different velocities. This could be found by taking the average weight from stable experimental data at one velocity and subtracting the average weight from the lower velocity (ΔW), and then multiply with the fluid density (ρ_m).

7. Plot ΔV versus ΔP and add a linear trend line to find k in the linear relationship (4.7):

$$\Delta V = k \cdot \Delta P \quad (4.7)$$

8. Use equation (4.7) to calculate ΔV , multiply with ρ_m and find the loss in weight from experimental data that is caused by expansion
9. Subtract this value from experimental data to find the total weight difference caused by cuttings

The idea was to use the stabilised average value of tank weight for each velocity step, plotted against the corresponding pressure drop. After plotting the data needed to find k it was observed that the average value might not be representative because of two reasons; weight in the tank was increasing, not decreasing, which is the opposite effect we would have from expansion, and measurement deviations from noise. The noise, which can be seen in Figure 30, seemed to be a result of pump vibrations caused by the unfit size of impeller.

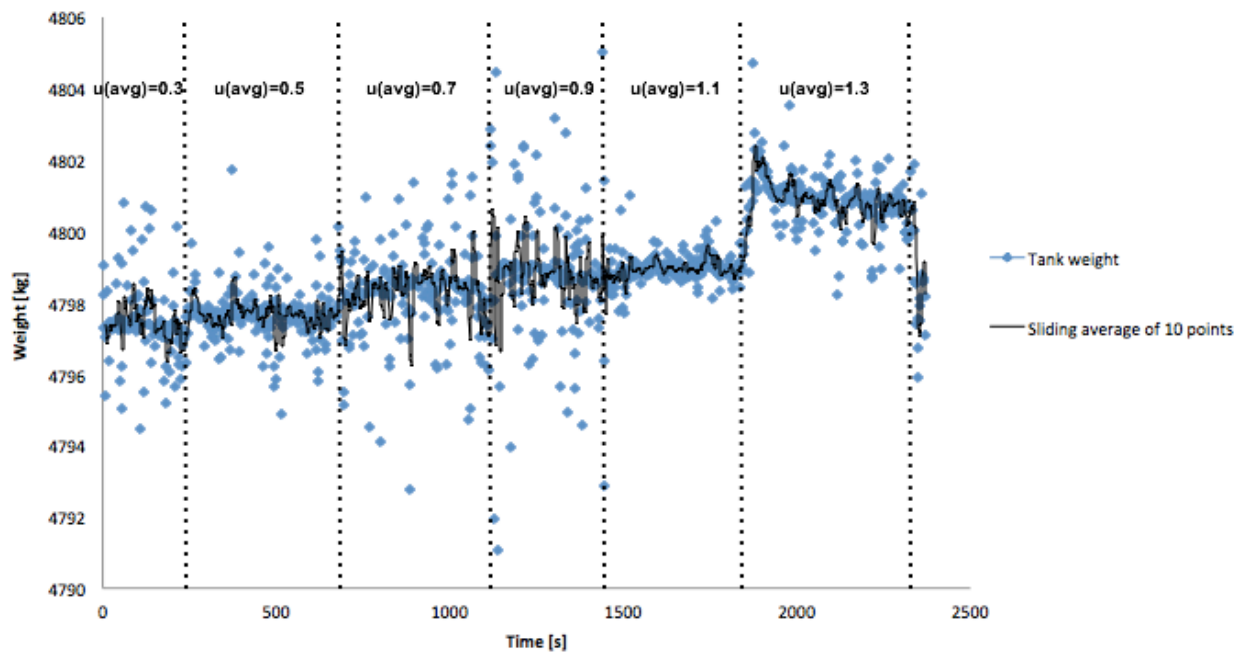


Figure 30 Tank weight measurement vs. time with noise from vibrating pump, with the velocity ramped up 0.3-0.5-0.7-0.9-1.1 to 1.3 (SINTEF, 2017)

The noise of data points was not successfully excluded from the measurements until after the hand-in time limit for this report. Average values of tank weight differences were therefore compared to the median tank weight difference for each velocity in Table 5:

Table 5 Average tank weight difference in average and median for each velocity-step, in three experiments without rotation and sand injection (SINTEF, 2017)

Velocity steps:	Weight difference average [kg]	Weight difference median [kg]
0,3-0,5	0,05	0,01
0,5-0,7	0,42	0,48
0,7-0,9	0,59	0,40
0,9-1,1	-0,19	-0,07
1,1-1,3	1,26	1,28

As the deviations are found in the intermediate velocities (0.7-0.9), calculated values that include measurements for these velocities deviate the most in median compared to the average value. It is therefore reasonable to believe the vibrations have a significant effect on tank weight results.

The calculated pressure drop from the velocity-increase in the hoses was added to the difference in pressure drop of the test section measured by the DP-cells under velocity increase. Further the change in pressure drop was plotted versus change in tank weight with increasing velocity in Figure 31:

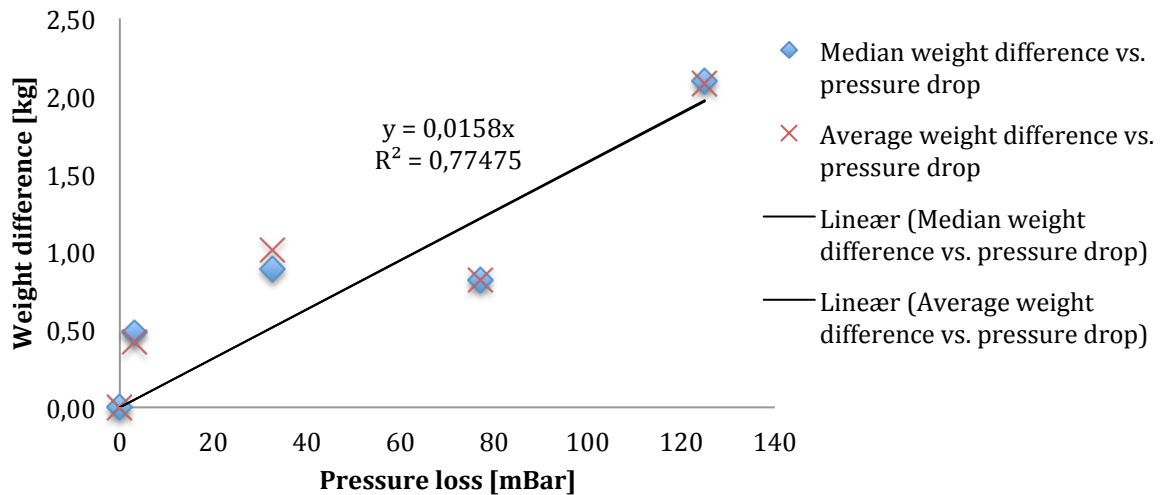


Figure 31 Average and median weight differences versus average pressure drop of three experiments, without rotation and sand-injection (SINTEF, 2017)

Even though the median and average values have similar linear curve-fittings, the vibration has a clear effect on the results. The k-value is estimated to be 0.0129, but the R-value suggests that it is not well representable for the plotted data. Comparably in Figure 30 we see an increase in weight per increased velocity, while in Figure 31 an increase in pressure drop (and therefore increase in velocity) gave lower weight-values for intermediate velocities compared to lower velocities. The data have to be cleaned by a statistical model prior to finding a suitable k-value to account for the expanding hoses.

Previous experiments show decrease in tank weight for increasing pressure drop, which gives reasons to believe that expansion of hoses has an impact on the measurements (SINTEF, 2017). As the tank weight in this case increases, it raises reasons to believe that another parameter is affecting the weighing data. Dynamic momentum of the fluid when it hits the tank in return, was suggested as an influencing parameter (SINTEF, 2017). At increasing pressures, an increased force down on the tank loading cells will be applied, by the return of drilling fluids.

In addition, the possible temperature effect shown in subchapter 4.3 should also be accounted for at the end of an experiment with increasing temperature, more expansion of the fluid and therefore decreasing rheology measurements.

Gravity segregation

Prior to circulating OBM WARP in the flow loop, there was raised suspicion of gravity segregation of the fluid, as it had been at rest for several weeks. It was discovered that a sample taken from the top of one of the tanks, seen in Figure 33, had a very light density (1.20 g/cm^3) compared to its design (1.46 g/cm^3). The solution was to stir the mud with pressurized air. The results before and after mixing are illustrated in Figure 32 where density-measurements prior to mixing are in red and after mixing in blue.

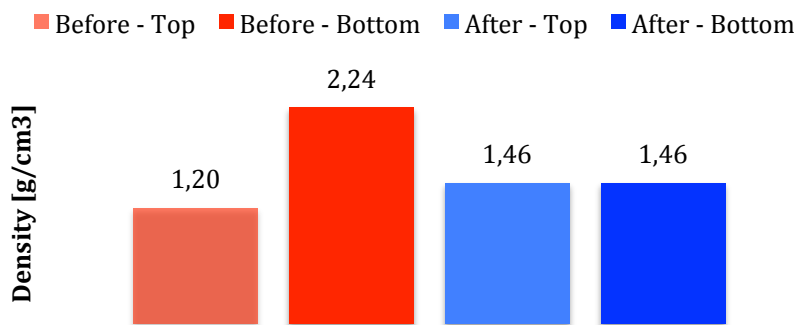


Figure 32 Density of OBM WARP measured at the top and at the bottom of an IBC-tank before and after agitation

The effects of gravity segregation can be seen as the heavier particles and fluid have clearly fallen to the bottom and created a density of 2.24 g/cm^3 . After agitation the fluid samples showed similar densities of 1.46 g/cm^3 . However, after agitation, a layer of particles was still suspended at the bottom. Continuous agitation is therefore recommended for best preserving the fluid with its original design and avoiding gravity segregation.



Figure 33 OBM WARP in the IBC-tank from *M.I. Swaco – A Schlumberger Company*

The density was relatively stable throughout the flow-loop experiments performed during this master thesis, as can be seen in Figure 34. An increase in fluid density is seen around 26.05.17. Few days later (30.05.17) we started experiments with sand particles. It is likely that sand particles are being crushed by the rotating drill pipe into smaller particles and passing through the small gaps in the filter-mesh. But it is difficult to say if the small increase of density is affected by crushed sand-particles, uncertainties during measurements in the pycnometer or fluid sampling (fluid sample not representative).

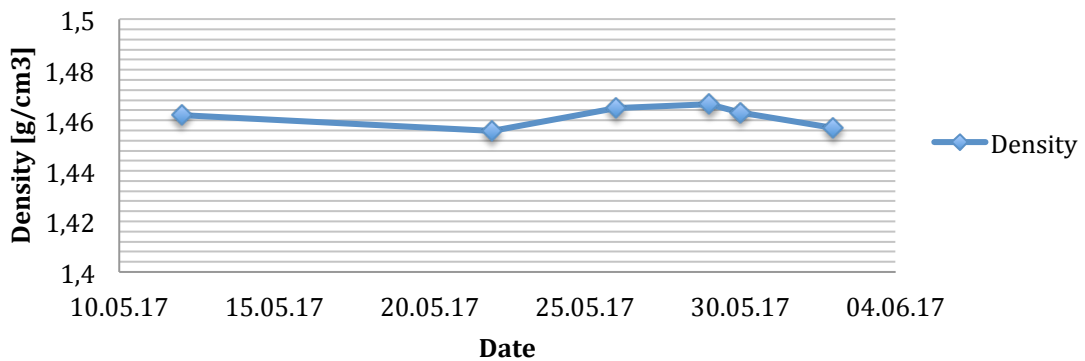


Figure 34 Density measurements of OBM WARP in flow-loop over time from 10.05.17 to 04.06.17

One of the main concerns in this project in particular was that the rheology of the fluid was uneven and therefore would influence the cuttings transport experiments. If so, the velocity- and rotation-effects could not be analysed without influence by other parameters. All in all, fluid-properties did not seem to be a disturbance for the results if temperature was kept constant.

5 ANALYSIS AND EVALUATION OF LABORATORY OBSERVATIONS

In chapter 5 we present a unique observation and results of cuttings bed height from experiments in the laboratory. Experiments were performed by *SINTEF* as a result of a joint industry project in examining hole cleaning. An interesting connection between cuttings bed height, drill pipe rotation and inclination of wellbore is found in the laboratory data. The objective is to try to understand the observed behaviour and then analyse and evaluate our hypothetical understanding.

5.1 OBSERVATIONS

In previous laboratory experiments (Sayindla et al., 2016), cuttings transport in inclined and horizontal sections were analysed from numerous circulations through a semi full-scale loop. The loop consisted of a pipeline composed of elements made of concrete to imitate an open hole in the field, with an inner, freely rotating drill pipe.

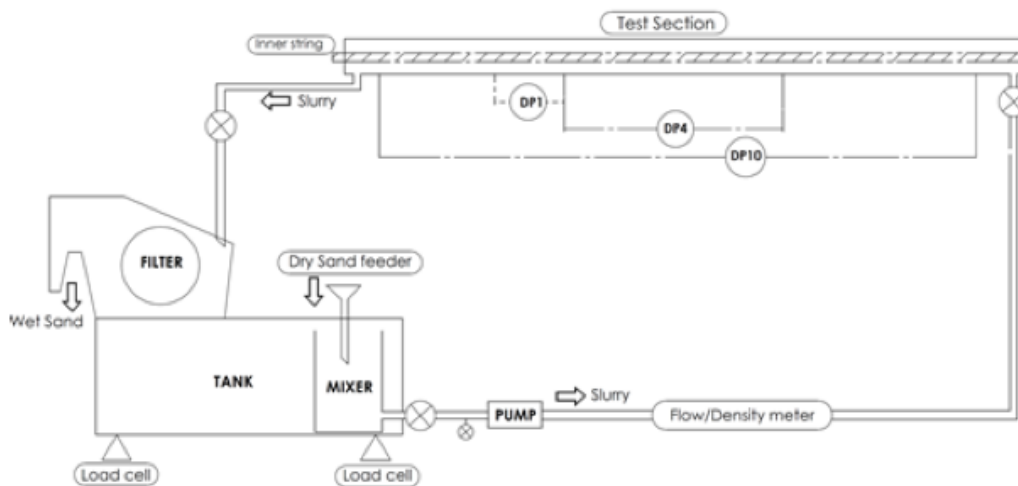


Figure 35 Illustration of the main components in the full-scale flow loop (Ytrehus J, 2015)

Figure 35 illustrates the main components of the semi full-scale flow-loop (2016). Dry sand is added to the drilling fluid at the rate of 43 g/s and blended in the mixer. From there the drilling fluid is pumped through a flow meter and eventually through the annuli in test section with the rotating pipe. Differential pressure measurements were logged in a section of 4 and 10 meters over the test section. The drilling fluid with sand

was sent back to the tank unit, where a meshed filter separates the sand from the liquid and sends it to a tray for wet sand, while the drilling fluid flows back to tank. The dimensions of the test-related objects in the test section are listed in Table 6.

Table 6 Dimensions of factors contributing to cuttings transport

Object	Size	Unit
Sand particle diameter	0,0013	m
Inner pipe diameter	0,0508	m
Outer pipe diameter	0,1016	m
Pipe length	10	m
Inclination	60/90	degrees (from vertical)

The flow-loop has a unique weighing system under the tank, which makes it possible to measure the difference from no sand in the flow loop to cuttings bed build-up. With information about the sand density, we can find the cuttings bed height based on the volume sand lacking from the tank area.

Fluid was circulated through the loop with constant flow rate and sand was evenly injected into the drilling fluid before circulating through the annular space, resembling a rate of penetration (ROP) equivalent to 8 m/hr. After a short amount of time, a constant bed height was established. The experiments were run at two different angles of 60° and 90° and the rotation of drill pipe varied from 0, 50 to 150 rpm. Flow rates that gave velocities of 0.5, 0.7, 0.9 and 1.1 m/s were chosen for the horizontal section (90°), and 0.5, 0.75 and 1 m/s for the inclined section (60°).

The drilling fluid used in the experiments is referred to as OBM C (Oil-based mud C) in previous work by Sayindla et al. (2016) and Werner et al. (2016b). The mud is of the type Versatec and was delivered by *M.I. Swaco - A Schlumberger Company*. The fluid is used in real drilling operations with a density of 1270 kg/m³ and an oil-water ratio of 75/25.

Sayindla et al. (2016) and Werner et al. (2016b) analysed the fluid in a Herschel Bulkley-model, as Bingham plastic gave some deviations in the low shear region and an overestimated yield point (Werner et al., 2016b). Its flow curve is illustrated by Figure 36 and properties listed in Table 7:

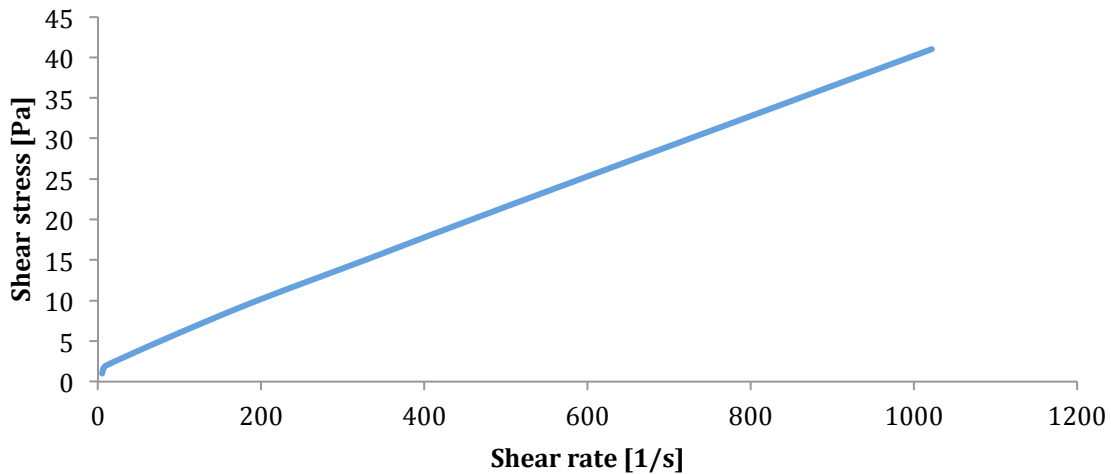


Figure 36 Flow curve of OBM C obtained by Fann 35 (Werner et al., 2016b)

Table 7 Herschel Bulkley parameters for OBM C (Sayindla et al., 2016)

Density [kg/m ³]	Consistency factor [Pas]	n-exponent	Yield point [Pa]
1270	0.144892	0.8285	2.83713

The results of the experiments are presented in Figure 37, where sand bed height is compared to the range of velocities. For no rotation of drill pipe (0 rpm), the inclined section has significantly higher cuttings bed compared to the horizontal pipeline.

It is interesting to see that at 150 rpm we can observe the opposite; the cuttings bed in the horizontal section is higher compared to the inclined section. This can be explained by Figure 6 in Chapter 2, which illustrates shorter settling distance for cuttings particles in horizontal wellbores, compared to inclined wellbores.

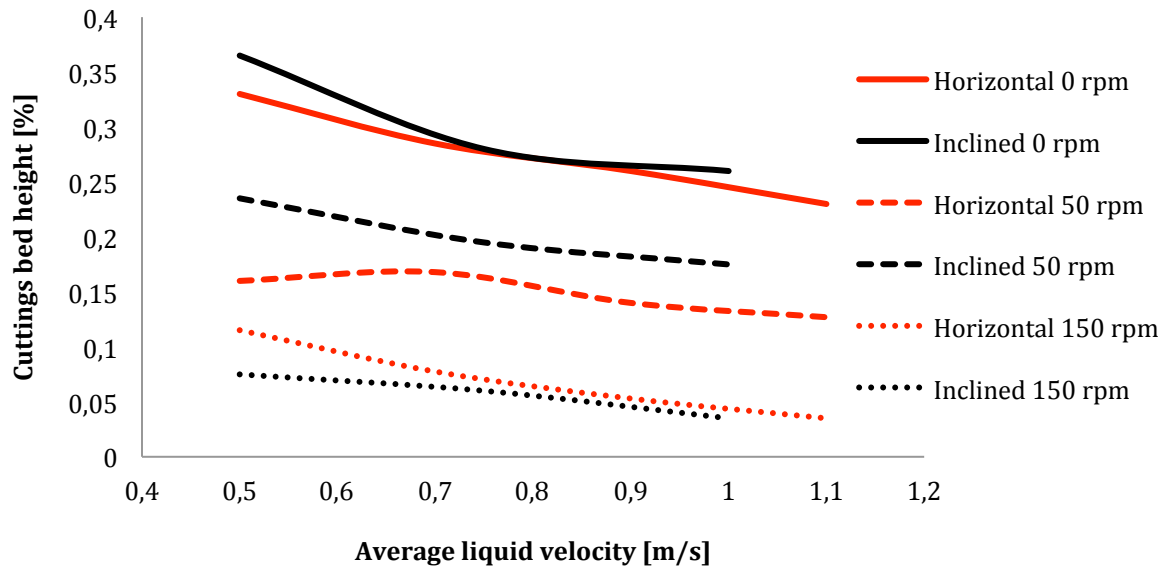


Figure 37 Effect of rotation on hole cleaning in inclined and horizontal experiments (SINTEF, 2017)

The most interesting observation is found when rotating the drill pipe at 50 rpm, where the difference between inclined and horizontal wellbore increases significantly, compared to 0 rpm. This may be a sufficient rotation to lift the particles enough to trigger backsliding, while slightly higher rpm may have triggered increased cuttings suspension in the drilling fluid.

These data will be analysed and used as comparison for the development of a model in the next sub-chapter. The physics contributing to cuttings particle movement will be outlined in sub-chapter 5.2.

5.2 PHYSICS INVOLVED

In subchapter 5.2 we will suggest what physical mechanisms are involved in cuttings transport and bed formation. A mechanistic model is developed to evaluate the observations described in Figure 37.

Contributing forces to cuttings transport

A mechanistic model for cuttings transport was developed by Ramadan et al. (2003), where the critical flow to initiate movement of the solid bed particles was the key parameter. Simplifications and assumptions must be made for idealization of the fluid dynamics. As the force field acting upon a cuttings particle changes rapidly, mean values

must be calculated for mathematical simplicity. The following assumptions was made for that purpose (Ramadan et al., 2003):

- 1 Uniform thickness of cuttings bed
- 2 Stationary bed
- 3 Uniform rearrangement of bed
- 4 Uniform cuttings size
- 5 Spherical particles
- 6 Uniform density
- 7 Uniform angle of repose
- 8 No velocity fluctuations
- 9 Obeys law of the wall
- 10 Steady state

There are usually four main forces that are contributing to transporting the cuttings; gravity, plastic, drag and lift. Step one in finding the cuttings bed area, is to set up the balance of forces acting against the gravity- and plastic-forces. Gravity force (F_G) is mainly contributing to bed settlement and transports particles suspended in the mud down with the slip velocity. For an inclined wellbore section, gravity force can be expressed as (Ramadan et al., 2003):

$$F_G = W \cdot \sin(\alpha) = \frac{\pi}{6} \cdot d_p^3 \cdot (\rho_s - \rho_f) \cdot \sin(\alpha) \cdot g \quad (5.1)$$

When the gravity force has transported the particle to become a part of a cuttings bed, the gel strength of the fluid surrounding particles in the static bed will act upon the settled particle. In the mechanistic model, this is called the plastic force (F_P) and is expressed by equation (5.2):

$$F_P = \frac{\pi}{4} \cdot d_p^2 \cdot \tau_0 \quad (5.2)$$

In the opposite direction from the plastic force, is the lifting force (F_L). The lifting force acts perpendicular to the borehole wall and outwards from the bed of cuttings. For lifting force to occur, the flow field should have asymmetry. For a cuttings particle on the top of a cuttings bed, the slip condition ceases and the particle will experience this asymmetry. This will give lift to the particle with a magnitude defined by (5.3) (Ramadan et al., 2003):

$$F_L = \frac{\pi}{8} \cdot d_p^2 \cdot C_L \cdot \rho_f \cdot u^2 \quad (5.3)$$

u is the local velocity and C_L is the lift coefficient defined as (Ramadan et al., 2003):

$$C_L = 4.11 \cdot \left[\frac{d_p}{u \cdot Re_p} \cdot \frac{du}{dr} \right]^{0.5} \quad (5.4)$$

In the formula (5.4) the shear rate is written as du/dr and the particle Reynolds number is defined as:

$$N_{Rep} = \frac{u^2 \cdot \rho_f}{\tau} \quad (5.5)$$

When making the assumption that there is no friction in between particles, the summation of forces in the perpendicular to the borehole wall will determine if the particles are lifted or deposited on the bed. If the summation of these forces is zero with the y-axis in direction of the lifting force, the cuttings bed is experiencing equilibrium. Under equilibrium between deposition and lifting we can find the critical velocity (u) (Ramadan et al., 2003):

$$F_y = F_L - F_p - F_G = 0 \quad (5.6)$$

$$F_y = \frac{\pi}{2} \cdot d_p^2 \cdot \rho_f \cdot \left(\frac{C_L \cdot u^2}{4} - \frac{\tau_0}{2 \cdot \rho_f} - \frac{d_p \cdot \sin(\alpha) \cdot (s - 1) \cdot g}{3} \right) \quad (5.7)$$

where s is the ratio of solid density to fluid density.

Step two of finding the cuttings bed area for sections without rotation is to find the critical (local) lifting-velocity where equation (5.7) is zero. For the expression (5.7) to be zero, the expression within the bracket has to be zero. This will lead to the expression for the critical velocity determined by the lifting force (u_L) (Ramadan et al., 2003):

$$u_L = \left(\frac{2 \cdot \tau_0}{C_L \cdot \rho_f} + \frac{4 \cdot d_p \cdot \sin(\alpha) \cdot (s - 1) \cdot g}{3 \cdot C_L} \right)^{0.5} \quad (5.8)$$

As can be seen in equation (5.8), the critical velocity for lifting is highly dependent on the lifting coefficient (C_L), which again is also dependent on the lifting velocity. This means that the velocity should be found by iterations. For this thesis, the iterations were performed in Microsoft Excel.

As can be seen in Figure 38, one additional force in the direction of flow is not yet mentioned; the drag force (F_D), defined by equation (5.9):

$$F_D = \frac{\pi}{8} \cdot d_p^2 \cdot D_R \cdot C_D \cdot \rho_f \cdot u^2 \quad (5.9)$$

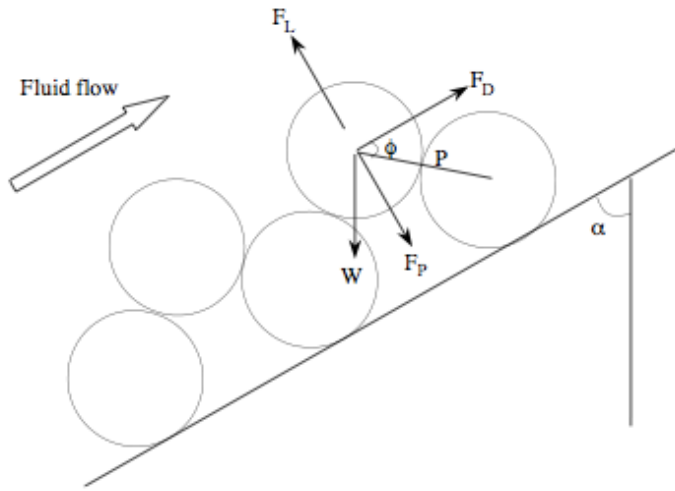


Figure 38 Forces acting upon a cuttings particle (Ramadan et al., 2003)

The drag force is a contributor to another transport type; rolling. A rotating torque around the point P in Figure 38, initiates rolling of a particle. Assuming no friction in between particles, the formula for rotating torque can be expressed as (Ramadan et al., 2003):

$$T_P = \frac{d_p}{2} \cdot (F_D \cdot \sin(\phi) + F_L \cdot \cos(\phi) - F_P \cdot \cos(\phi) - W \cdot \sin(\alpha + \phi)) \quad (5.10)$$

After inserting expressions for the forces involved:

$$T_P = \frac{\pi \cdot d_p^3 \cdot \rho_f}{4} \left(\frac{D_R \cdot C_D \cdot \sin(\phi) + C_L \cdot \cos(\phi)}{4} u^2 - \frac{\tau_0 \cdot \cos(\phi)}{2 \cdot \rho_f} - \frac{d_p \cdot g \cdot (s - 1) \cdot \sin(\phi + \alpha)}{3} \right) \quad (5.11)$$

where the drag coefficient (C_D) is:

$$C_D = \frac{24}{N_{Rep}} + \frac{6}{1 + N_{Rep}^{0.5}} + 0.4 \quad (5.12)$$

The drag force introduces a local, critical velocity with rolling mechanism as the dominating transport force. This is typical for highly inclined or horizontal wellbores and high mud flow rates. The local critical velocity for rolling is found where the rotating torque is zero. The same approach as used when finding the critical lifting velocity can be utilized where the bracket alone can be set as zero, to find an expression for rolling critical velocity (step three):

$$u_R = \left(\frac{6 \cdot \tau_0 \cdot \cos(\phi) + 4 \cdot d_p \cdot g \cdot (s - 1) \cdot \sin(\phi + \alpha)}{3 \cdot (D_R \cdot C_D \cdot \sin(\phi) + C_L \cdot \cos(\phi))} \right)^{0.5} \quad (5.13)$$

We will evaluate what critical velocity has the lowest calculated value out of the two; rolling or lifting, which will decide what is the dominating transport force and what critical velocity to use for further calculations.

The next step for predicting the cuttings bed height at no rotating conditions is to find the average velocity. As the flow rate (Q) is constant over the whole pipeline, the critical velocity at the cuttings bed will represent a mean velocity that is higher compared to corresponding areas in the pipeline without a reduced area.

Two simple steps are pursued to find the mean velocity in annuli. In step four, the maximum velocity (U_{max}) could be found from the velocity profile of the outer layer (Gerhart et al., 1992):

$$\frac{u}{U_{max}} = \left[\frac{2 \cdot y}{D_h} \right]^{n_f} \quad (5.14)$$

where y is the distance from the bed where the critical velocity is found, illustrated in Figure 39, and n_f is related to the friction factor between the cuttings and the bore hole-

or casing-wall ($n_f = f^{-0.5}$). The critical velocity cannot be found directly at the bed, as the velocity there would be zero.

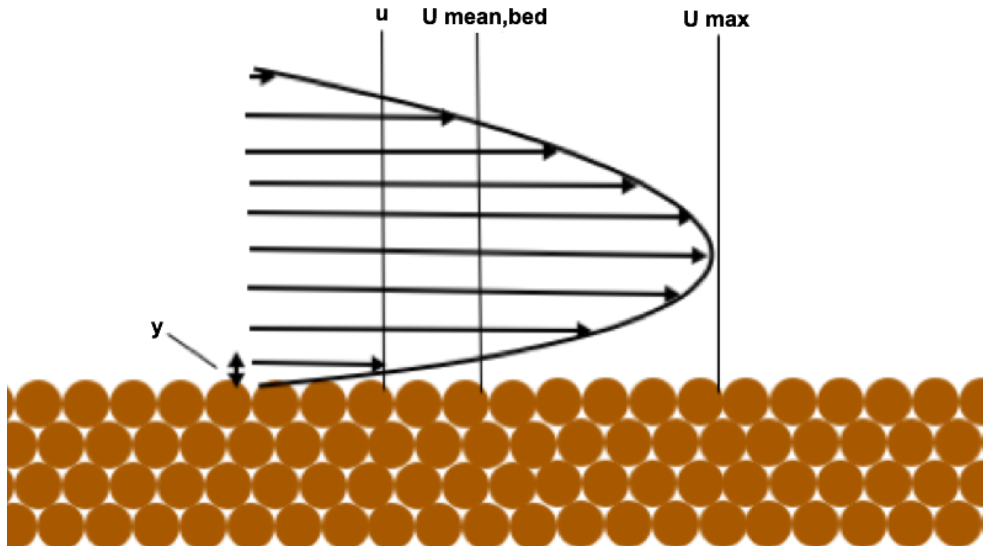


Figure 39 Velocity profile with the critical velocity (u), average velocity ($U_{mean,bed}$), max velocity (U_{max}) and distance (y) to the critical velocity from the bed (this author)

In step five we use the formula for maximum velocity (5.15) to obtain the value for the mean velocity ($U_{mean,bed}$) (Gerhart et al., 1992):

$$U_{max} = \frac{(n_f + 1) \cdot (2 \cdot n_f + 1)}{2 \cdot n_f^2} \cdot U_{mean,bed} \quad (5.15)$$

Area occupied by cuttings can be found by the simple relationship between flow rate, area and mean velocity (step six and seven):

$$A_{cuttings,0rpm} = \left(\frac{\pi}{4} (d_o^2 - d_i^2) - \frac{Q}{U_{mean,bed}} \right) \cdot (1 - \phi) \quad (5.16)$$

The porosity of the bed is assumed to be around 50% (SINTEF, 2017), which was the bed porosity estimate from a similar experiment (2017) described in Chapter 4. The bed porosity was found by measuring the weight of sand particles saturated in OBM WARP in a cup with a known volume. Knowing the density of both the sand and fluid, the

fraction between the two could be found, with the fluid volume representing the porosity.

The model for inclined and horizontal cuttings transport in systems without rotation can be summarized in the flow chart in Figure 40.

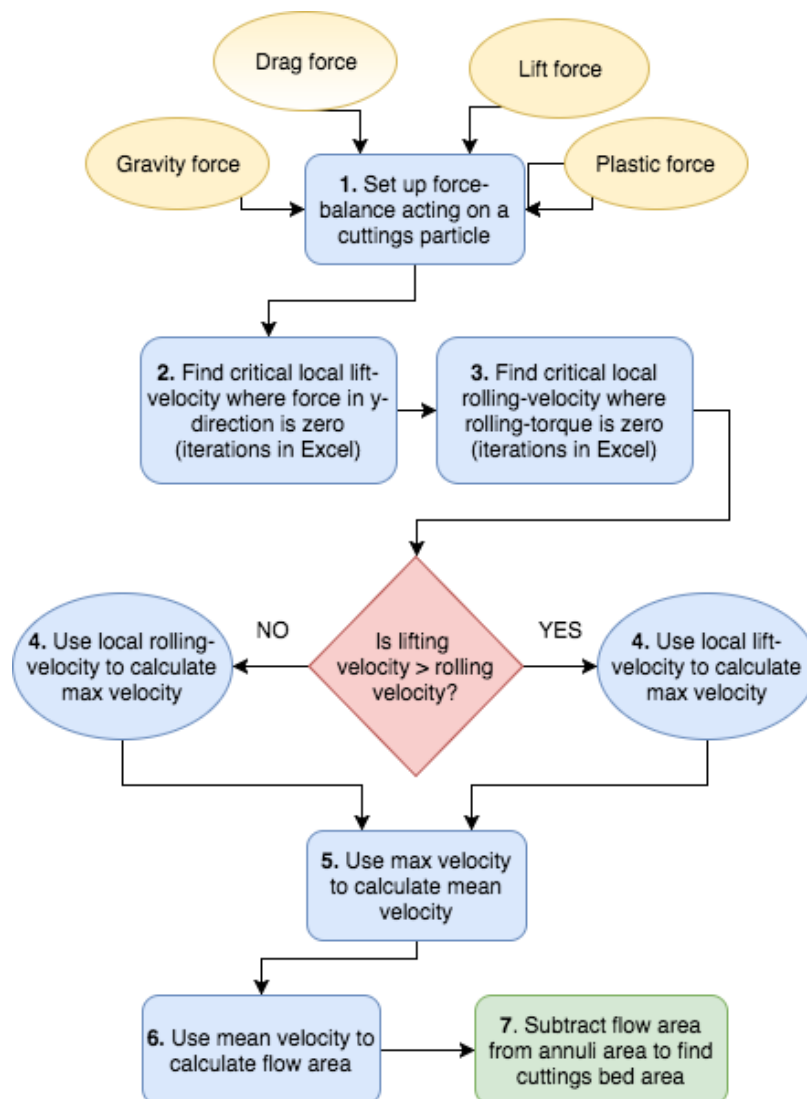


Figure 40 Flow chart for finding cuttings bed flow area without rotation

Transport force from the rotating drill pipe

Transporting sand from the borehole is affected by two cuttings feeds; the cuttings feed from the rate of penetration (ROP) transported with the axial velocity, and the cuttings feed that is transported from the bed as a result of drill pipe rotation, illustrated by Figure 41.

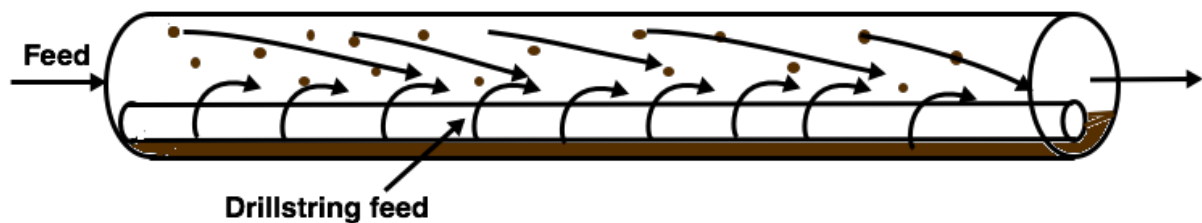


Figure 41 Cuttings transport of ROP- and RPM-feed (this author)

Previously we have presented the bed estimate as a result of balance between eroding and settling forces due to axial flow. When the cuttings bed was stable, the sum of forces was zero at the top of the bed. With rotation, an additional shear force acts in the radial flow around the drill pipe. To successfully develop a model within this thesis, a list of assumption had to be made:

1. The two dominating forces are gravity force and shear force induced by rotating drill pipe
2. Cuttings particles are perfect spheres and experience no spinning
3. Neglect effect of pressure drop along the bed from rotation and velocity
4. Effect from Taylor vortices neglected
5. Sand lifting velocity is equal to the velocity of an incompressible fluid in the Taylor Couette-flow, created by the rotating drill pipe, combined with particle slip velocity
6. Axial flow velocity

The flow for estimating drill string evoked lifting-velocity is presented in Figure 42 and is an extension of the model for cuttings transport without rotation. The aim is to calculate the volume of sand-particles that are exposed to the shear force induced by

rotating drill pipe that is greater than the gravity force. The sufficient shear force that is great enough to lift a particle is in between the drill string and red dotted line in Figure 42. If drill string rotation is increased, the red dotted line will shift to the left, further towards the annuli wall, as shear force is increased along the hydraulic diameter. The height whereas the particles are lifted to, will determine how far the particles are transported along the drill pipe, limited by the axial- and slip-velocity.

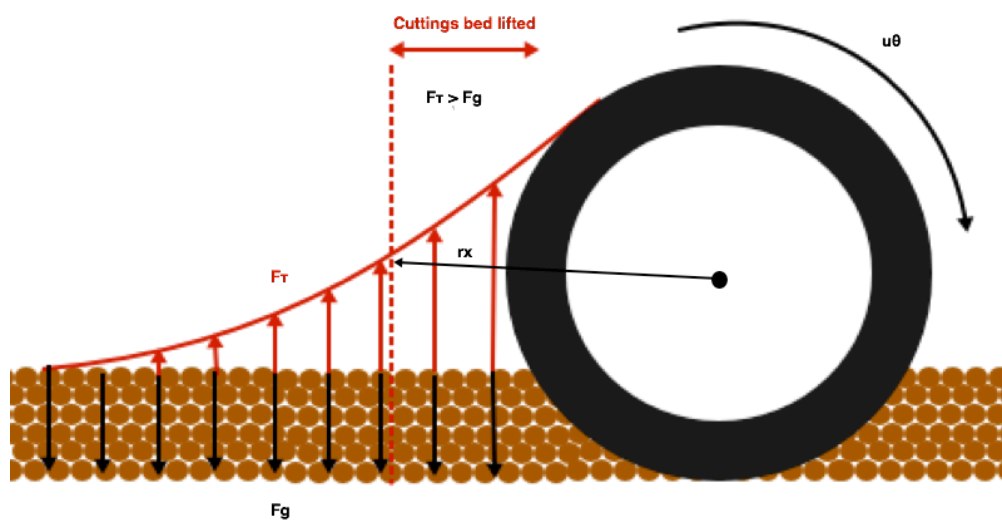


Figure 42 Radius of particle lifting (this author)

A force-balance will lead to finding the effective radius whereas the shear force is large enough for lifting. Fluid models described in sub-chapter 3.2, demonstrate the relationship between shear force and shear rate, which can be utilized to find the corresponding shear rate where shear force is equal to gravity force. Shear rate is defined as difference in velocity over radial distance, and can therefore be used to find the effective radius (r_x) where velocity of particles is above zero.

Step one is setting up the force balance between the shear force from the rotational movement of the drill string and the gravity force acting upon a cuttings particle, in equation (5.17).

$$F_G = F_{shear} \quad (5.17)$$

Rewriting (5.17) leads to an expression that includes the drill string induced shear stress (τ) sufficient to lift a cuttings particle:

$$m_p \cdot g \cdot (1 - s) = \tau \cdot A \quad (5.18)$$

In step two we calculate the minimum shear stress for lifting, by rearranging equation (5.18):

$$\tau = \frac{m_p \cdot g \cdot (1 - s)}{A} \quad (5.19)$$

Further, in step three, we use the minimum shear stress for lifting in the Herschel Bulkley-relationship from equation (2.6), to find the corresponding shear rate in equation (5.20). Herschel Bulkley parameters are found in previous work (Sayindla et al., 2016).

$$\dot{\gamma} = \left(\frac{\tau - \tau_0}{K} \right)^{\frac{1}{n}} \quad (5.20)$$

The shear rate from equation (5.20) can be utilized in step four by equation (2.2) to find the effective radius of lifting (step four). The length of the radius will describe how many particles in the radial distance that are lifted. The cuttings closest to the drill pipe wall will experience the highest velocity, as they follow the rotational speed of the drill string. This can be defined as the circumference of the drill pipe times its rotational speed:

$$u_{rpm} = \frac{\pi \cdot r_i}{30} \cdot \Omega_i \quad (5.21)$$

The velocity defined by equation (5.21) is set as the maximum velocity for the lifted particles. An expression of shear rate ($\dot{\gamma} = \frac{du}{dr}$) can be defined as the maximum velocity minus the minimum velocity (=0), over the effective radius (r_x) for lifting in annuli:

$$\dot{\gamma} = \frac{\frac{\pi \cdot r_i}{30} \cdot \Omega_i - 0}{r_x} = \frac{\pi \cdot r_i}{30 r_x} \Omega_i \quad (5.22)$$

Equation (5.22) can be inserted in the Herschel Bulkley model and tie the rotational velocity directly to shear force:

$$\tau = \tau_0 + K \left(\frac{\pi \cdot r_i}{30 r_x} \cdot \Omega_i \right)^n \quad (5.23)$$

Now that we have found the effective radius of lifting, the next step is to calculate the heights, which as the single particles are lifted to, a distance r from the rotating drill pipe. First we need to find the start velocity of different particles and utilize this in the equation of movement, to find the max lifting height, assuming gravitational acceleration back towards the bed.

In step five we find the velocity profile of the particles surrounding the drill string. The velocity field around the drill pipe as a result of the centrifugal force is illustrated in Figure 43. This velocity will be set as the starting velocity of each individual particle, towards the maximum height, which they will be lifted to. The velocity distribution can be expressed mathematically (White, 2016):

$$u_{\theta} = \Omega_i \cdot r \cdot \frac{\frac{r_o}{r} - \frac{r}{r_o}}{\frac{r_o}{r_i} - \frac{r_i}{r_o}} \quad (5.24)$$

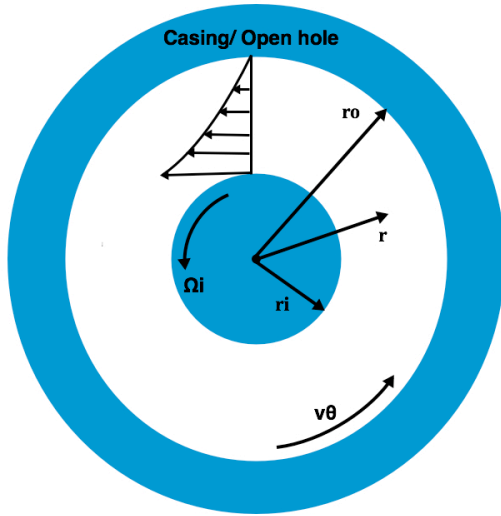


Figure 43 Flow between an inner concentric, rotating cylinder and an outer fixed cylinder

Equation (5.24) represents the Couette flow solution, a system-description of a concave, and two-dimensional velocity profile with an incompressible fluid and concentric drill pipe. Even so, we assume for simplicity that the start-velocity of the particle is defined by the velocity distribution of the fluid rotated by the drill pipe in equation (5.24). Couette-flow describes a laminar flow regime, but will experience instabilities at low rotation in accordance to Taylor's number in equation (2.9) (White, 2016).

In step six we will find the magnitude of the particle transport max height, limited by the particle's gravitational acceleration. We use the equation of movement to calculate the maximum height of the cuttings particles. With the maximum travelling height we can calculate how far the cuttings particle can be transported out of annuli comparing the axial- and slip-velocity. The maximum height and slip-distance for a particle to fall back to the bed is given by equation (5.25):

$$u_2^2 - u_1^2 = 2 \cdot g \cdot h_{max} \quad (5.25)$$

where the maximum height (h_{max}) of the cuttings particle, as a result of the rotating speed of drill pipe, can be illustrated in Figure 44.

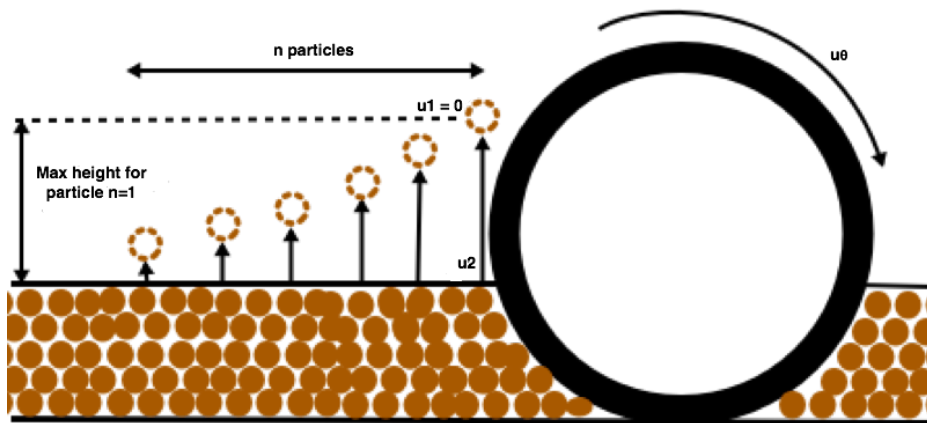


Figure 44 Max height for n particles, transported by the rotating drill pipe (this author)

We have defined the time required to move one layer of particles as $t_1 = d_p/u_2$, where u_2 is the velocity of rotating drill pipe. We assume that layer 2 and the following layers will use the time $t_2 = 3t_1$ to be lifted, as they experience forces from the surrounding particles and are not as loose as the first layer of particles.

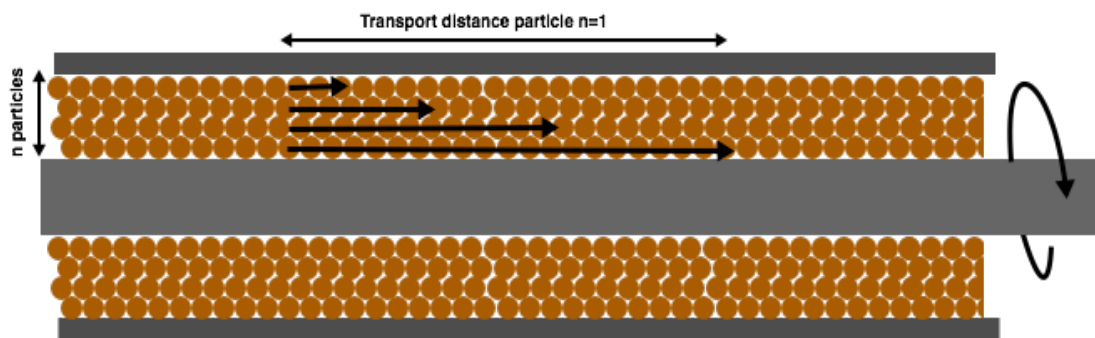


Figure 45 Transport distance for cuttings transport depending on radius length from the rotating drill pipe seen from above (this author)

Figure 45 represents the transport distance for a particle-row n counted from the outer radius of the drill pipe towards the inner casing radius. As the particles closest to the drill pipe are transported to a higher max height compared to particles closer to the annuli wall, this particular particle will also have the longest transporting distance by axial velocity before it falls back down to bed (slip velocity). Step seven is comparing slip- and axial-velocity and determining the volume of particles transported out of the

10-meter section. We start by calculating the available transport time ($t_{transport}$) as a function of the slip velocity:

$$t_{transport} = \frac{h_{max}}{v_{slip}} \quad (5.26)$$

The transport length ($L_{transport}$), which a particle will be transported with the available transport time, can be calculated as:

$$L_{transport} = v_{avg} \cdot t_{transport} \quad (5.27)$$

Then the volume of particles transported out for column n particles can be calculated in equation (5.28):

$$V_{transport} = \frac{L_{transport}}{d_p} \cdot V_{sphere} \quad (5.28)$$

After calculating the transport distance and the volume of particles to reach the end of the test section before falling back down, we can find the flow rate of particles ($q_{cuttings}$) cleaned out of annuli:

$$q_{cuttings} = \frac{V_{transport,1}}{t_{transport,1}} + \dots + \frac{V_{transport,n}}{t_{transport,n}} \quad (5.29)$$

The flow rate of cuttings ($q_{cuttings}$) transported away from the cuttings bed is subtracted from the bed area for the model without rotation. As the surface of cuttings bed exposed to the fluid is unknown, we estimate the new ROP-feed that make up a new bed the volume made up of the area of particles that make up the inner diameter length annuli and the maximum, vertical slip-velocity, with the entire length of test section:

$$q_{new\ feed} = d_o \cdot v_{slip} \cdot \frac{L}{v_{avg}} \quad (5.30)$$

Subtracting the new feed that builds new bed from the volume that escapes the test section in equation (5.29), will give the volume out of the test section when multiplied with the experiment time (3.5 minutes for a 10 meter section):

$$V_{net\ cuttings\ out} = (q_{cuttings} - q_{new\ feed}) \cdot t_{experiment} \quad (5.31)$$

Then the relative cuttings area can be found by subtracting the area of cuttings transported out from annuli, from the cuttings area for 0 rpm:

$$A_{cuttings,rpm} = A_{cuttings,0\ rpm} - \frac{V_{net\ cuttings\ out}}{L} \quad (5.32)$$

From this point, the cuttings bed hold up can be calculates as:

$$H = \frac{A_{cuttings,rpm}}{A_a} \quad (5.33)$$

Through experimental data from previous years, SINTEF (2017) has developed a curve-fitting between cuttings hold-up and the actual bed height that can be utilized for estimating the height of the bed in this model:

$$H = 6.7066 \cdot h^{0.567} \quad (5.34)$$

The process flow for calculating cuttings transport out of annuli is presented in Figure 46.

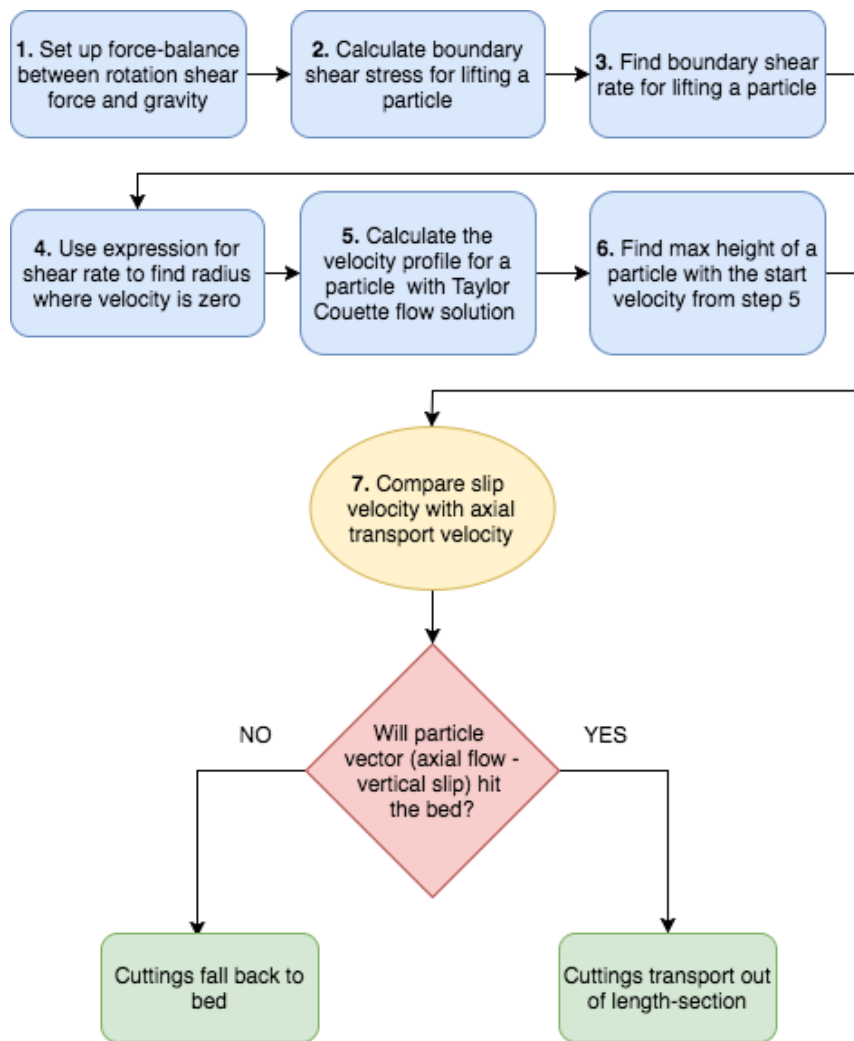


Figure 46 Flow chart for calculating cuttings bed reduction

5.3 COMPARISON WITH LABORATORY DATA

In this sub-chapter we will evaluate the model developed in 5.2 and test it against true laboratory experiments with the same dimensions, presented in Table 6, in sub-chapter 5.1. The comparison will be separated in two parts; before and after the effect of rotation.

Experiments vs. model without rotation

Modelling cuttings bed height without rotation gave the results in Figure 47, which shows lower bed heights compared to the data obtained from the laboratory experiments in the low velocity-area. In addition, we observe slightly overestimation of the high-velocity area for the model compared to experimental data.

According to the model, rolling was the dominating transport force in horizontal and inclined section with no rotation, as critical rolling velocity was lower than critical lifting velocity. The model does not show the similarity between bed height in horizontal and inclined wellbores at intermediate velocities, as the experimental data imply. However, in similarity to the experimental data, the model also suggests that the velocity-increase alone is not enough to lift and suspend the particles in the drilling fluid.

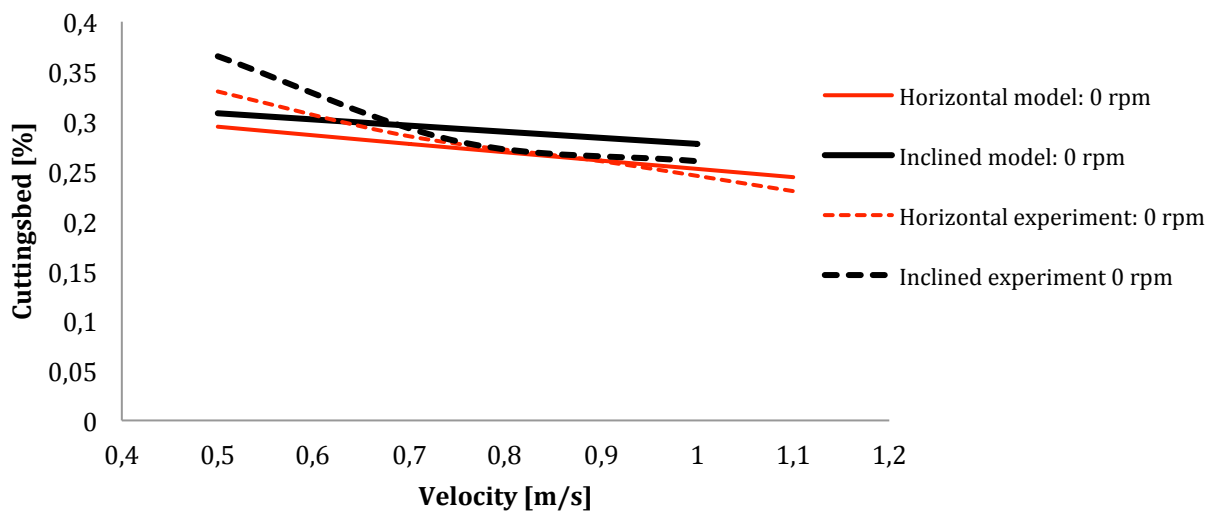


Figure 47 Comparison of model and experimental data from SINTEF for cuttings transport without rotation

The gap between the SINTEF-data points and model points can also be explained by the uncertainties inserted in the model. The model is to a high degree dependent on

simplifying assumptions, e.g. the distance to the critical velocity for lifting and rolling (y) and assuming a friction factor between particles and the borehole wall ($n_f = f^{-0.5}$) in the equation (5.14) for $\frac{u}{U_{max}}$. Small deviations of these values had significant impact on the results.

Experiments vs. model with rotation

In part two of the model, we used the rotational speed for adding the effect of drill string feed of cuttings, to the total transport-estimate. Tested for a range of rpms, the shear stress radius was sufficient enough to work across the total hydraulic diameter of the annuli for all rpms above 5 rpm. Knowing that the shear stress works along the total area for our desired measure points (50 and 150 rpm), means that we can assume that the velocity field calculated by Taylor Couette equation (5.24), goes from maxima at the inner rotating drill pipe to a minimum at the outer static annuli ($r_x = r_h$).

Finding the radius r_x , is the only place where mud rheology is included in the drill string-feed modelling. The mud rheology is more central in the modelling of critical velocity for cuttings transport without rotation. The mud rheology is therefore of less importance as the drill pipe rotation increases, especially above 5 rpm.

From communication with SINTEF (2017) we know that at low rpms the expected result is an increase in bed height. The drill pipe rotation is efficient to move cuttings particles a small distance along the axial flow, but they will accumulate further up in the bore hole, making room for more particles at the initial resting point. Therefore it is not surprising to have an efficient shear force along the annuli radius even at low rpms.

In Figure 48 the model and experimental results for 50 rpm in horizontal and inclined annuli, are plotted as cuttings bed height versus annular velocity. The plot anticipates that rolling mechanism is still a significantly dominating factor contributing to the cuttings bed height, both for the experimental data and in the model. It seems like the rotational velocity is not sufficient for suspending the cuttings in the axially flowing mud.

Higher degrees of inclination has a tendency to trigger back sliding of cuttings bed that move slower through the annular space (Piroozian et al., 2012). In experiments from Chapter 4, the stabilization took longer for inclined sections at each velocity, and it took in general longer for the sand bed front to reach the end of test section (measured by differential pressure cells). As the horizontal test section will not experience backsliding, it is natural to assume that the difference between horizontal and inclined results will increase, as in the experimental data. The model only includes the difference in settling distance between inclined and horizontal wellbores and stabilization of bed height between eroding and building-forces. Therefore the backsliding of cuttings particles cannot be analysed in this this model.

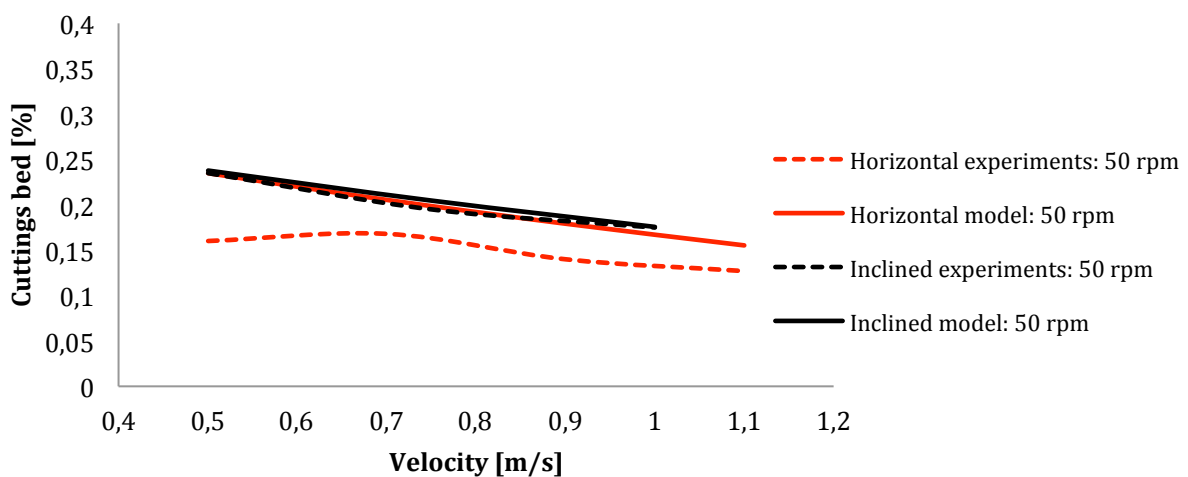


Figure 48 Comparison of model and experimental data from SINTEF for cuttings transport with 50 RPM

The cuttings bed height for horizontal and inclined section is increasingly similar for 50 rpm, compared to 0 rpm in the model, which can indicate that the gravitational forces are increasingly important for increased rpm in the model as the lift mechanism becomes more dominating. As can be seen in Figure 49, for a particle suspended in mud, more energy is needed to transport a cuttings particle in the inclined section. The gravity force works against the drag force, causing less efficient cuttings transport compared to the horizontal.

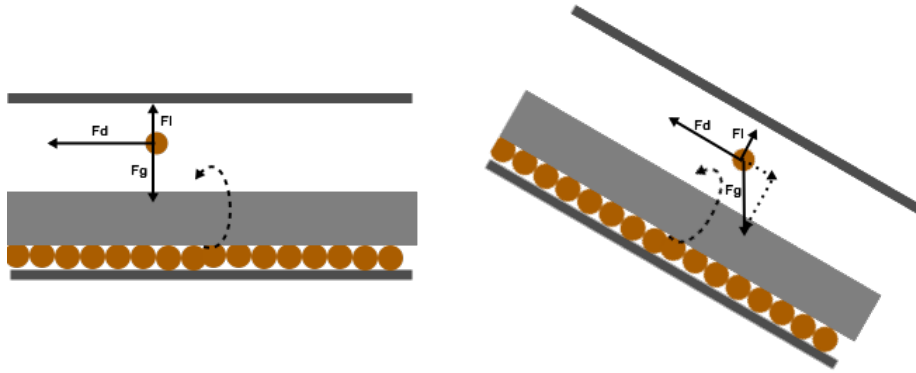


Figure 49 Forces acting upon a cuttings particle suspended in mud, in horizontal and inclined annuli

In Figure 50 we see the cuttings bed height versus velocity at 150 rpm. The model shows total sufficiency of hole cleaning and no cuttings bed build-up. Well-improved hole cleaning was suspected at 150 rpm, as more cuttings particles will be thrown back up in annuli to be suspended in the drilling fluid.

One reason for not put completely trust in the cuttings bed height modelled compared to experimental data may be due to not including the free whirling effect the drill pipe has in annuli when under high rotation. The drill pipe will climb on the wall, which it is climbing against and not lay in the bottom as much as without rotation. This effect would in general give an overestimation of cuttings bed, but with the lack of inclusion of other physical physics, this does not show in the model.

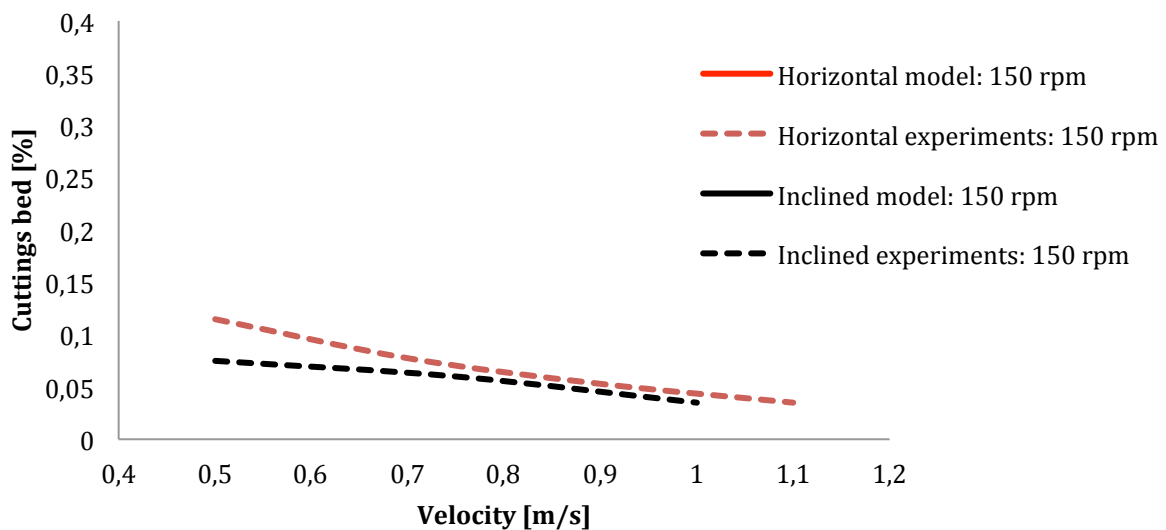


Figure 50 Comparison of model and experimental data from SINTEF for cuttings transport with 150 RPM

In the case of 150 rpm, most of the cuttings particles will be lifted by the drill pipe and suspended in the fluid. Gravity will in this case be the dominant factor for cuttings bed estimation. The settling distance for cuttings particles in inclined boreholes are longer compared to horizontal boreholes, where the settling distance is the radius of the annuli for a centred particle. This may cause the experimental data-plots to shift from 0 rpm and 50 rpm to the opposite trend seen with 150 rpm, where the inclined borehole experienced the highest cuttings bed height.

Cuttings bed height percentage for 0, 50, 80 and 150 rpm is plotted in Figure 51. Cuttings bed height for 80 rpm was added to show the shifting effect, which is seen for 150 rpm from experimental data in Figure 37, where the horizontal section had higher cuttings bed. The plots of cuttings bed height at 150 show approximately 0 for all velocities, making the trend not visible. From the model, this effect is simply a result of higher lift of single particles at 80 and 150 rpm in both sections, and longer slip distance in inclined sections.

Experimental data show in general a more complex pattern of bed height estimation, while the model has similar slopes in the two plots for horizontal and inclined. The model estimates a linear relationship between cuttings bed height and average velocity. These differences points towards two directions:

1. Average velocity has low impact on the modelled cuttings bed height
2. The model lacks inclusion of important, influencing physics

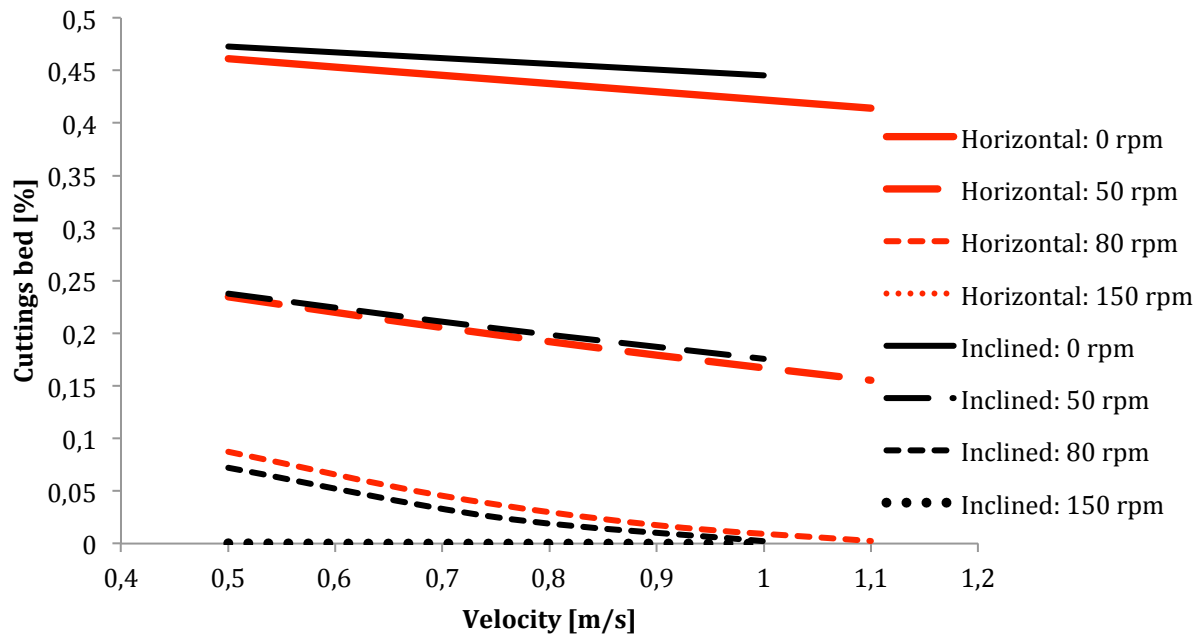


Figure 51 Modelled cuttings bed height in inclined and horizontal sections for 0, 50, 80 and 150 rpm

The cuttings bed height is given as an exponential function of cuttings hold-up in Figure 52. Its comparison by SINTEF (2017) with previous experimental data, estimates that the function is applicable for cuttings bed height up to 90% of the annuli diameter, although as unrealistic that is.

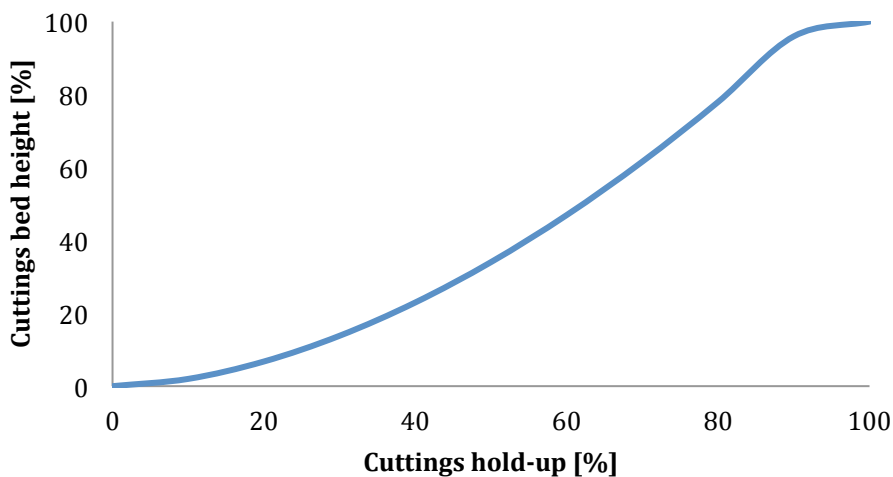


Figure 52 Cuttings bed height vs. cuttings hold-up (SINTEF, 2017)

6 SELF-ASSESSMENT

In self-assessment we will discuss the limitations and uncertainties related to hole cleaning-experiments and rheological characterization. This part is important for analysing the results from Chapter 4 and 5 with scepticism and realistic consideration.

The second part of this self-assessment is to suggest improvement areas to measurement of rheological properties and density, and handling experimental results from the flow-loop tests. Improvement areas are an important part of the cuttings transport model, as few developed models are applicable for many well cases. Our model will be discussed and excluded physics will be highlighted in this chapter.

6.1 UNCERTAINTY AND LIMITATIONS

In this subchapter we will discuss the uncertainty and limitations in three parts; rheological characterization in Chapter 4 for the experimental part, and flow induced transport and drill pipe induced transport for the theoretical modelling in Chapter 5.

Rheology characterization

During rheology characterization, Fann 35 deviated from Anton Paar. Two Fann 35-viscometers were used to measure flow curves, whereas the first gave deviations in the high shear-area. When the first Fann 35-viscometer broke, a new Fann 35-viscometer was tested, which gave deviations from Anton Paar in the low shear area. Deviations from Anton Paar-flow curves have previously been observed in plots by Werner et al. (2017) with lower shear stress at high shear rates and higher stress for lower shear rates. Preferably the same Fann 35- viscometer should be used for all measurements, so that apparatus-deviations are excluded.

In general, temperature control is a challenge for measurements in Fann 35, as it is not possible to monitor it constantly during measurements. Anton Paar has lower temperature deviations as the heating of the system is designed to be very precise. In

addition, Fann 35 has dial reading-uncertainty by the operator. The dial reading can change ± 0.5 from what angle the value is read off the dial.

The density measurements were experimentally found by weighting a filled pycnometer with a known volume. Pycnometers have a relatively high measuring accuracy compared to the mud weight scale. Gravity segregation in the tank was an issue prior to filling the loop with drilling fluids. A layer of particles has fallen to the bottom of the IBC-tank and may result in rheological measurements slightly lower than its initial design. Gravity segregation could also have been an issue for measurements after 24 hours where OBM WARP was at rest. For drilling fluids that are not utilized for weeks, frequent agitation is recommended to avoid particle settling.

Individual pressure measurements in the flow-loop utilized to see results of rheology measurements in context with operational data, as well as the expansion data, may deviate from the average values. The reasoning is because the pumps impeller is not fit for the pump itself and caused vibrations in the tank. The pump is a part of the tank-weight and will therefore influence the weight measured during experiments. The deviating points were found especially at intermediate velocities without sand injection.

In data from the flow loop measurements, deviations also occur on the tank weight loading cells. If we experience leakage, or something is added to the tank during experiments, this will affect the tank weight measurements. Calculating an average value for finding the tank weight difference when examining the expansion-effect of the hoses was no easy task. Data cleaning is needed to obtain a reasonable estimate for weight change between different flow-rates as well as finding the deviation in tank weight that comes from fluid momentum when the drilling fluid hits the tank on return, which causes extra pressure towards the loading cell.

A summation of uncertainties in rheological examination and flow loop-data is listed in Table 8, where the flow-loop uncertainties also can be applied to the experimental data compared to the model in Chapter 5:

Table 8 Uncertainties related to rheological characterization and flow-loop experiments

Uncertainty Rheological Characterization	Error estimate
Weight (density measurements)	$\pm 0.001g$
Spill of volume pycnometer	$\pm 1g$
Dial readings	± 0.5
Fluid sampling	Fluid not representable
Temperature Fann 35	$\pm 1^{\circ}C$
Temperature Anton Paar	$\pm 0.01^{\circ}C$
Uncertainty flow-loop experiments	
Expansion error on tank weight	$\pm 2 kg$
Load cell error	–
Sand rate	$\pm 1 g/s$
DP cells-error	–
Temperature flow-loop	$\pm 2.5^{\circ}C$

Flow induced transport

An attempt was made to simulate the hydraulic effect on cuttings transport in horizontal and inclined annulus-sections. A mechanistic model was utilized for the purpose of simulating the cuttings bed height without rotation. Numerous assumptions were made to give results for both the horizontal and inclined section, with the following limitations and uncertainties:

- The critical velocity for a stable bed height was assumed to be 0.5 mm over the stationary cuttings bed. At critical velocity the forces between lifting and gravity are zeroed out and the bed height will remain constant. An assumption of the distance from the bed to the radius of critical velocity can strongly influence the end-result for cuttings bed heights, without rotation.
- The particles applied were sand, which were close to spherical, with the assumption of no friction working between them. The true friction by sand gliding against sand will be approximately $f = 0.3$. The sand's imperfect spheres

will affect the transport, as they will have a complex flow pattern with swirling, impossible to simulate once lifted or rolled by the critical velocity.

- For fluid modelling we utilize the Herschel Bulkley-parameters of the fluid. Herschel Bulkley is often a preferred model when analysing drilling fluids, but its limitations in finding a universal expression for viscosity and other fluid properties, make it difficult to include in a master thesis.

Drill pipe induced transport

An attempt of adding rotation by using a mechanistic model and comparing slip velocity to the traveling-distance and -time was made. The greatest uncertainties regarding such a model can be listed as:

- The flow complexity had to be simplified to laminar flow along the axial- and rotational flow paths in this mechanistic model. Adding rotation will add Taylor vortices at relatively low rotational speeds. These vortices are not modelled.
- The start velocity of a single particle follows the Couette Taylor-velocity profile for incompressible fluids, where friction forces are neglected. The peripheral velocity of the pipe defines the velocity pattern induced by rotation in the model. In reality the velocity field will be a vectorial result of the drill pipe, transporting particles from the flowing mud, and not only from the cuttings bed top. However, assumed to not take part in bed height variation, some particles will also be transported back down to bed by the rotational effect.
- Excluded from this model is also the climbing of the drill pipe against the cuttings bed and annuli wall, especially during high rotations. This effect will contribute to better hole cleaning, as a greater part of the cuttings will be in contact with the rotating drill pipe. That particular effect may be the key parameter for improved hole cleaning in inclined and horizontal wellbores.
- Pressure loss is a dominant cuttings transport contributor (Saasen, 1998) but is not accounted for in this model. The pressure difference will be the force that

pushes the cuttings from one side of the pipeline to the other. Pressure drop is increased by flow rate and rotation, and will influence the results at high velocities and rotations if included.

6.2 FUTURE WORK AND IMPROVEMENT AREAS

In this subchapter we will reflect on the topics studied that need further research or improvement of testing procedures. A proposal for further work to be done within the area of research will also be suggested. The future work and improvement areas will be divided into rheological examination and cuttings transport modelling.

Rheology characterization

In rheology characterization there is some blurry zones in embodiment of procedure. The oil industry should preferably develop a common, detailed API-procedure for testing of drilling fluid in both Fann 35-viscometer and other rheometers (Anton Paar etc).

Especially the procedures for pre-treatment of the fluid should be set as a common practice in API standards, as studies have shown that it has an impact in rheological characterization. Pre-shearing the sample in a mixer can have several positive effects on the sample, as breaking down gel structure and give a more homogeneous sample. Oil-based drilling fluids tend to take longer to stabilize, and in addition to pre-shearing the sample in a mixer, a standard time should be set for pre-stirring at 1022 s^{-1} in the rheometer to avoid uncertainty in measurements between researchers. In work done by this author in Werner et al. (2017), pre-stirring the fluid sample had a significant impact on the measurements, especially after being at rest for a longer period of time. The effect was more reproducible results, for both testing after 0h rest and 24h rest.

With a procedure of pre-shearing and pre-stirring, a scope for further work could be to see if the centrifugal force will have similar effect to the hydro-cyclone and cause particles that hit the outer wall fall to the bottom of the fluid container. This effect may contribute to underestimation of the fluid's viscosity increasingly with time.

Cuttings transport modelling

In total the uncertainties added up throughout the model makes it unfit for use in the industry. Additional research is needed in fluid mechanics, especially for fluid modelling and viscosity- and pressure loss-calculations for Herschel Bulkley. The field of research lacks universal expressions for drilling fluids transporting cuttings in annuli. Models developed for a small fraction of a wellbore, e.g. 10 m, are not valid for the complete well.

Studies on flow regimes in axial flow should be combined with studies on Taylor-couette flow to better understand the flow pattern in annuli with different rotational speeds. An expression for Taylor vortices is developed for Newtonian fluids, but not adequate to use on drilling fluids.

A mechanistic model alone is not sufficient for modelling the complexity and enormous amount of input data and parameters that are dependent on each other. Statistical analysis of input data from the field, compared with each other may be a good foundation for such a model. A cuttings transport model should be compared to huge amount of experimental data with different types of formations, drilling fluids, velocities, rotational speeds and dimensions.

For models including high-inclination wells, the effect of backsliding of cuttings bed in the medium inclined part needs to be included. The increasing difference in bed height between inclined and horizontal sections at intermediate rpm (50 rpm) was not fully explained by the mechanistic model, and backsliding is the suspected contributor to the higher bed height for inclined section.

7 CONCLUSION

Fluid control was obtained during testing of OBM WARP from flow-loop experiments and while testing Laptonite-fluids under procedure evaluation (results published in Werner et al. (2017)), in Fann 35-viscometer and Anton Paar-rheometer. From the measurements we can conclude that:

- Pre-stirring has a significant effect on reproducing results of rheological flow curves for Laptonite fluids (Werner et al., 2017) and OBM WARP
- Low concentration of salt in Laptonite fluids increased reproducibility of pre-stirred samples after both 0 and 24 hours waiting time (Werner et al., 2017)
- The temperature increases during flow loop experiments, which may lower the viscosity of the fluid resulting in deviations of pressure loss gradients
- Anton Paar deviates from Fann-obtained rheology by exhibiting lower stress at low shear rates and higher stress at high shear rates

Experimental data from SINTEF with varying cuttings bed height as a function of rotational speed was attempted modelled in a mechanistic model. By comparing the experimental result with the model, we can conclude that:

- The rheology of drilling fluids has in general low impact on hole cleaning efficiency in the model. Rheology is a decreasingly dominant factor with increasing rotational speed
- Changes in velocity of the drilling fluid had less impact in the modelled cuttings bed height estimate, compared to experimental
- Comprehensive statistical modelling and handling a large amount of input-data needs to be included to lower the model-uncertainties from excluded physics
- At medium-inclined wells, back-sliding is an important part of cuttings transport efficiency, that needs to be included in future models

NOMENCLATURE

A	Area
A_a	Annular area
A_c	Cross sectional area of cuttings
A_l	Area between liquid layers
A_{sphere}	Area of a sphere
C_L	Lift coefficient
C_D	Drag coefficient
d	Diameter
d_i	Drill pipe diameter
d_o	Casing-/Open hole-diameter
d_h	Hydraulic diameter
d_p	Diameter of particle
$\frac{dP}{dx}$	Pressure loss
F	Force
F_D	Drag force
F_G	Gravity force
F_L	Lift force
F_P	Plastic force
F_y	Forces along y-axis
f	Friction factor
g	Gravity acceleration
H	Cuttings hold-up
h_{max}	Max height
h	Cuttings bed height
K	Consistency factor
k	Expansion constant
L	Pipe length
$L_{transport}$	Transport length

m_p	Particle mass
n	Flow behaviour index
n_f	Function related to friction between cuttings and borehole wall
N_{Re}	Reynolds number
$N_{Re,p}$	Reynolds particle number
P	Pressure
Q	Flow rate
$q_{cuttings}$	Flow rate of cuttings
$q_{new\ feed}$	Flow rate of ROP-cuttings
r	Radius
r_i	Diameter of drill pipe
r_o	Diameter of annulus
r_x	Effective lifting radius
s	Distance
Ta	Taylor's number
T_P	Rolling torque
$t_{transport}$	Transport time
u	Local velocity
u_L	Critical lift velocity
U_{max}	Maximum velocity in velocity profile
$U_{mean,bed}$	Mean velocity over cuttings bed
u_R	Critical rolling velocity
u_{rpm}	Velocity of rotating drill pipe wall
$u(r)$	Velocity as a function of radius
u_*	Friction velocity
V	Volume
V_{sphere}	Volume of a sphere
$V_{transport}$	Volume of transported cuttings
v_{avg}	Average velocity
v_{slip}	Slip velocity
v_{sa}	Axial slip velocity

v_{sr}	Radial slip velocity
v_{θ}	Rotational velocity
W	Weight
y	Height from cuttings bed

α	Wellbore inclination
β	Buoyancy factor
γ	Shear rate
μ_{eff}	Effective viscosity
μ_{pl}	Plastic viscosity
Ω_i	Angle velocity
ρ	Density
ρ_f	Density of mud
ρ_p	Density of particle/cuttings
τ	Shear stress
τ_0	Yield shear stress
τ_w	Wall shear stress
θ	Inclination of wellbore
ϕ	Angle of repose
φ	Porosity

REFERENCES

- Anton-Paar (2011) 'Instruction Manual - MCR Series'.
- Assembayev, D. V. and Skalle, P. (2015) *Evaluation of Rheology and Pressure Losses for Oil-based Drilling Fluids in a Simulated Drilling Process*. Norwegian University of Science and Technology (NTNU),
<https://brage.bibsys.no/xmlui/handle/11250/2350995>.
- Azar, J. J. and Sanchez, R. A. 'Important Issues in Cuttings Transport for Drilling Directional Wells', 1997/1/1/. SPE: Society of Petroleum Engineers.
- Caenn, R., Gray, G. R. and Darley, H. C. H. (2011) *Composition and Properties of Drilling and Completion Fluids*. Waltham, MA: Gulf Professional Publishing.
- Clark, R. K. and Bickham, K. L. 'A Mechanistic Model for Cuttings Transport', 1994/1/1/. SPE: Society of Petroleum Engineers.
- Fann, I. C. (2016) *Model 35 Instruction Manual*.
- Fischer, J. M. and Kloiber, L. A. (2006) 'Base Plate and Anchor Rod Design', *American Institute of Steel Construction, inc*, Second Edition.
- Gavignet, A. A. and Sobey, I. J. (1989) 'Model Aids Cuttings Transport Prediction', *SPE: Society of Petroleum Engineers*.
- Gerhart, P. M., Gross, R. J. and Hochstein, J. I. (1992) *Fundamentals of Fluid Mechanics*. Addison-Wesley.
- Iyoho, A. W. (1980) *Drilled-cuttings Transport by Non-Newtonian Drilling Fluids Through Inclined, Eccentric Annuli*. University of Tulsa.
- Kim, Y.-J., Yoon, C.-H., Park, Y.-C., Park, J., Kang, J. S., Kwon, S.-K., Woo, N. S. and Hwang, Y. K. 'A Study On the Rotating Flow In an Annulus', 2008/1/1/. ISOPE: International Society of Offshore and Polar Engineers.
- Kosberg, B. R. (2016) 'Comparison of Rheology and Pressure Loss for Water- and Oil-Based Drilling Fluids', *TPG4560 Petroleum Engineering, Specialization course at the Norwegian University of Science and Technology (NTNU)*.
- M.I-Swaco (2011) *Drilling Fluid System & Products*. Oil-base Systems: WARP Advanced Fluids Technology.
- M.I.Swaco (2017) *Drilling and Completion fluids*.
- OFI Testing Equipment, I. (2014) 'OFITE Product Catalog',
http://www.ofite.com/doc/131-50_brochure.pdf.

- Okrajni, S. and Azar, J. J. (1986) 'The Effects of Mud Rheology on Annular Hole Cleaning in Directional Wells', *SPE: Society of Petroleum Engineers*.
- Omosebi, A. O. and Adenuga, K. A. 'Pressure Drop versus Flow Rate Profiles for Power-Law and Herschel-Bulkley Fluids', 2012/1/1/. SPE: Society of Petroleum Engineers.
- Ooms, G. and Kampman-Reinhartz, B. E. (2000) 'Influence of Drillpipe Rotation and Eccentricity on Pressure Drop Over Borehole With Newtonian Liquid During Drilling', *SPE: Society of Petroleum Engineers*.
- Ozbayoglu, M. E., Saasen, A., Sorgun, M. and Svanes, K. 'Estimating Critical Velocity to Prevent Bed Development for Horizontal-Inclined Wellbores', 2007/1/1/. SPE: Society of Petroleum Engineers.
- Ozbayoglu, M. E., Saasen, A., Sorgun, M. and Svanes, K. 'Effect of Pipe Rotation on Hole Cleaning for Water-Based Drilling Fluids in Horizontal and Deviated Wells', 2008/1/1/. SPE: Society of Petroleum Engineers.
- Piroozian, A., Ismail, I., Yaacob, Z., Babakhani, P. and Ismail, A. S. I. (2012) 'Impact of drilling fluid viscosity, velocity and hole inclination on cuttings transport in horizontal and highly deviated wells', *Journal of Petroleum Exploration and Production Technology*.
- Ramadan, A., Skalle, P. and Johansen, S. T. (2003) 'A mechanistic model to determine the critical flow velocity required to initiate the movement of spherical bed particles in inclined channels', *Chemical Engineering Science*, 58(10), pp. 2153-2163.
- Ravi, K. and Hemphill, T. 'Pipe Rotation and Hole Cleaning in Eccentric Annulus', 2006/1/1/. SPE: Society of Petroleum Engineers.
- Sayindla, S., Lund, B., Taghipour, A., Werner, B., Saasen, A., Gyland, K. R., Ibragimova, Z. and Ytrehus, J. D. (2016) 'Experimental Investigation of Cuttings Transport With Oil Based Drilling Fluids', *ASME Proceedings*, Volume 8: Polar and Arctic Sciences and Technology; Petroleum Technology.
- Schlumberger (2017) 'Biocide', *Oilfield Glossary*.
- Schlumberger, I. M. F. f. (2016) 'Rheology ', *The defining series*.
- Sifferman, T. R. and Becker, T. E. (1992) 'Hole Cleaning in Full-Scale Inclined Wellbores', *SPE: Society of Petroleum Engineers*.
- SINTEF 2017. RE: *SINTEF Petroleum: Unpublished data*.
- Skjeggstad, O. (1989) *Boreslamteknologi : teori og praksis*. Bergen: Alma Mater.

- Saasen, A. 'Hole Cleaning During Deviated Drilling - The Effects of Pump Rate and Rheology', 1998/1/1/. SPE: Society of Petroleum Engineers.
- Saasen, A. and Løklingholm, G. 'The Effect of Drilling Fluid Rheological Properties on Hole Cleaning', 2002/1/1/. SPE: Society of Petroleum Engineers.
- Tomren, P. H. (1979) 'The Transport of Drilled Cuttings in an Inclined Eccentric Annulus', *MS thesis, University of Tulsa, OK*.
- Wang, Z., Zhai, Y., Hao, X., Guo, X. and Sun, L. 'Numerical simulation on three layer dynamic cutting transport model and its application on Extended Reach Drilling', 2010/1/1/. SPE: Society of Petroleum Engineers.
- Werner, B. 2017. *RE: Personal Communication*.
- Werner, B., Lund, B., Myrseth, V., Saasen, A. and Gyland, K. R. 'Comparison of Rheological Properties of Oil-Based and KCl Drilling Fluids', 2016/4/20/. SPE: Society of Petroleum Engineers.
- Werner, B., Lund, B. r., Birgitte, R. K., Johansen, E., Giil, G. L. and Ytrehus, J. D. (2017) 'Effect of Preconditioning and Ageing on Rheological Properties of Model-Drilling Fluids', *The Annual European Rheology Conference*.
- Werner, B., Myrseth, V., Lund, B., Saasen, A., Ibragimova, Z., Ytrehus, J. D. and Gyland, K. R. (2016b) 'Effects of Oil-Based Drilling-Fluid Rheological Properties on Hole-Cleaning Performance', (49996), pp. V008T11A038.
- White, F. M. (2016) 'Fluid Mechanics', pp. XIV, 773 s.
- Ytrehus J, T. A., Sayindla S, Lund B, Werner B, Saasen A (2015) 'Full Scale Flow Loop Experiments of Hole Cleaning Performances of Drilling Fluids.', *ASME International Conference on Offshore Mechanics and Arctic Engineering, Volume 10: Petroleum Technology ()*:V010T11A041. doi:10.1115/OMAE2015-41901.
- Ytrehus, J. D., Taghipour, A., Lund, B., Werner, B., Opedal, N., Saasen, A. and Ibragimova, Z. (2014) 'Experimental Study of Cutting Transport Efficiency of Water Based Drilling Fluids', *OMAE - American Society of Mechanical Engineers*.

APPENDICES

Appendix A: Flow curves for procedure evaluation (Werner et al., 2017)

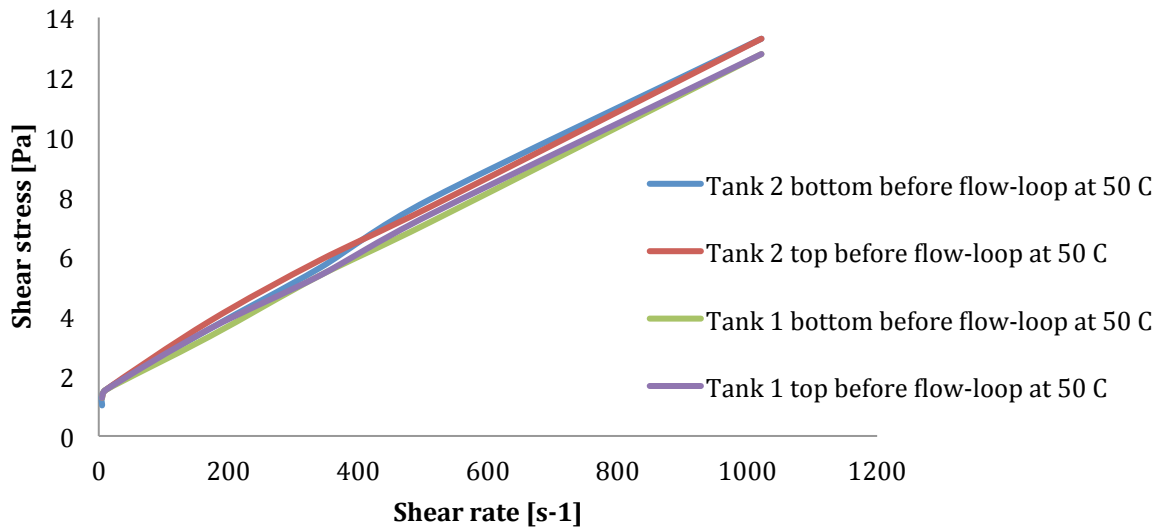
Appendix B: Flow curves from rheology control (SINTEF 2017)

Appendix C: Laboratory procedures

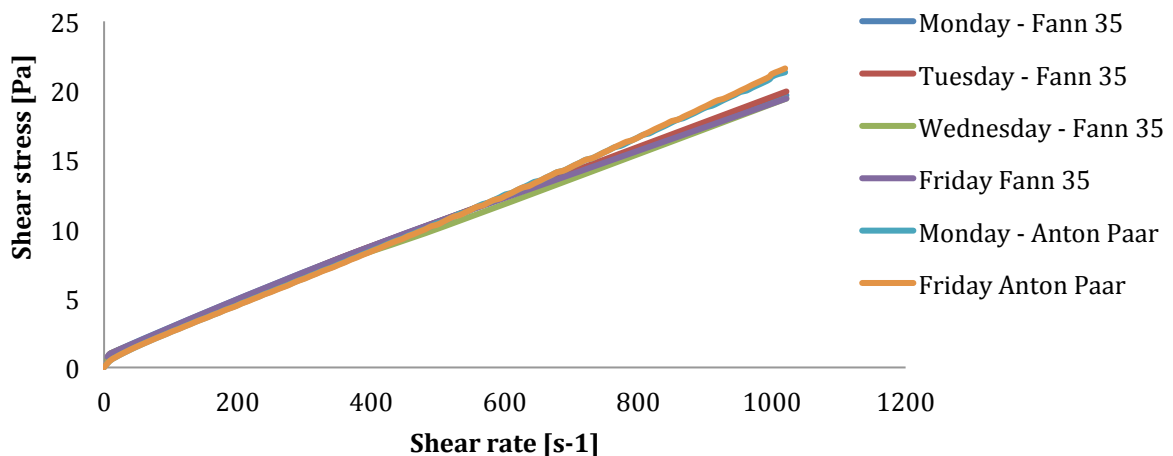
Appendix E: Risk assessment

APPENDIX A: FLOW CURVES FOR PROCEDURE EVALUATION

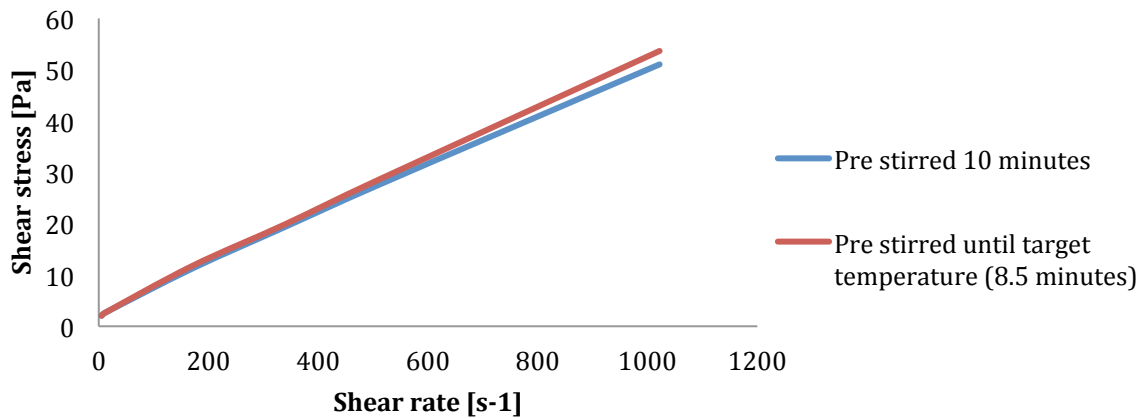
Flow curves of the tanks with OBM WARP at 50 °C on bottom and top to be able to evaluate if the tanks were evenly mixed. The plots show that there is similarity between the different tanks in rheology profile:



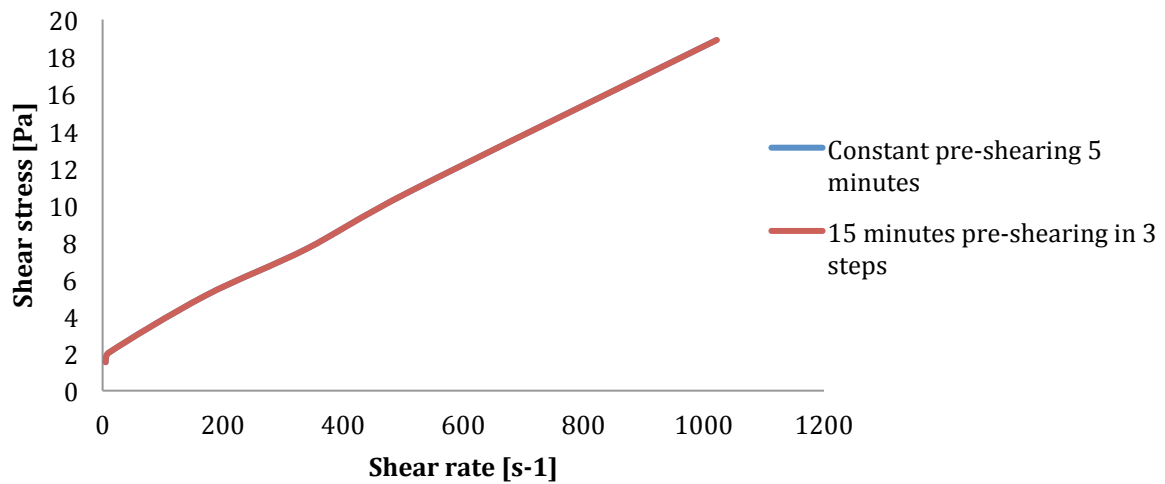
Flow curves of the first week's test over the flow loop-experiments with OBM WARP at 25°C. The flow curves show Anton Paar deviates from the Fann 35 measurements at high shear-rates:



Flow curves examining different durations of pre-stirring in Fann 35 at 600 rpm prior to the measurement.

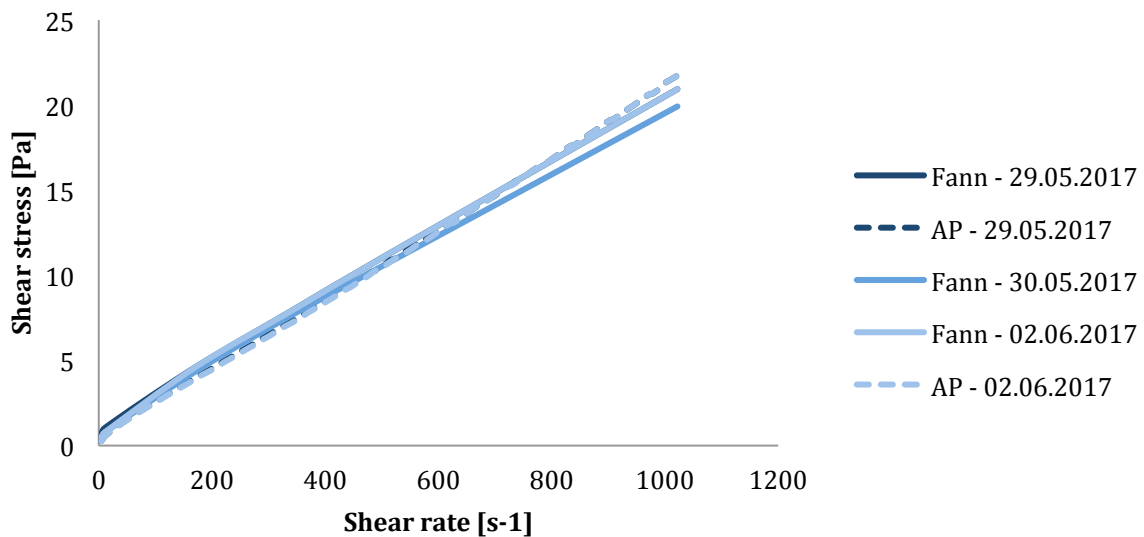


Flow curves of examining the procedure of pre-mixing in Hamilton blender; 15 minutes straight mixing vs. mixing in 3 x 5 minutes intervals with 5 minutes resting in between and after.

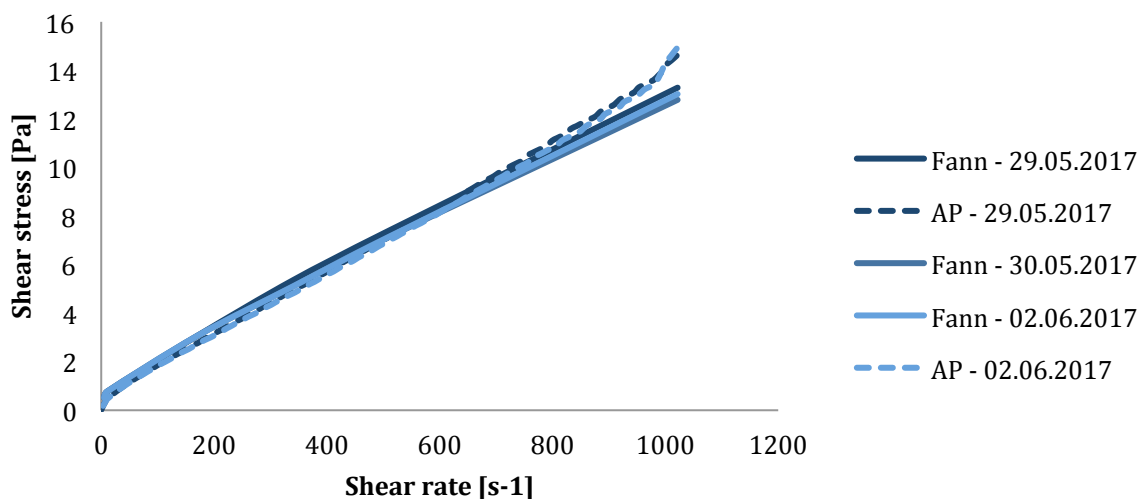


APPENDIX B: FLOW CURVES FOR RHEOLOGY CONTROL (*SINTEF*)

In Appendix B we will list the flow loop measurements done for obtaining rheology control in the flow-loop during experiments conducted by *SINTEF*. The first plot shows flow-loop measurements from week 2 in Fann 35 and Anton Paar. Measurements show stable rheology at 25°C throughout the experiment-period.



The second plot shows flow-loop measurements from week 2 in Fann 35 and Anton Paar. Measurements show stable rheology at 50°C throughout the experiment-period.



APPENDIX C: LABORATORY PROCEDURES

In Appendix C the laboratory procedures for testing emulsion stability, density and rheological properties within the fluid will be closely gone through. The procedures utilized in this master thesis is inspired and developed in cooperation with MI Swaco – A Schlumberger Company.

C.1 PROCEDURE FOR FANN 35-VISCOMETER AND ES MEASUREMENTS

The procedure for obtaining the rheology profile, gel strength and electrical voltage is mentioned in the same procedure as the measurements are done simultaneously. Measurements in Fann 35-viscometer is done in the following way:

1. Pre-shear the fluid at low shear for 15 minutes in the Hamilton Beach drink blender
2. Pour the fluid over in a Fann-thermo cup with the pre-set temperature of your choice and bring the fluid level to the mark on the cylinder surrounding the bob
3. Start rotating at 600 rpm in 10 minutes for the OBM to stabilize at high shear
4. When stabilized at 600 rpm – read off the value on the display. Continue ramping down from 600-300-200-100-6 and then 3 rpm.
5. After reading off the value at 3 rpm, measure the emulsion stability by using the *OFITE Emulsion Stability Tester*.
6. Measure gel parameters by rotating at 600 rpm for 10 seconds – wait 10 seconds at rest – then read off the 3 rpm reading. Then repeat the same procedure for 10 seconds at 600 rpm – 10 minutes at rest and then read off the 3 rpm reading.

Successfully following this procedure will lead to obtaining the rheological profile, gel strength and emulsion stability.

C.2 PROCEDURE FOR ANTON PAAR-RHEOMETER

In C.2 we will go through the procedure for obtaining the rheological profile from the Anton Paar-rheometer. The Anton Paar differs from the Fann-viscometer as it can achieve a lot more measured points, as well as it gives other useful data as i.e. yield point. This procedure was done with references to the manual (Anton-Paar, 2011):

1. Pre-shear the fluid in a Hamilton Beach blender for 15 minutes

2. Turn on Anton Paar during the wait and wait for it to boot for approximately 1 minute. The text "ok" will then appear on the digital display.
3. Start up the rheo-plus program on the computer connected to Anton Paar.
4. Open the water- and air-inlets
5. Connect the right bob for the fluid you are testing
6. Choose the shear stress versus shear strain option and initialize the instrument so that it is connection between the instrument and the software
7. Set the required temperature to the water bath
8. Set up a profile for measuring the shear stress versus the shear strain. In this case 10 minutes at 1022 s⁻¹ and then ramp down from 1022-1 s⁻¹ with 120 measured points with 2 seconds between them
9. Put the measuring cup in place
10. Set the bob down to measuring position and keep it there for the rest of the wait, so that the bob can hold the same temperature as the fluid and reduce uncertainty
11. Start measurements at temperature equilibrium

When measurements are obtained the apparatus will by itself lift the bob from measuring position so that it will be easy to remove the cup with the fluid sample. Clean both the fluid container and the bob prior to starting up new measurements.

C.3 PROCEDURE FOR DENSITY MEASUREMENTS WITH PYCNOMETER

The density measurements from the pycnometer is a rather simple procedure, but will be listed in this appendix:

1. Weigh the pycnometer with its top-part and zero out the weighing cell at that particular weight
2. Fill the pycnometer with the fluid sample
3. Put on the top part and make sure the pycnometer is totally clean prior to weighing the sample
4. Weigh the pycnometer with the fluid inside and write down the fluids weight
5. Write down the volume of the pycnometer and find the density

APPENDIX D: RISK ASSESSMENT

In Appendix C the Risk Assessment needed prior to entering the lab is attached. Risk assessment is required for all work in the laboratory or field for master students at the Norwegian University of Science and Technology (NTNU). The document contains possible hazards and solutions to issues regarding use of the laboratory, and the calculated risk of operations.

ID	16790	Status	Date
Risk Area	Risikovurdering: Helse, miljø og sikkerhet (HMS)	Created	19.12.2016
Created by	Birgitte Ruud Kosberg	Assessment started	19.12.2016
Responsible	Birgitte Ruud Kosberg	Actions decided	
		Closed	19.12.2016

Risk assessment for the mud-laboratory

Valid from-to date:

11/20/2016 - 12/19/2019

Location:

4 - Sydområdet / 444 - Petroleumsteknisk senter / 1030 - 3. etasje / 313A

Goal / purpose

We will perform measurements of the drilling fluids rheology with respect to health, safety and environment. We want to become aware of what unconformities that can occur while working in the laboratory and the outcome. We also want to know how these unconformities can be prevented.

Background

This autumn's specialization project will be based on measurements in the drilling fluids laboratory and a risk assessment will be familiar with the possible risks of the different work tasks and how these in a best way can be prevented.

Description and limitations

Prerequisites, assumptions and simplifications

[Ingen registreringer]

Attachments

[Ingen registreringer]

References

[Ingen registreringer]

Summary, result and final evaluation

The summary presents an overview of hazards and incidents, in addition to risk result for each consequence area.

Hazard: Fire

Incident:

Not to be analyzes.





Hazard: Toxic inhalation

Incident:

Not to be analyzes.

Hazard: Slippery floor

Incident: Oil spillage

Consequence area:	Helse	Risk before actions:		Risiko after actions:	
	Materielle verdier	Risk before actions:		Risiko after actions:	

Final evaluation

The health, safety and environmental risks involved are acceptable to perform laboratory-measurements for the specialization project this autumn. Under a oil spillage, be sure to clean up the oil with an oil absorbing rag and soap water. Also be sure to have high level of ventilation available.

Units this risk assessment spans

- NTNU

Participants

[Ingen registreringer]

Readers

[Ingen registreringer]

Others involved/stakeholders

[Ingen registreringer]

The following accept criteria have been decided for the risk area Risikovurdering: Helse, miljø og sikkerhet (HMS):

Helse



Materielle verdier



Omdømme



Ytre miljø



Overview of existing relevant measures which have been taken into account for this risk assessment

The table below presents existing measures which have been taken into account when assessing the likelihood and consequence of relevant incidents.

Hazard	Incident	Measures taken into account
Slippery floor	Oil spillage	Guidelines

Existing relevant measures with descriptions:

Ventilation

Ventilation is provided as a lot of oil-based fluids are used in the experiments.

Personal protective wear

Lab coat is provided to avoid spill of oil or corrosive fluids or powders on skin or clothing.

Glasses are worn at all times to avoid damage to eyes because of the substances that is included in this project.

Safety shoes are worn to avoid the consequences of dropping heavy objects that can hurt our feet.

Latex gloves are worn when exposed to harmful fluids or powders, in example corrosive mediums.

Guidelines

The following guidelines were pursued:

- Master students are not allowed to stay in the lab before 08:00 am and after 15:45 pm to ensure that other people are around if anything were to happen
- Guidelines of treatment of hazardous waste
- Guidelines in how to use the instruments correctly to avoid damage

Risk analysis with evaluation of likelihood and consequence

This part of the report presents detailed documentation of hazards, incidents and causes which have been evaluated. A summary of hazards and associated incidents is listed at the beginning.

The following hazards and incidents has been evaluated in this risk assessment:

- **Slippery floor**
 - Oil spillage

Overview of risk mitigating actions which have been decided, with description:

Slippery floor (hazard)

Slippery floor as a result of oil spillage can result in people falling.

Slippery floor/Oil spillage (incident)

Oil was spilled onto the floor, making it extra slippery. In a worst case scenario this could lead to people falling and hurt themselves or equipment.

Cause: Lost the measuring cup

Description:

We lost the measuring cup containing oil that was to be mixed into the drilling fluid sample.

Overall assessed likelihood of the incident: Less likely (2)

Comment to likelihood assessment:

If you are careful, the likeliness of losing the cup is relatively low.

Assessment of risk for the consequence area: Helse

Assessed likelihood (common for incident): Less likely (2)

Assessed consequence: Medium (2)

Comment to consequence assessment:

[Ingen registreringer]



Overview of risk mitigating action which have been decided:

Below is an overview of risk mitigating actions, which is intended to contribute towards minimizing the likelihood and/or consequence of incidents:

Overview of risk mitigating actions which have been decided, with description:

